A NUMERICAL INVESTIGATION OF MICROGRAVITY ETHYLENE/OXYGEN/NITROGEN SPHERICAL DIFFUSION FLAMES AT THEIR SOOT FREE LIMIT

A THESIS SUBMITTED TO THE GRADUATE DIVISION OF THE UNIVERSITY OF HAWAI‘I AT MĀNOA IN PARTIAL FULFILLMENT OF THE REQUIREMENTS FOR THE DEGREE OF

MASTER OF SCIENCE

IN

MECHANICAL ENGINEERING

AUGUST 2012

By

Mahmood Dehnavi

Thesis Committee:

Beei-Huan Chao, Chairperson

Michael Antal Jr.

Weilin Qu

2012

Acknowledgements

The funding for this project was made possible by the National Aeronautics and Space Administration. In addition, Research and Teaching Assistantship support was provided by the Department of Mechanical Engineering.

I would like to express my gratitude to my adviser, Prof. Beei-Huan Chao, for his help and support throughout my studies and for giving me the opportunity to work on this project. I would also like to thank my committee members, Profs. Qu and Antal, for their guidance.

Last but not least, I would like to acknowledge Dr. Peter Sunderland and Dr. Vivien Lecoustre from the Department of Fire Protection Engineering at the University of Maryland and Dr. Richard Axelbaum from the Department of Energy, Environmental and Chemical Engineering at Washington University at St. Luis for the technical discussions and guidance.

Abstract

Soot, which is a byproduct of incomplete combustion from hydrocarbon/air flames, is a major cause of premature deaths and lung cancer among pollutants generated from burning of carbon-based fuels. It also is responsible for the reduction of combustion efficiency due to the decrease of thermal energy and radiative heat losses. In this study, the sooting behavior of spherical diffusion flames using ethylene as the fuel was investigated to improve the understanding of soot formation processes in diffusion flames. Microgravity experiments using the 2.2-s drop tower operated by NASA Glenn Research Center were conducted to observe the sooting behavior and provide guidance to the theoretical study of such flames. Fifteen flames that were found to reach their soot-free conditions between 1 and 2 seconds from the experiments were selected in this study. A numerical code with detailed chemistry and transport properties as well as realistic radiation model was adopted to simulate these flames. Results show that for the formation of soot particles, both the local temperature and carbon to oxygen atom ratio need to exceed certain critical values, which were found to be 1425 K and 0.47, respectively, for the flames investigated in this study.

Contents

List of Tables

List of Figures

Nomenclature

C_p	Mixture molar heat capacity at constant pressure
C_v	Mixture molar heat capacity at constant volume
C/O	Carbon to oxygen atom ratio
D	Diffusion coefficient
Da	Damkohler number
E_a	Activation energy
$\vec{f}_k$	Body forces acting on k^{th} species
h^s	Sensible enthalpy
h_k^0	Enthalpy of formation of k^{th} species per unit mass
II	Number of elementary reactions
K_{ci}	Equilibrium constant of the i^{th} reaction
k_{fi}	Rate of the i^{th} forward reaction
k_{ri}	Rate of the i^{th} backward reaction
KK	Number of species
Le	Lewis number
$\dot{m}$	Mass flow rate
p	Pressure
Pe	Peclet number
$\vec{q}_r$	Rate of radiative heat loss
r	Radius
R	Ideal gas constant
Re	Reynolds number
S	Entropy
Sc	Schmidt number
T	Time
T	Temperature
T_f	Flame temperature
$\vec{U}$	Velocity vector

$\vec{U}_{d,k}$	Diffusion velocity of the k^{th} species
W_k	Molecular weight of the k^{th} species
$\overline{W}$	Mean molar weight of the mixture
X_k	Mole fraction of the k^{th} species
Y_k	Mass fraction of the k^{th} species
Z	Mixture fraction
Z_{st}	Stoichiometric mixture fraction

Greek Symbols

χ	Scalar dissipation rate
$\dot{\omega}_k$	k^{th} species molar production
η	Mixture viscosity
λ	Mixture thermal conductivity
ν	Stoichiometric coefficient
ρ	Mixture density

Subscripts and Superscripts

0	Conditions inside the burner
∞	Condition at infinity
b	Burner property
f	Fuel property
k	Property of the k^{th} species
ox	Oxidizer peoperty
s	Surface property

Chapter 1
Introduction

1.1 Influence of Fire on Human life

Domestication of fire started a new chapter in the history of mankind and it can be considered as one of the biggest achievements of our kind. Learning to manipulate fire enabled humans to dominate other species, both animals and plants. Armed with fire, humans were able to open up impenetrable tracks of bush and drive away animals [1].

Higher standard of living was achieved by the possibility of heating, lighting and cooking as a consequence of the discovery of fire. Pointed arrows, earthenwares, metal tools and weapons were made by controlling fire and thus providing humans with more safety and access to food [1]. Agriculture was further developed utilizing fire to burn up unwanted plants, creating land for cultivating new crops. This resulted in settlement of large populations and formation of societies. Thus competition for resources was increased and unavoidably ignited the engine of war between these societies. Further development of technology has increased the extent of destruction since the industrialization of human societies.

Although fire has been in use for an extensive period of time, the first hypothesis of the true nature of combustion was posited in the late eighteenth century by a French chemist, Antoine-Laurent Lavoisier. Lavoisier proposed a phlogiston theory and explained combustion as a

chemical process induced by a combination of oxygen and some other reactive components. His theory can be considered as a keystone to the development of modern combustion science [2]. The invention of steam engines and establishment of thermodynamics in subsequent years expedited utilization of fire in industrial scale and made a major contribution to the industrial revolution.

1.2 The role of combustion in current societies

During the 20^{th} and 21^{st} centuries, our dependence on energy has increased drastically. Transportation, industry, agriculture, lighting and daily life rely heavily on various sources of energy, especially electricity. A great portion of the energy consumed, including electricity, is provided through combustion of fossil fuels. Figure 1.1 shows the United State's energy consumption from 1949-2010. It can be noticed that despite the growing interest in and supply of renewable and nuclear energy, fossil fuels are the primary sources of energy. A breakdown of the major sources of energy consumption in 2010 is presented in Figure 1.2.

The energy flow in 2010, depicted in Fig. 1.2, emphasizes the significance of more efficient combustion processes and devices which can be achieved through a better understanding of combustion phenomena. The results of our work can be applied to reduce the formation of soot, and lead to improved performance of combustion devices.

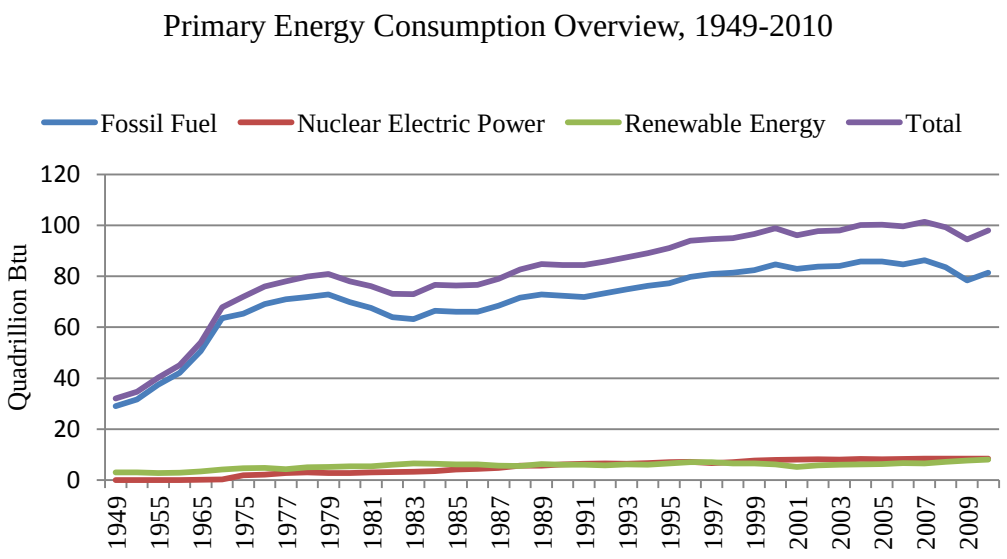

Figure 1.1. Primary energy consumption in the United States, 1949-2010. Adapted From [3]. Note: 1 Btu = 1.06 kJ

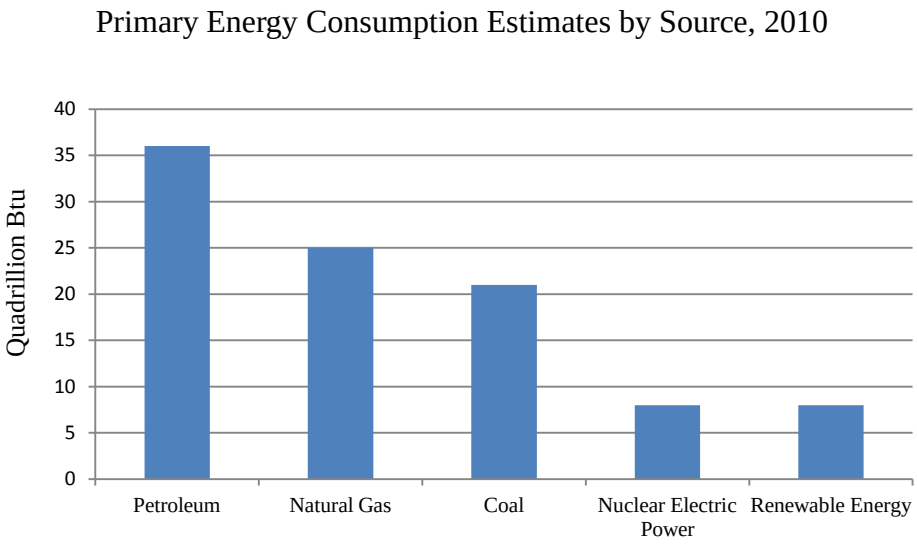

Figure 1.2. Primary energy consumption estimates in the United States, by source. Adapted From [3].

Note: 1 Btu = 1.06 kJ

In addition to the improvements of the quality of our life by the use of flames, burning of carbon-based fuels produces various forms of pollutants that may negatively impact our environment. The most common combustion pollutants include carbon monoxide, nitrogen oxides, sulfur dioxide, particulates and polycyclic aromatic hydrocarbons (PAHs), which are soot precursors. Among these pollutants, soot is responsible for the highest number of premature deaths and lung cancer. Roughly 50,000 premature deaths per year are caused by inhalation of soot particles in USA alone. In New Jersey, for instance, nearly 400 premature deaths, 16,000 asthma attacks and 1,800 emergency-room visits could be avoided each year by reducing soot emissions by 20 percent [4, 5].

Realizing the significance in the negative impact of soot, the primary purpose of this research is to understand the soot formation from combustion processes and identify the soot free conditions, that is, the conditions under which soot cannot be formed. Because most of the practical combustion devices adopt diffusion flames for heat generation, the investigation focuses on the soot formation processes in diffusion flames.

1.3 Conservation Equations

Diffusion flames, such as candle flames, are the most common type of flames in nature. A diffusion flame is established by combustion of fuel and oxidizer, which are supplied from separate sources and are brought together in the reaction zone by convection and diffusion transports. In the case of premixed flames, fuel and oxidizer are mixed before the premixture is transported to the flame. A diffusion flame is situated at where the stoichiometry between the

fuel and the oxidizer is attained while a premixed flame is a combustion wave that propagates into the premixture.

The conservation equations governing the transport and reaction processes are the same for these two types of flames despite their difference in characteristics. For low Mach number combustion systems, the governing equations are [6]:

I. Conservation of mass:

$$\frac{\partial \rho}{\partial t} + \nabla . \left(\rho \vec{U}\right) = 0 \tag{1.1}$$

II. Conservation of species:

$$\frac{\partial \rho Y_k}{\partial t} + \nabla . \left[\rho Y_k \left(\vec{U} + \vec{U}_{d,k}\right)\right] = \dot{\omega}_k, \qquad k = 1, \dots, KK \tag{1.2}$$

III. Conservation of momentum

$$\rho \frac{\partial \vec{U}}{\partial t} + \left(\rho \vec{U} . \nabla\right) \vec{U} = -\nabla . \mathrm{P} + \rho \sum_{\mathrm{k=1}}^{\mathrm{KK}} Y_k \vec{f}_k \tag{1.3}$$

IV. Conservation of energy:

$$\frac{\partial \rho C_p T}{\partial t} + \nabla . \left(\rho C_p T \vec{U}\right) = -\nabla . \left(\vec{q}_r + \rho \sum_{\mathrm{k=1}}^{\mathrm{KK}} Y_k C_{p,k} T \vec{U}_{d,k} - \lambda \nabla T \right) + \frac{dp}{dt} - \sum_{\mathrm{k=1}}^{\mathrm{KK}} h^0{}_k \dot{\omega}_k \tag{1.4}$$

In these equations, ρ is density and $\vec{U}$ is velocity vector. Y_k , $\vec{U}_{d,k}$ and $\dot{\omega}_k$ are the mass fraction, diffusion velocity and molar production of the k^{th} species, respectively. $\vec{f}_k$ is the body force (such as the gravitational force) acting on species k, C_p is the heat capacity of the mixture at

constant pressure, T represents temperature, $\vec{q}_r$ is the rate of radiative heat loss, $C_{p,k}$ is the k^{th} species heat capacity at constant pressure, λ is the thermal conductivity of the mixture, and ${h^0}_k$ is the k^{th} species formation enthalpy per unit mass at the standard reference state.

For a multi-step reaction consisting of numerous intermediate elementary steps and many intermediate species before the formation of products, the general reactions that convert the reactants to the products can be expressed as

$$\sum_{k=1}^{KK} \nu'_{k,i} M_k \rightleftarrows \sum_{k=1}^{KK} \nu''_{k,i} M_k \,, \qquad i = 1,2,\dots,II \tag{1.5}$$

where II represents the total number of reaction steps, ν_{ki} represents the stoichiometric coefficients, and M is the chemical species. The stoichiometric coefficients of the reactants of the forward reactions are denoted by a superscript ’ while those of the reverse reactions are denoted by ”. The rate constants of the backward reactions can be easily determined using the equilibrium constant, given by

$$k_{r_i} = \frac{k_{f_i}}{K_{c_i}} \tag{1.6}$$

and the equilibrium constant for the ith reaction is:

$$K_{c_i} = \left(\frac{P_{atm}}{RT}\right)^{\sum_1^K (\nu''_{k,i} - \nu'_{k,i})} \exp\left(\frac{\Delta S_i^0}{R} - \frac{\Delta H_i^0}{RT}\right) \tag{1.7}$$

In the above, k_{f_i} and k_{r_i} are the reaction rate constants of the forward and backward reaction, and S_i^0 and H_i^0 are the entropy and enthalpy of formation per unit mole of species of the l^{th} reaction. The reaction rate for each of these steps is expressed by law of mass action and the Arrhenius law as:

$$\dot{\omega}_k = W_k \sum_{i=1}^{II} \left(\nu''_{k,i} - \nu'_{k,i}\right) A_i T^{\beta_i t} \exp\left(-\frac{E_{i,k}}{RT}\right) \prod_{j=1}^{KK} c_j^{\nu'_{j,i}} \tag{1.8}$$

Finally, these equations are complemented by the equation of state with the assumption that the gases are ideal gas:

$$p = \rho \frac{R}{\overline{W}} T \tag{1.9}$$

where $\overline{W}$ is the mean molecular weight of the mixture.

These nonlinear partial differential equations are three dimensional in general and are difficult to solve. Even with the use of powerful supercomputers, simulation of combustion problems demands tremendous computational time. To ensure that the study can be performed within realistic time, the results can be analyzed and the controlling parameters can be unambiguously identified, simplified one-dimensional flames have been adopted in numerous previous studies and are considered in this work.

1.4 Influence of Gravity on Flames

The densities of gaseous combustion products at the flame front are typically 7-10 times less than those of unburned reactants at their supply. In the presence of gravity, these density

differences generate buoyancy forces that drive the gases with higher/lower density towards/away from the center of gravity, and modify the flow field [7, 8]. Because this natural convection process is not symmetric in a flow field, existence of gravity complicates the convective-diffusive transport of the gases.

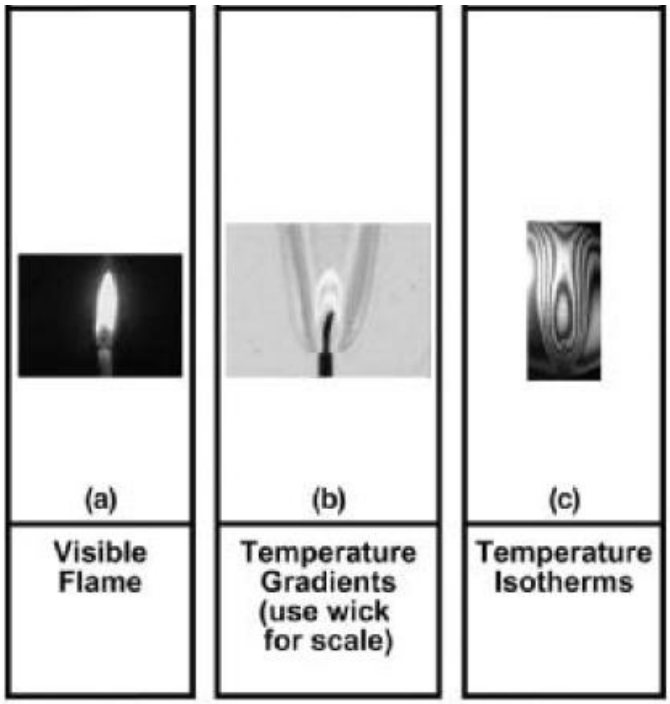

Figure 1.3. Temperature and chemical species measurement of a candle burning at earth's gravity: (a) flame image; (b) temperature gradients; (c) temperature isotherms. From [7].

Using a candle flame, a type of flame that has been widely used for various purposes, as illustration, Fig. 1.3 underlies the effects of gravity on the shape of the flame. This figure shows the asymmetric behavior caused by gravity, which results in complex temperature and density distributions. These complexities make the solution of the governing equations extremely difficult due to the following reasons.

All the conservation equations are coupled through the gas density, which depends on the temperature gradient, and must be solved simultaneously. The addition of exponential dependence on temperature in the reaction rates as shown in Eq. (1.8) further renders the problem very sensitive to temperature variations. As a result, the equations are computationally stiff such that obtaining of the solution is beyond the state of the art even for the simplest three-dimensional combustion systems [7]. The unidirectional nature of the gravity force makes the problem inherently multi-dimensional and difficult to solve both numerically and analytically.

Elimination of gravity causes the candle flame to be spherical as depicted in Fig. 1.4. In the upper half of the flame, the variations along angular directions can be ignored such that the only spatial dependence is the radial direction and the flame can be considered one-dimensional in the spherical coordinates. In the presence of gravity, the flame is elongated as shown in Fig. 1.3 and is inherently multi-dimensional.

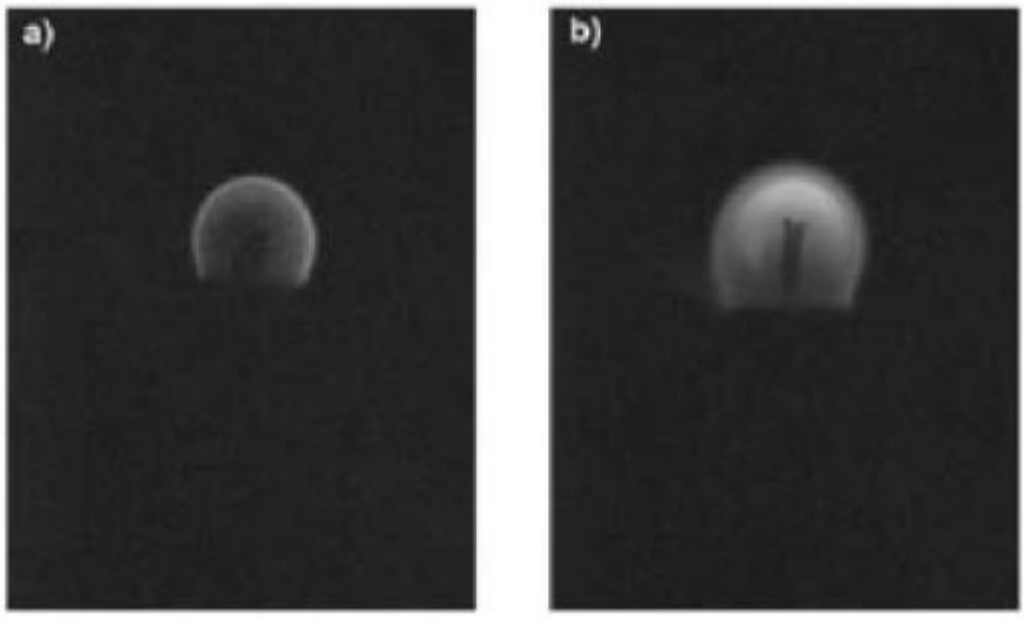

Figure 1.4. Shape of candle flame burning in microgravity (a) early in flame lifetime, (b) just after the wax melts completely. From [7]

It can be shown mathematically [9] that among the three possible one-dimensional flame configurations (planar, cylindrical and spherical flames) burning in an infinite domain, the only flame that can reach steady state is the spherical flame. Spherical flames with negligible gravity effect can be established experimentally by the combustion of fuel droplets or by the use of a spherical burner. A burner supported flame can be obtained by issuing a reactant from a porous sphere into a large quiescent environment filled with the other reactant.

1.5 Fuel Droplet Combustion and Burner-stabilized Diffusion Flames

The combustion of a fuel droplet in microgravity is an ideal example of a spherical diffusion flame burning in an unbounded environment. The heat conducted from the flame to the liquid droplet is used to vaporize the liquid fuel at the droplet surface into the fuel vapor. The fuel vapor is subsequently transported to the flame to support further combustion. Although quasi-steady combustion can be achieved for most of the burning period, and reasonably good predictions can be made through analysis for this case, the process is inherently unsteady because of the reduction in the droplet size with time. For droplet combustion, the rate of fuel vaporization, or the fuel consumption rate, and the flame location cannot be independently controlled. They are determined by the coupling between the heat conduction from the flame to the droplet and the latent heat of the liquid fuel [6]. In addition, the flow direction is always from the fuel side to the oxidizer.

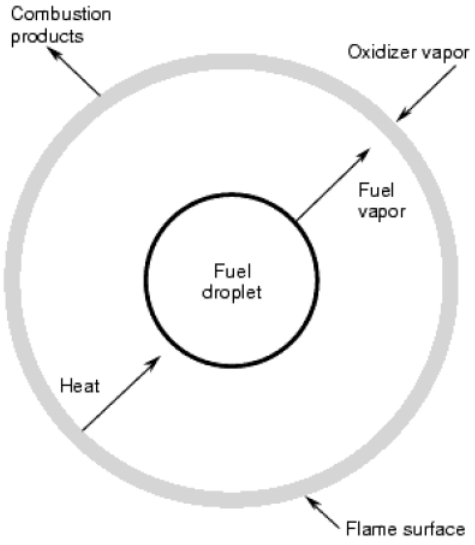

Fig. 1.5. Schematic of a burning fuel droplet.

As an alternative, we chose a burner-stabilized configuration as illustrated in Fig. 1.6 in this study. There are many advantages for the adoption of this burner-stabilized flame. The flame can be in truly steady state by fixing the mass flow rate issued from the burner, and the flame location is controllable by adjusting the flow rate. In addition, the flow direction can be from the fuel to the oxidizer by supplying the fuel from the burner into a large chamber filled with the oxidizer or from the oxidizer to the fuel by injecting the oxidizer from the burner into a fuel environment. The fuel and oxidizer concentrations can also be individually controlled by varying the amount of inert gas (e.g., nitrogen) that is supplied with each of the reactants. Finally, the inert gas selection depends on the objectives of study.

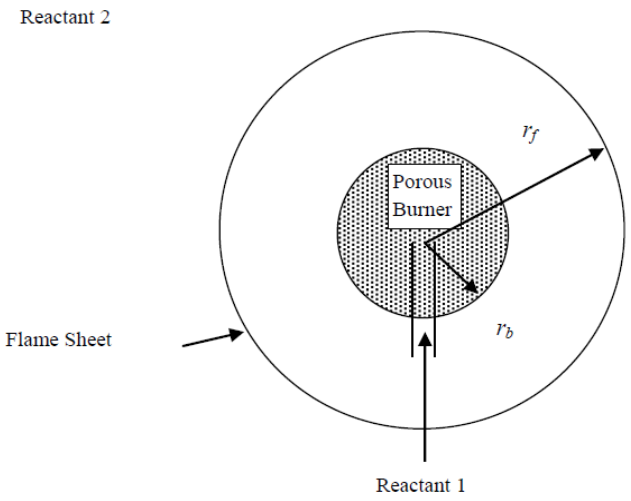

Fig. 1.6. Schematic of a burner-generated spherical diffusion flame

The burner-generated spherical diffusion flames resolve the difficulties that cannot be removed from droplet flames and can be used for fundamental studies. To employ the configuration, experiments must be conducted in microgravity. Experiments conducted in the drop towers provided by NASA exhibit that the flames can be sufficiently spherical and appropriate for this study. Figure 1.7 shows a soot-free flame at 2 seconds after release into microgravity, with 80% oxygen (balanced by nitrogen) issued from the burner into a chamber filled with 11% ethylene.

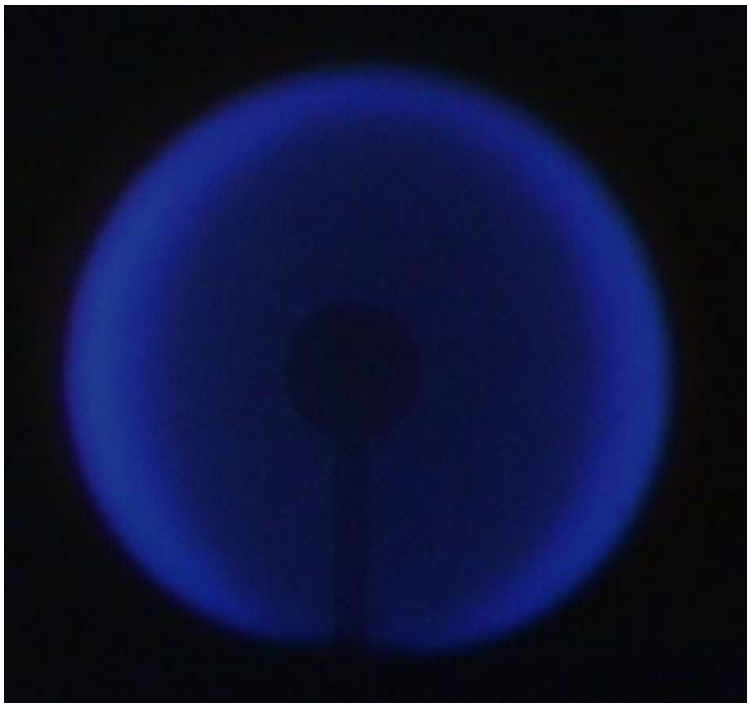

Fig. 1.7. Spherical diffusion flame with 80% oxygen issued into 11% ethylene at 2 seconds.

Chapter 2

Experimental Setup

2.1 NASA Drop Tower

The microgravity experiments for this project were conducted using NASA's ground-based 2.2 second drop tower, Zero Gravity Research Facility, located at the NASA Glenn Research Center. This facility is one of the two drop towers used to study combustion, fluid physics, biotechnology and material science in the United States. It has been in operation since 1966 and is the largest facility of its kind in the world. The facility capabilities are as follows [10]:

- Operational Parameters:

Microgravity Duration: 2.2 seconds;

Free Fall Distance: 79 feet (24m);

Gravitational Acceleration: $< 0.001g$

- Experimental Drop Package:

Payload width: 38 in. (96 cm);

Payload height: 33 in. (84 cm);

Payload depth: 16 in. (40 cm);

Payload weight: up to 350 lbs (159 kg);

Gross vehicle weight: 1075 lbs. (487 kg)

- Instrumentation/Data Acquisition:

Video Cameras, Digital Frame Grabbers; Analog-Digital Data Acquisition; 24 VDC Battery Power; Programmable Logic Controller; Pressure Transducers; Flow Meters; Thermocouples, Radiometers and Lasers.

A layout of the drop test is illustrated in Fig. 2.1.

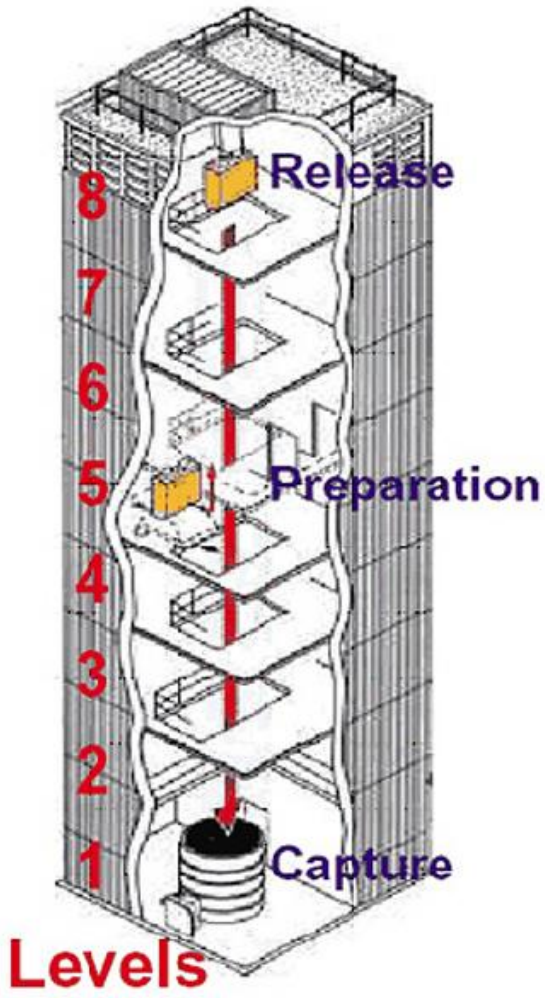

Figure. 2.1. Layout of 2.2 s drop tower at NASA's Zero-G Research Facility

To prepare the chamber for each experiment, it was first evacuated to 0.03 bar and filled to 0.98 bar (with the uncertainty of ±0.005 bar) with the appropriate ambient gas at the room temperature [11].

2.2 Drop Package

The experimental apparatus used for the experiments was described in detail by Sunderland et. al [11]. The combustion rig has the general features as mentioned in section 2.1. The burner reactant is supplied from a storage tank mounted on the rig, and then flows through a pressure regulator, a solenoid valve, a calibrated mass-flow meter and a second solenoid valve into the burner. The uncertainty of the flow rate was estimated to be 5%. The burner is a stainless steel porous sphere with a diameter of 6.4 mm, which is placed at the center of a cylindrical chamber with a volume of 26 liters. A picture of the combustion rig is shown in Fig. 2.2.

The tests used in this research include ethylene (99.9% purity), oxygen, synthetic air consisting of 0.21 mole fraction oxygen balanced with nitrogen (99.999% purity) and diluted ethylene by volume in nitrogen. Ethylene was diluted with different amounts of nitrogen to enable studying of soot formation with a wide range of fuel concentrations.

Both the normal and inverse flames were investigated. For normal flames, the fuel was supplied from the burner and flowed into the chamber filled with the oxidizer gas. As to the inverse flames, the oxidizer was supplied from the burner with the fuel in the chamber. The flame was ignited immediately after the drop by a spring-loaded nichrome wire energized at 28 VDC. All

the flames in the test had ethylene consumption rate of 1.51 mg/s [11]. A schematic of the flow system in the combustion rig is depicted in Fig. 2.3.

Figure. 2.2. Schematic of the combustion rig used in the 2.2-s drop tower

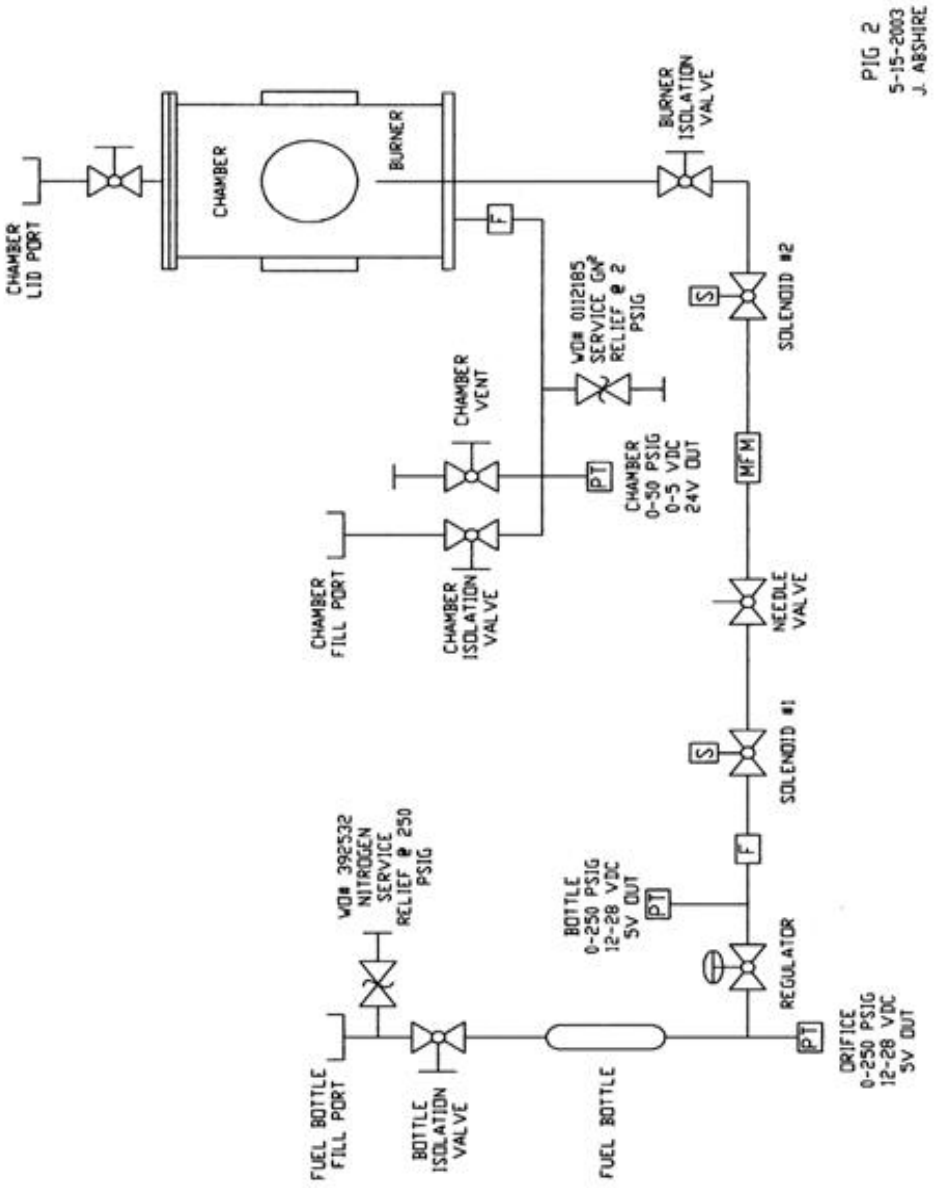

Figure. 2.3 Schematic of flow system used in the combustion rig

A color charge-coupled device (CCD) was used to record the image of the flames through the chamber window. The camera has a 16 mm fixed iris-lens with apertures (f 1.4-8). Flame diameters were measured using the peak blue emission in the videos [11, 12]. Fig. 2.4 presents snap shots of an inverse and a normal flame recorded from the experiments.

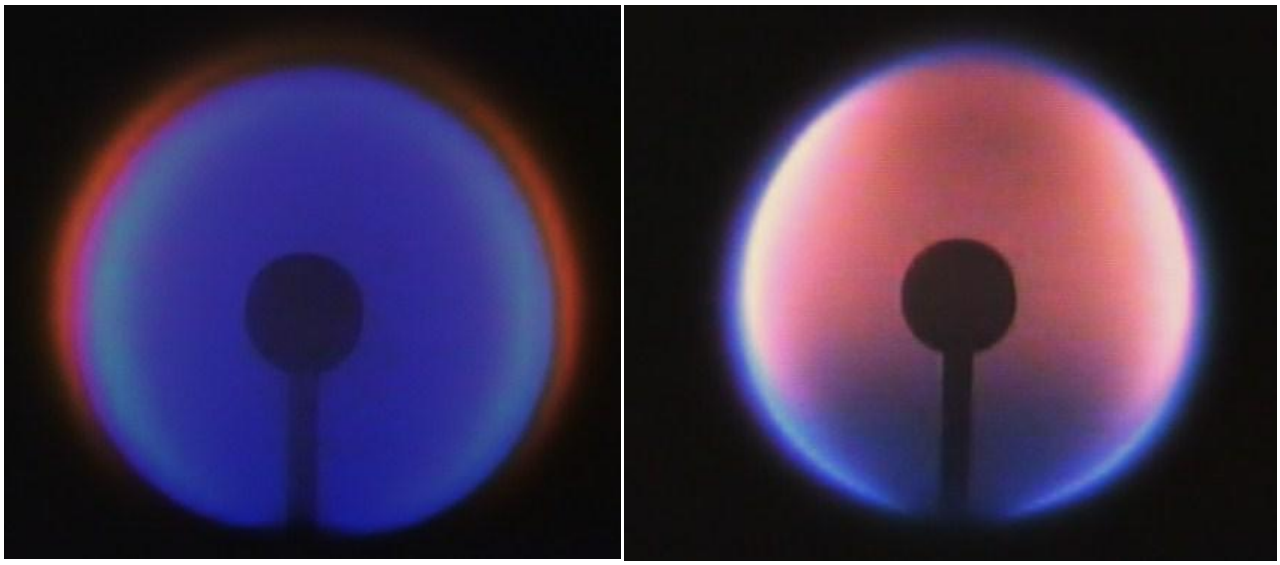

(a) (b)

Figure. 2.4. (a) Inverse flame 80% oxygen→ 11% ethylene and (b) Normal flame 18% ethylene→ 26% oxygen

The pictures show that both these flames produce soot and soot is formed on the fuel side of the flame. In addition, both of the flames are very close to spherical configuration, which suggests that the flow field and flame are spherically symmetric and can be modeled by a one-dimensional system as considered in this research.

Chapter 3

Numerical Modeling

This chapter begins with a brief literature review of previous works on spherical diffusion flames and is then followed by a discussion of governing equations and numerical methods that were used to model the flames. The chapter will be closed by the description of the structure of the numerical code used in this study.

3.1 Literature Review

As mentioned earlier, spherical flames stabilized by a porous burner are of particular interest in fundamental studies of diffusion flames due to their simplicity in geometry and existence of a steady-state solution. This configuration allows for variation of flow direction either from the fuel to the oxidizer (normal flames) or from the oxidizer to the fuel (inverse flames). In addition, mass flow rate and inert distribution can be controlled independently. These flexibilities cannot be achieved in droplet combustion. These features have enabled researchers to study the sooting and extinction behaviors of diffusion flames for both the transient and steady-state cases [13-28].

Radiative and kinetic extinctions of spherical diffusion flames were studied analytically by Mills and Matalonet [13, 14] and Wang and Chao [23] employing activation energy asymptotics and

optically-thin radiation model. They found that radiative heat loss renders extinction at high flow rates, which does not exist for adiabatic flames. They also determined critical radiation intensities beyond which steady burning is not possible. This phenomenon, named radiative extinction limit, was previously predicted by Chao et al. [15] for droplet combustion. Wang and Chao [23] further examined the effects of radiation intensity and residence time on the extinction of steady spherical diffusion flames. It was noticed that for flames with low/high radiation intensity, extinction is dominated by residence time/radiative heat loss rate.

Tse et al. [16] investigated the transient burner-generated spherical diffusion flames both experimentally and numerically using H_2/CH_4/inert mixtures issuing into atmospheric air. Their numerical work was performed using a code with detailed chemistry, transport and radiation models. They observed that steady-state behavior could not be reached within the 2.2 second microgravity duration for their experiments conducted in NASA's drop tower. The possibility of radiative extinction for diffusion flames was also confirmed by Atreya et al. [18-20].

Chernovsky et al. [21, 22] used NASA's 2.2-s drop tower to investigate the transient behavior of microgravity spherical ethylene diffusion flames. Their work included experimental measurements of flame growth, temperature and radiation intensity of the flames. The effect of diluents (N_2, CO_2 and He) on the flame structure was studied and the presence of CO_2 on the oxidizer side was found to decrease the flame temperature and soot formation. They also observed that the Lewis number of the oxidizer does not have a dominant effect on the flame growth.

Santa et al. [17] studied radiative extinction of transient microgravity spherical diffusion ethylene and propane flames numerically and experimentally, with both normal and inverse

configurations. Nitrogen was used as an inert gas to dilute either the fuel or oxidizer. Numerical simulation was performed using a code similar to that used by Tse et al. [16]. The results indicated that for transient flames, extinction time, peak temperatures and the fraction of the radiative loss compared to the heat generation were independent of flow rate except at very low flow rates. At low flow rates, extinction is cause by low residence time instead of radiation.

Liu et al. [24] theoretically investigated the soot inception of burner-generated spherical diffusion flames. A simplified three-step model with high activation energies was used to describe the combustion, soot formation and soot oxidation reactions. Four limiting configurations, namely the flame with fuel issuing into air, diluted-fuel issuing into oxygen, air flowing into fuel and oxygen flowing into diluted-fuel, were compared to determine the importance of hydrodynamics (flow direction) and flame structure (inert distribution) on soot inception. This analysis indicates that the sooting behavior corresponding to the variation of the mass-flow rate and the rate of the soot formation reaction is qualitatively similar. They also observed that flame structure has a profound impact on the soot inception while hydrodynamics only has secondary effect on the process. The results agree with the experiments of Sunderland et al. and Du and Axelbaum [25, 26].

Sunderland et al [25] conducted experiments in NASA's 2.2-s drop tower and studied the importance of hydrodynamics and flame structure using the four limiting flames as Liu et al. [24]. They observed that the effect of flame structure on the sooting behavior of diffusion flames is the dominant effect. These results were extended to identify the sooting limits of spherical diffusion flames [27] by considering 17 ethylene/oxygen flames with a wide variety of concentrations that reach their sooting limits at 2 second after the drop. Nitrogen was used as diluent to vary the structure of these flames. Results of this study show that sooting limits follow

a linear relation between adiabatic flame temperature and stoichiometric mixture fraction, Z_{st} , indicating that inception of soot precursors, requires the local C/O atom ratio and temperature to be above their threshold values. Mixture fraction is defined as follows:

$$Z = \frac{Y_F - \frac{1}{r_S} Y_{O_2} - Y_{F,ox} + \frac{1}{r_S} Y_{O_2,ox}}{Y_{F,f} - \frac{1}{r_S} Y_{O_2,f} - Y_{F,ox} + \frac{1}{r_S} Y_{O_2,ox}} \tag{3.1}$$

where, subscripts *ox* and *f* represent oxidizer and fuel side, respectively, r_S is the stoichiometric oxidizer to fuel mass ratio given by (based on a global reaction $F+\nu O_2 \rightarrow (\nu+1)\, P$):

$$r_S = \frac{\nu W_{O_2}}{W_F} \tag{3.2}$$

and *W* is the molecular weight. Z_{st} is the value of *Z* at the flame sheet. These threshold values of the local temperature and C/O atom ratio were later determined to be 1305 K and 0.53, respectively, for ethylene flames by Lecoustre et al. [28].

In this thesis, ten normal and inverse flames, which reach their soot free conditions within 1 and 2 seconds after the drop, were modeled numerically. These flames were originally yellow, but turn blue during the aforementioned time period. The soot free conditions were defined as the conditions at the time the flames become blue from the video images recorded from the experiments. The flames cover a broad range of adiabatic flame temperatures, stoichiometric mixture fraction, and scalar dissipation rate. Scalar dissipation rate is related to the mixture fraction, *Z*, and diffusion coefficient of the mixture, D, though:

$$\chi = 2D \left(\frac{\partial Z}{\partial r}\right)^2 \tag{3.3}$$

3.2 Governing Equations

The governing equations were reduced from the general equations presented in section 1.3 by considering the flow field and flame to be spherically symmetric. In a spherical coordinate system, the only variation of the variables, such as the flow velocity and temperature, is along the radial direction. Images recorded in the experiments showed that most of these flames are sufficiently spherical as illustrated in Fig. 2.4. Both the flow field and flame are laminar under the conditions specified in the experiments. Other assumptions adopted in the study include constant pressure and negligible body forces. Moreover, the gases are considered as ideal gases, and the absorption and emission of radiant energy in the burner is neglected. Applying these assumptions, the governing equations, Eqns. 1.1 – 1.4 are simplified to:

I. Conservation of mass:

$$\frac{\partial \rho}{\partial t} + \frac{1}{r^2}\frac{\partial}{\partial r}(\rho r^2 U_r) = 0 \tag{3.4}$$

II. Conservation of species:

$$\frac{\partial}{\partial t}(\rho Y_k) + \frac{1}{r^2}\frac{\partial}{\partial r}\left[\rho r^2 Y_k\left(U_r + U_{rd,k}\right)\right] = \dot{\omega}_k, \qquad k = 1, \ldots, KK \tag{3.5}$$

III. Conservation of momentum:

$$\rho\frac{\partial U_r}{\partial t} + \rho U_r\frac{1}{r^2}\frac{\partial}{\partial r}(r^2 U_r) = 0 \tag{3.6}$$

IV. Conservation of energy:

$$\frac{\partial}{\partial t}\left(\rho C_p T\right) + \frac{1}{r^2}\frac{\partial}{\partial r}\left(\rho r^2 C_p T U_r\right) =$$

$$-\frac{1}{r^2}\frac{\partial}{\partial r}\left(r^2 \vec{\mathrm{q}}_{\mathrm{r}} + \rho r^2 \sum_{\mathrm{k=1}}^{\mathrm{KK}} Y_k C_{p,k}\, \mathrm{T} U_{rd,k}\right) + \frac{1}{r^2}\frac{\partial}{\partial r}(r^2 \lambda \frac{\partial T}{\partial r}) - \sum_{\mathrm{k=1}}^{\mathrm{KK}} h_k^0 \dot{\omega}_k$$

(3.7)

V. Equation of State, which is Eq. 1.9.

Equations 3.4 through 3.7 can be rearranged and expressed in terms of the surface area at any radial distance from the center of the burner, $A(r) = 4\pi r^2$, and the mass flow rate, $\dot{m} = \rho A(r) U_r$. The mass flow rate is controllable during the experiments. Adopting these quantities, the above equations can be rearranged to:

i. Conservation of mass

$$A(r)\frac{\partial \rho}{\partial t} + \frac{\partial}{\partial r}(\dot{m}) = 0 \tag{3.8}$$

ii. Conservation of species

$$\rho A(r)\frac{\partial Y_k}{\partial t} + \dot{m}\frac{\partial Y_k}{\partial r} + \rho \frac{\partial}{\partial r}\left[A(r) Y_k U_{rd,k}\right] = A(r)\dot{\omega}_k, \qquad k = 1, \ldots, KK \tag{3.9}$$

iii. Conservation of energy

$$\rho A(r)\frac{\partial T}{\partial t} + \dot{m}\frac{\partial T}{\partial r} = -\frac{\partial}{\partial r}(A(r)\mathrm{q_r}) - \frac{\rho}{C_p}\frac{\partial}{\partial r}\left(\mathrm{A(r)}\sum_{\mathrm{k=1}}^{\mathrm{KK}} Y_k C_{p,k}\,\mathrm{T}U_{rd,k}\right)$$

$$+\frac{1}{C_p}\frac{\partial}{\partial r}(A(r)\lambda\frac{\partial T}{\partial r}) - \frac{A(r)}{C_p}\sum_{\mathrm{k=1}}^{\mathrm{KK}} h^0{}_k\dot{\omega}_k \qquad (3.10)$$

These equations are solved subject to the following user-specified boundary conditions:

- Initial radius: r_b = 0.3175 cm (radius of the burner)
- Outer radius is input by the user depending on the computational domain intended for the simulation
- Mass flow rate through the burner: $\dot{m}_b$
- Initial temperature of the reactant supplied from the burner: T_b= 300 K
- Temperature at the outer boundary (ambient temperature): T_∞ = 300 K.
- Pressure of the chamber: p = 0.98 bar.
- Mass flow rate of reactants at the burner exit and the concentration of species at the outer boundary are specified by the user.

3.3 Numerical Model

The code used to simulate the flames is a modified version of Sandia PREMIX code [29]. PREMIX was originally developed to solve one-dimensional burner-stabilized and freely-propagating laminar premixed flames. To run the code, use of Sandia's CHEMKIN package [30] is necessary. CHEMKIN allows for the use of various detailed chemistry mechanisms such that the rates of all reaction steps can be evaluated. The code also requires the Sandia's TRANSPORT package [31] for the evaluation of transport properties of the species. After the differential equations are discretized to difference equations, the matrix was inverted by the TWOPNT package [32], which employed a modified Newton algorithm to solve the variables iteratively.

Because of the steep gradient of temperature and species concentrations near the flame, a non-uniform mesh distribution was used to discretize the governing equations to ensure accuracy of the solution. The number of grids per length is gradually increased from the burner to the flame, and then decreased from the flame to the outer boundary. More mesh points are needed in the areas adjacent to the flame where the gradients are high to yield convergence and obtain accurate results. A coarse mesh grid near the outer boundary affects the results only minimally, but significantly reduces the computation time. The code allows a maximum number of 300 mesh points, but normally 200 points are sufficient for a domain of r_b = 0.3175 cm to r_∞ = 100 cm [9]. An initial guess of the flame location needs to be provided by the user. The code then uses these initial values to solve for the actual flame solution over the domain of computation.

The mesh generation can be done either by the code, which uses a pre-programmed mesh refinement procedure, or by the user. To increase the speed of computations, a set of smooth

uniform mesh grids generated by a tangent hyperbolic function was adopted as an input for the code. This mesh is then refined by the refinement procedure in the code during the simulation.

The code uses the first and second order finite difference algorithm to discretize the governing equations. The transient terms in the governing equations are discretized using an implicit Euler method [33]. The spatial derivative of continuity equation (3.9) is solved using a first order backward difference operator [9, 31, 33]. For the momentum, species and energy equations, the diffusion terms are discretized by a second order central difference formulation while the convection term can be discretized by either a first order upwind difference operator or a second order central difference operator. The central difference method is more accurate but is very sensitive to the boundary conditions. For problems with low mass flow rates, the central difference was used for the convection terms. When the mass flow rate is high, the upwind difference algorithm is more likely to obtain convergence and yield meaningful solutions. A more detailed description can be found in [31-33].

3.3.1 Structure of the Code

The structure of the code is presented by the use of Fig. 3.1. The figure shows the different components of the code and their relations.

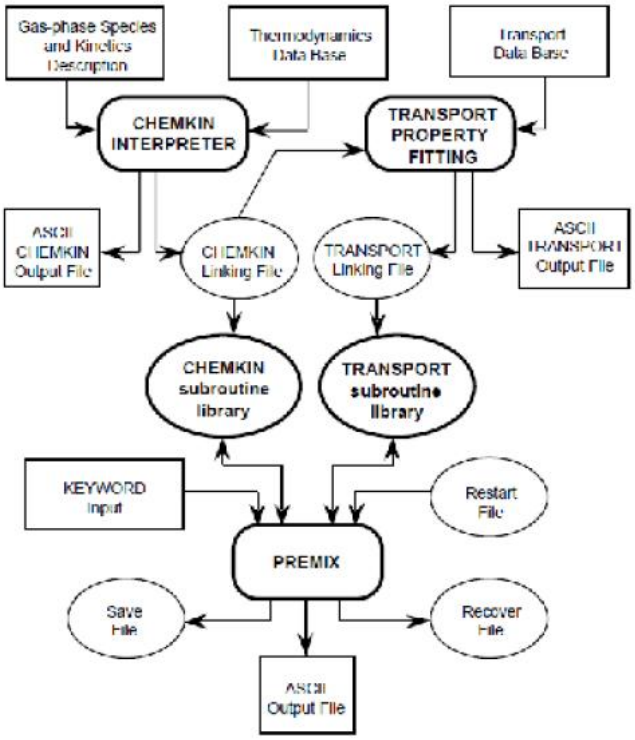

Figure. 3.1. Different components of the main code. Adapted from [16]

It can be seen that the code requires thermodynamics data and transport-properties databases in addition to the input from the user. To solve a problem using the code, the CHEMKIN and TRANSPORT preprocessors must be executed first. The operations of these sub-programs are introduced in the following sections.

3.3.1.1 Chemistry Model

The rates of all the reaction steps and the concentration of all the species are integrated to the code by the CHEMKIN subroutine. CHEMKIN uses a detailed and complex chemistry model to simulate the chemical reaction of combustion processes. Combustion reactions involve numerous

elementary reactions and intermediate species, and the exact reaction steps are still unknown. Various mechanisms have been developed based on kinetic theory and quantum mechanics. These models were then modified and validated by comparison with experimental results. GRI-Mech 3.0, ABF-Model and USC-Mech 2.0 are examples of commonly used chemical mechanisms. To illustrate the complexity of these models, the USC-Mech 2.0 mechanism [34] is listed in Appendix A, which contains 111 species and 784 reactions in its H_2/CO/C1-C4 kinetic model. This model was developed based on GRI-Mech 1.2 and 3.0, and is the most recent mechanism, and is the mechanism employed in the present study.

CHEMKIN assumes that the thermodynamic properties of gas species are functions of temperature only at the standard-state (1 atm and 298 K), and are expressed in terms of polynomials of temperature. As an example, the molar heat capacity of a species at constant pressure is given by [30].

$$\frac{C_{pk}^0}{R} = \sum_{n=1}^{N} a_{nk}\, T_k^{(n-1)} = \; a_{1k} + a_{2k}T_k + a_{3k}\, T_k^2 + a_{4k}\, T_k^3 + a_{5k}\, T_k^4 \tag{3.11}$$

The values of the coefficients are obtained by fitting of the actual values. Properties at standard-state are represented by the superscript 0. Other thermodynamics properties such as enthalpy and entropy can be obtained from integrating Eq. (3.11) as

$$\frac{H_k^0}{RT_k} = \; a_{1k} + \frac{a_{2k}}{2}T_k + \frac{a_{3k}}{3}\, T_k^2 + \frac{a_{4k}}{4}\, T_k^3 + \frac{a_{5k}}{5}\, T_k^4 \tag{3.12}$$

$$\frac{S_k^0}{R} = a_{1k} ln T_k + a_{2k} T_k + \frac{a_{3k}}{2} T_k^2 + \frac{a_{4k}}{3} T_k^3 + \frac{a_{5k}}{4} T_k^4 + a_{7k} \quad (3.13)$$

These values can be used in the calculation of reaction rates. Consider a general expression for elementary reactions involving KK species as shown in Eq. (1.5). Each of the forward and backward reactions has a reaction rate that can be expressed similar to that of Eq. (1.6). The pre-exponential factor A_i, the temperature exponent β_i, and the activation energy E_i are specified by the thermodynamics database. The rate constants of the reverse reaction can be easily determined using the equilibrium as shown in Eq. (1.6).

3.3.1.2 Transport Property Model

The next step in running the code is to execute TRANSPORT property program. Similar to CHEMKIN, this program needs input from a transport property data base. TRANSPORT computes the values of viscosities, thermal conductivities, and binary diffusion coefficients for individual species as functions of temperature using polynomial fits similar to that of Eq. (3.11). A brief description of this code is provided below. More detailed information about TRANSPORT can be found in [29, 31]. TRANSPORT computes the properties of each species and then the mixture-averaged properties.

The binary diffusion coefficients are given in the following form:

$$D_{jk} = \frac{3\sqrt{2\pi k_B^3 T^3 / m_{jk}}}{16\, P\pi\sigma_{jk}^2 \Omega^{(1,1)*}} \quad (3.14)$$

where m_{jk} is the reduced molecular mass for the (j,k) species pair, σ_{jk} is the reduced collision diameter and $\Omega^{(1,1)*}$ is the collision integral based on Stockmayer potentials.

$$m_{jk} = \frac{m_j m_k}{m_j + m_k} \tag{3.15}$$

The mixture-average diffusion coefficient for species k is calculated as

$$D_{km} = \frac{1 - Y_k}{\sum_{j \neq k}^{k} X_j / D_{jk}} \tag{3.16}$$

For mathematical expressions of σ_{jk} , η_k and λ_k refer to [30, 31]. In the Eqn. (3.16), X_j is the mole fraction of the jth species. With this value we can compute the ordinary diffusion velocity below. The thermal diffusion velocity formulation can be found in [30].

$$V_k = -D_{km} \frac{1}{X_k} \frac{\partial X_k}{\partial r} \tag{3.17}$$

while the mixture-averaged thermal conductivity can be determined from:

$$\lambda = \frac{1}{2}\left(\sum_{k=1}^{K} X_k \lambda_k + \frac{1}{\sum_{k=1}^{K} X_k / \lambda_k} \right) \tag{3.19}$$

After the execution of CHEMKIN and TRANSPORT, two linking files are generated, which will be used by CHEMKIN and TRANSPORT libraries. These libraries can be accessed by the code any time during the computation.

3.3.1.3 Input and Output Files

The flames to be modeled are defined by the user in the input file using a Keyword format [29]. This input file contains the problem specifications such as mass flow rate, reactant composition and convection direction, approximate flame temperature and location, boundary conditions, steady-state or transient, etc. Approximate flame temperature is prescribed through the procedure described earlier to initialize the chemical and transport properties. Results of a successful simulation, which is stored in the Save and Output files, can be used as the input for a subsequent simulation. In this approach, the saved file is read as Restart to initialize the iterations.

The output of a converged computation is stored in a few files:

- FlameEvolution.out reports the properties at the flame, such as flame radius, flame temperature, stoichiometric mixture fraction and C/O ratio, etc.
- Sphdif.out includes the iterations, intermediate and elementary species distribution over the entire mesh grid, etc. This is the most comprehensive output of the code.
- The other output files are in ".tec" format which are accessed through Tecplot software to visualize and post-process the data.

3.3.2 Radiation model

The radiation model consists of two models: radiation property model and radiative transfer model. In radiation property model, the emission and absorption properties of the radiative species CO_2, H_2O and CO are calculated. These properties are calculated by a statistical narrow-band model in which the spectrum is divided into numerous spectral bands with a bandwidth of 25 cm^{-1}. The emissivities were extracted from the line-by-line values given by the HITRAN database [35] and the average radiation properties are calculated for each of the narrow bands. To account for the angular variation of the radiation intensity, the discrete ordinates method was employed, with a discrete representation that included 20 different directions. The rate of radiative heat transfer was then evaluated by integrating over all directions using Gaussian quadrature. The radiative transfer equation (RTE) is then solved in the radiative transfer model using the calculated properties as the input data. More detailed information about the radiation model can be found in [9, 36].

Chapter 4

Results and Discussion

In this chapter, definition and formation of soot will be discussed first. It will be followed by an analysis of the numerical and experimental results to determine the soot-free limits of ethylene spherical diffusion flames from the flames that were observed to turn blue (soot-free) between 1 and 2 seconds after the drop in the experiments.

4.1 Background

Combustion of hydrocarbons often results in formation of particulate carbon, or soot particles. Soot is a major pollutant produced from industrial furnaces, burners, engines and open fires. Formation of soot reduces the conversion from chemical energy to thermal energy and renders a higher amount of fuel consumption for a certain energy demand. Soot emits the yellowish or orange luminescence observed in most flames and is a main source of radiative heat loss from flames, which leads to additional decrease in thermal efficiency. Emission of soot into the atmosphere accelerates the greenhouse effect. Moreover, airborne particles of soot are known to be carcinogenic [6, 37]. Recognizing the negative impacts of soot particles, extensive research has been conducted to understand the soot formation processes from combustion devices and explore methods to reduce it [37-51].

In diffusion flames, soot is formed on the fuel rich side of the flame and it does not have a unique chemical composition. It consists of chain-like highly condensed polycyclic aromatic hydrocarbons (PAHs) that are nearly spherical [6]. A schematic of soot formation processes is presented in Fig. 4.1.

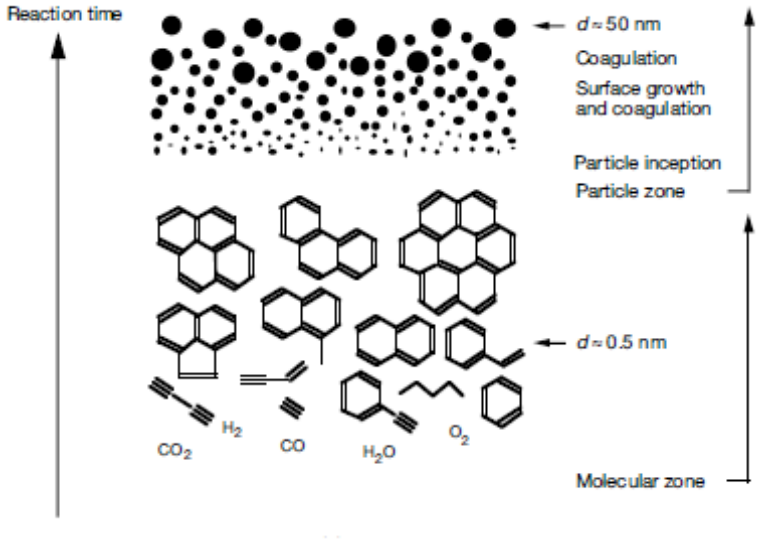

Figure 4.1. Soot formation process. From [45]

As it can be inferred from Fig. 4.1 mechanisms responsible for formation of soot are particle inception, surface growth and coagulation. It is generally believed that particle inception is initiated by the formation and coalescence of PAHs that are considered as soot precursors. These particles then grow by surface growth reactions from addition of gaseous species such as acetylene [6, 47]. Formation of soot can be reduced by suppressing the production of PAHs. To understand and control the soot formation process, it is necessary to understand the formation of PAHs. The mechanism responsible for the formation of the first aromatic ring, benzene, is presented in the following reactions (4.1 through 4.13) [6]:

$$C_2H_2 + CH_2 \rightarrow C_3H_3 + H \quad (4.1)$$

$$C_2H_2 + H \rightarrow C_2H_3 \quad (4.2)$$

$$C_3H_3 + CH_2 \rightarrow C_4H_4 + H \quad (4.3)$$

$$C_3H_3 + C_3H_3 \rightarrow C_6H_5 + H \quad (4.4)$$

$$C_2H_3 + C_2H_2 \rightarrow C_4H_4 + H \quad (4.5)$$

$$C_2H_3 + C_2H_4 \rightarrow C_4H_6 + H \quad (4.6)$$

$$C_4H_4 + H \rightarrow C_4H_3 + H_2 \quad (4.7)$$

$$C_4H_4 + OH \rightarrow C_4H_3 + H_2O \quad (4.8)$$

$$C_4H_6 + H \rightarrow C_4H_5 + H_2 \quad (4.9)$$

$$C_4H_6 + OH \rightarrow C_4H5 + H_2O \quad (4.10)$$

$$C_4H_3 + C_2H_2 \rightarrow C_6H_5 \quad (4.11)$$

$$C_4H_5 + C_2H_2 \rightarrow C_6H_6 + H \quad (4.12)$$

$$C_6H_5 + H \rightarrow C_6H_6 \quad (4.13)$$

As shown in these reactions, the presence of acetylene is crucial in the formation of benzene. Another critical intermediate species responsible for the formation of soot is propargyl (C_3H_3) [42-45, 48, 49]. Skeen et al. [49] has shown that the reaction of C_3H_3 to C_6H_5 as expressed in Eq.

4.4 contributes to more than 70% of phenyl production. In addition, H radical is necessary for the activation and deactivation of the radicals that form the first ring.

In general, soot formation occurs in a fuel rich region in which there is sufficient supply of carbon and shortage of oxygen to oxidize the PAHs. It also requires a high temperature to activate the reaction because of the high activation energy. Previous studies report that the minimum temperature required for the soot formation is between 1250-1650 K [41]. The carbon to oxygen atom ratio, C/O ratio, and temperature are then used to identify the tendency to form soot. As mentioned in Chapter 3, there have been numerous studies to identify the critical C/O ratio and temperature required for soot formation but resulted in different values for premixed and non-premixed flames [37]. These studies indicate that soot inception and growth are proportional to acetylene concentration [6, 37-51].

Another mechanism that should be taken into account is the oxidation of benzene which eliminates PAHs and therefore soot particles. It is generally accepted that the oxidation of the first aromatic ring follows the reaction pathway presented in reactions 4.14 through 4.27. Both the soot formation and oxidation mechanisms must be considered in the study of the sooting behavior of hydrocarbon flames.

$$C_6H_6 + H \rightarrow C_6H_5 + H_2 \quad (4.14)$$

$$C_6H_6 + OH \rightarrow C_6H_5 + H_2O \quad (4.15)$$

$$C_6H_6 + O \rightarrow C_6H_5O + H \quad (4.16)$$

$$C_6H_5 + O_2 \rightarrow C_6H_5O + O \quad (4.17)$$

$C_6H_5 + O_2 \rightarrow C_6H_4O_2 + H$ (4.18)

$C_6H_5O \rightarrow C_5H_5 + CO$ 4.19)

$C_5H_5 + H \rightarrow C_5H_6$ (4.20)

$C_5H_5 + O \rightarrow C_5H_4O + H$ (4.21)

$C_5H_5 + HO_2 \rightarrow C_5H_5O + OH$ (4.22)

$C_5H_5 + OH \rightarrow C_5H_4OH + H$ (4.23)

$C_5H_5O \rightarrow C_5H_4O + H$ (4.24)

$C_5H_4OH \rightarrow C_5H_4O + H$ (4.25)

$C_6H_4O_2 \rightarrow C_5H_4O + CO$ (4.26)

$C_5H_4O \rightarrow C_4H_4 + CO$ (4.27)

4.2 Identification of sooting-limit flames

The main objective of this study is to identify the soot free limit of spherical diffusion flames. Following the same approach as previous studies [40-42], ethylene/oxygen/nitrogen flames with different inert additions (flame structures) and convection directions were chosen. As discussed earlier [28, 42], flame structure has profound effect on the sooting behavior of these flames while the influence convection direction is secondary. In this work, reactant compositions were varied to explore the sooting behavior that corresponding to the given conditions. Convection direction also is changed to verify the previous findings.

For a particular convection direction, different tests were conducted with a wide range of oxidizer and fuel concentrations to study the flame structure in a comprehensive manner. Both the normal (ethylene issuing into oxygen) and inverse (oxygen flowing into ethylene) flames were considered. Reactant concentrations and mass flow rates were adjusted such that a constant ethylene consumption rate of 1.51 mg/s was maintained for all these flames. Specifications of the flames selected in this study are shown in Table 4.1.

Table 4.1. Specifications of the flames used for this study

Flame	Environment	$X_{C2H4,f}$	$X_{O2,ox}$	Z_{st}	$\dot{m}$ (mg/s)	$T_{ad}(K)$	$\chi_{st}(S^{-1})$	r^*	$r_{meas}(cm)$	$r_{pred}(cm)$	r_{pred}/r_{meas}	t(s)
(1)	Fuel	17	30	0.3241	15.74	2330	0.3323	0.1	1.517	1.441	0.95	2.0
(2)	Oxidizer	17	27	0.3296	8.87	2258	0.2573	0.09	1.505	1.528	1.01	1.7
(3)	Oxidizer	12	39	0.4971	12.58	2321	0.2258	0.12	1.205	1.651	1.37	1.77
(4)	Oxidizer	12	39	0.4978	12.58	2321	0.2284	0.11	1.384	1.665	1.20	1.87
(5)	Fuel	11	80	0.6568	6.31	2530	0.2147	0.04	1.451	1.441	0.99	1.9
(6)	Oxidizer	10	50	0.5931	15.1	2323	0.6272	0.10	1.108	1.307	1.18	1.9
(7)	Oxidizer	18	26	0.3092	8.38	2251	0.2495	0.04	1.3864	1.506	1.09	1.5
(8)	Fuel	8.51	85	0.7255	5.95	2370	0.1309	0.06	1.8408	1.638	0.89	1.83
(9)	Oxidizer	12	35	0.471	12.57	2263	0.4029	0.09	1.3582	1.463	1.08	1.87
(10)	Oxidizer	12	50	0.5558	12.57	2433	0.2911	0.11	1.18	1.452	1.23	1.8
(11)	Fuel	8.14	100	0.7544	5.06	2370	0.3983	0.10	1.44	1.188	0.82	1.27
(12)	Fuel	12	100	0.6866	5.08	2628	0.2189	0.04	1.627	1.307	0.80	2.0
(13)	Fuel	15	30	0.3527	15.74	2279	0.4581	0.09	1.521	1.379	0.91	1.2
(14)	Oxidizer	12	40	0.5013	12.58	2333	0.4977	0.11	1.232	1.359	1.10	1.8
(15)	Oxidizer	18	27	0.3167	8.38	2279	0.2225	0.06	1.545	1.563	1.01	1.93

It was noticed that decreasing the oxygen concentration for flames with a specified fuel concentrations reduces soot formation. Continuous decrease of oxygen concentration yields the flame to be soot free as is evident by the blue color of the flame. This behavior is understood because higher oxygen content results in a higher flame temperature, which favors the high-activation-energy soot formation reactions. The transition from sooty to soot-free flames by decreasing the amount of oxygen is demonstrated in Fig. 4.2. As shown in the figure, Flame (a) and (b) are sooty until the end of the 2.2-s drop tower test, Flame (c) turns blue and stops generating soot before the drop termination, while Flame (d) also reaches its soot-free conditions before the end of the test.

As mentioned earlier, soot formation is strongly affected by the C/O atom ratio. To understand this effect, tests were performed by varying the fuel content while keeping the oxygen concentration fixed. Representative results are shown in Fig. 4.3, which exhibits that flame transition from sooty to soot free as ethylene concentration is decreased. The reason is that when more fuel is provided, the carbon concentration in the fuel rich region is higher, and the formation of PAHs is increased.

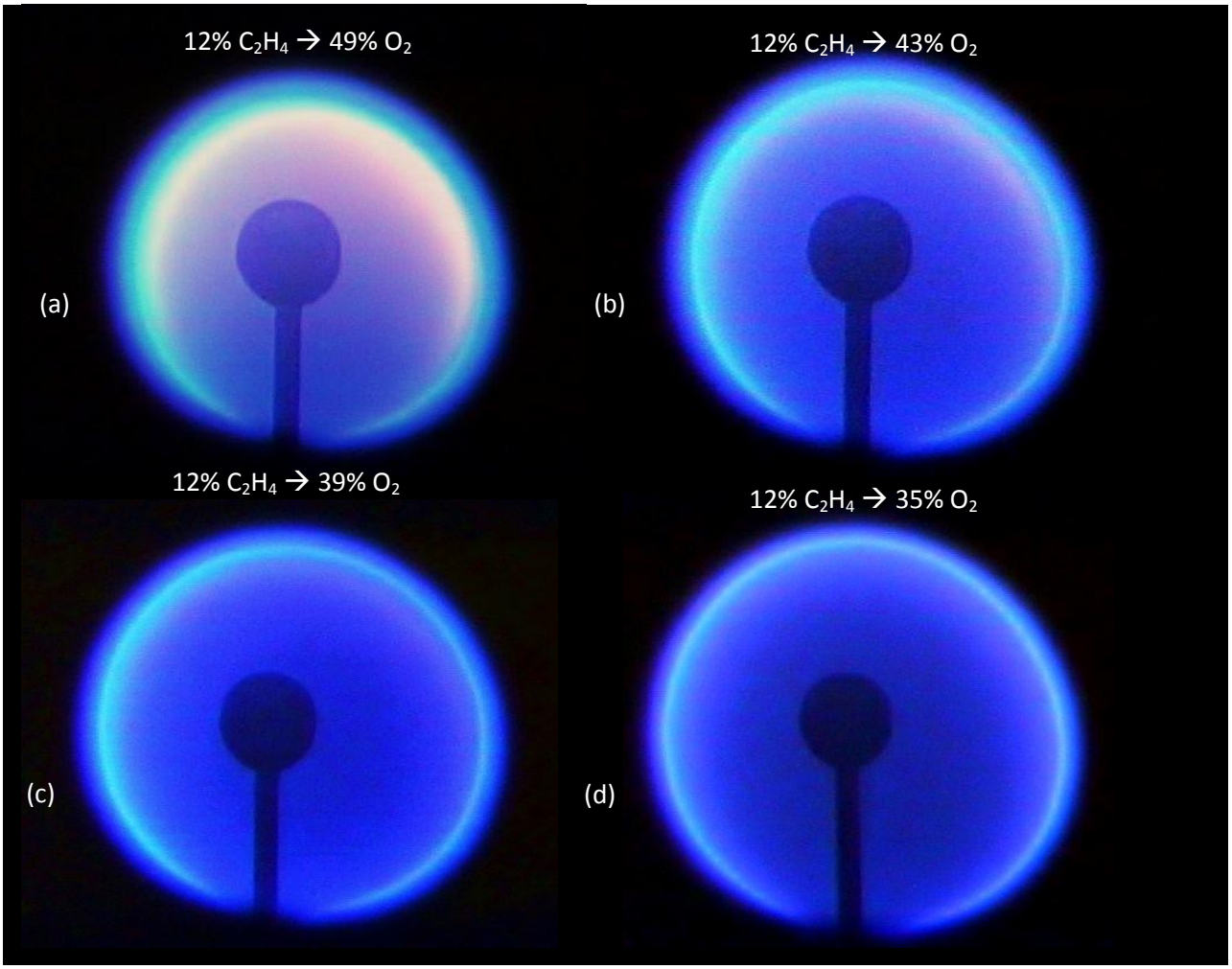

Figure 4.2. Transition from sooty to soot-free condition for 4 different flames with the same fuel concentration and different oxygen concentrations: (a) 12% C_2H_4→49%O_2 at 2.0s, (b) 12% C_2H_4→43%O_2 at 2.0s, (c) (sooting limit) 12% C_2H_4→39%O_2 at 1.9s(d) 12% C_2H_4→35%O_2 at 1.86s

It can be seen in Fig. 4.3 that Flame (a) still has soot at the end of the test, but Flames (b) and (c) are soot free before 2 seconds Flame (b) represents the concentration of fuel below which soot free conditions are achieved for the specified oxygen concentration (30% for this case). The flames presented in this figure are inverse flame and soot is formed outside of the flame if it exists.

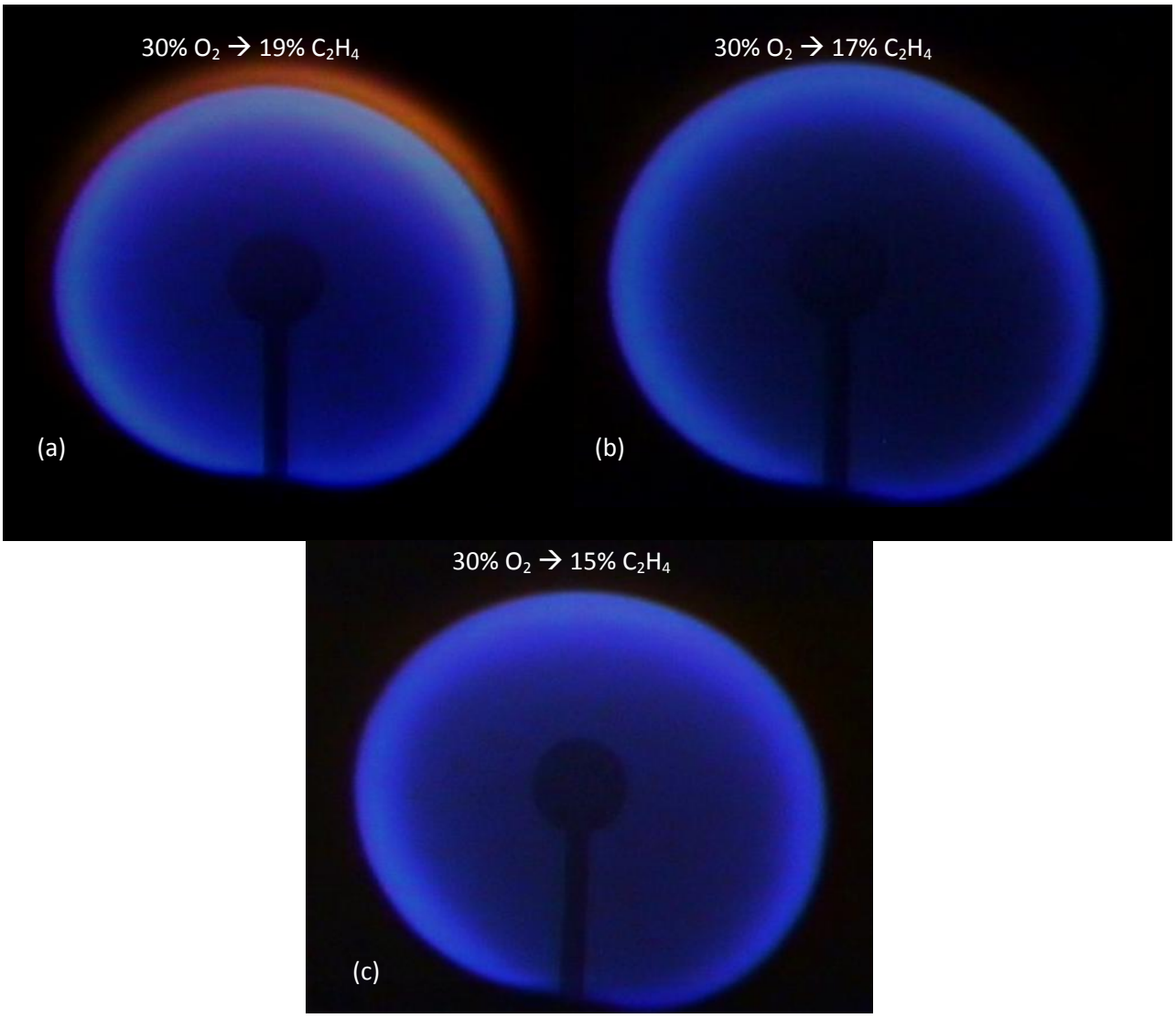

Figure 4.3. Effect of fuel concentration on sooting behavior of flames with the same amount of oxygen. (a) 30% O_2 → 19% C_2H_4 at 2.0s (b) 30% O_2 → 17% C_2H_4 at 2.0s (c) 30% O_2 → 15% C_2H_4 at 1.2s

Based on the observations from Figs.4.2 and 4.3, sooting limit is defined as the conditions under which the flame is transitioned from sooty to soot free conditions. Flame (c) in Fig. 4.2 and Flame (b) in Fig. 4.3 are the sooting limit flames according to this definition.

Following this approach, seven sooting limit flames that reached soot free conditions between 1.0s and 2.0s in the test were identified and the time these flames became soot-free were

recorded. Some soot-free flames (but not the sooting limit flames) that turned blue between 1.0s and 2.0s were also considered to broaden the range of compositions in the analysis. These flames are listed in Table 4.1. In the Table, Flames (1)-(7) are sooting limit and flames (8)-(15) are soot-free flames. These flames were simulated using the computer code described in Chapter 3. Because the flames were considered to be spherically symmetric in the simulations, comparison between the numerical and experimental results is meaningful only for flames that are sufficiently spherical in the experiments.

The sphericity of the flames tested in the experiments was determined using the images recorded during the experiments by measuring their radii at the time they become soot free. For each flame, the flame radii were measured in 8 evenly distributed directions and their mean is taken as the flame radius. The standard deviation of these values divided by their mean, expressed as r^* in Table 4.1, was used to indicate the sphericity of the flames. Flames with r^* exceeded 0.11 were excluded in our analyses. This method was adopted from [28].

Before the numerical results can be adopted for analysis, they should be validated by experimental results. However, due to the sensitivity of microgravity flames to disturbances, thermocouples were not used and temperatures cannot be measured in the experiments. Only the evolution and the color of the flames were recorded in the videos. The flames that passed the sphericity test were numerically modeled and their predicted radii were compared with those of experiments. The agreement between the predicted and measured radii was taken into account. Flames having a difference of more than 20% between these radii were also excluded from the analysis. Because of the uncertainties in microgravity experiments, some of the experimental results are not reliable. As an evidence, Flames (3) and (4) are repeated tests performed at different dates, but the results are quite different. Based on these criteria, Flames (3) and (10)

were eliminated. It should be mentioned that while the radii of the flames were measured as the outer edge of the blue-colored surface from the videos, the radii corresponding to the peak temperature are considered as flame radii in the numerical results

4.3 Numerical Modeling:

In the modeling approach, efforts have been attempted to minimize the numerical errors. There are two factors that need to be considered to ensure accuracy of the numerical results: domain size and initial conditions.

4.3.1 Initial Conditions

Initial conditions are defined by the user and represent the ignition conditions. For transient flames such as those studied in this research, the convergence and accuracy of the solution are very sensitive to initial conditions. The approach of Tse et al. [43] and Santa et al. [40] for the specification of the initial conditions was adopted. In this approach, the initial condition was taken as the steady-state solution of the same flame in a compressed domain, which was generated by forcing the outer boundary to be sufficiently close to the burner. This method yields a localized thin flame, which simulates the ignition source that was employed in the experiments. In the experiments, the flames were ignited by passing electric current into a Nichrome resistance wire to energize it. The wire was subsequently ruptured and retrieved. It should be noted that radiative heat loss was neglected in this preparation step because the ignition occurs in a very short period of time.

Santa et al. [40] studied different sizes of the compressed domain and chose the minimum domain for which a steady state solution exists. Lecoustre et al. [28], however, chose a compressed domain with the outer boundary located at 1.2 cm from the center of the burner to determine the initial condition. In this research, both of these approaches were considered. After the steady state solution was found for either case, it was used as the initial condition for the transient computation with the domain size of 20 cm (the selection of this domain size will be explained in Sec. 4.3.2.). All the results presented in this thesis were obtained from transient simulations in a 20 cm domain.

To understand the effect of the size of compressed domain, the temporal evolution of flame temperature, flame radius, stoichiometric mixture fraction and C/O atom ratio for Flame (1), which is an inverse flame, are shown in Fig. 4.4, with the size of compressed domain set as (a) 0.5 cm (minimum domain for this flame) and (b) 1.2 cm, respectively. It is observed that the profiles for the C/O atom ratio and the stoichiometric mixture fraction are the same for both of the cases. The flame radii are initially different, but approach each other soon after the flame is established, and become identical after 1 s. The flame temperature obtained from these approaches is approximately 15 K apart after 1 s, which is negligible. This allows us to use either method since all of the flames studied reach their soot-free conditions after 1 s.

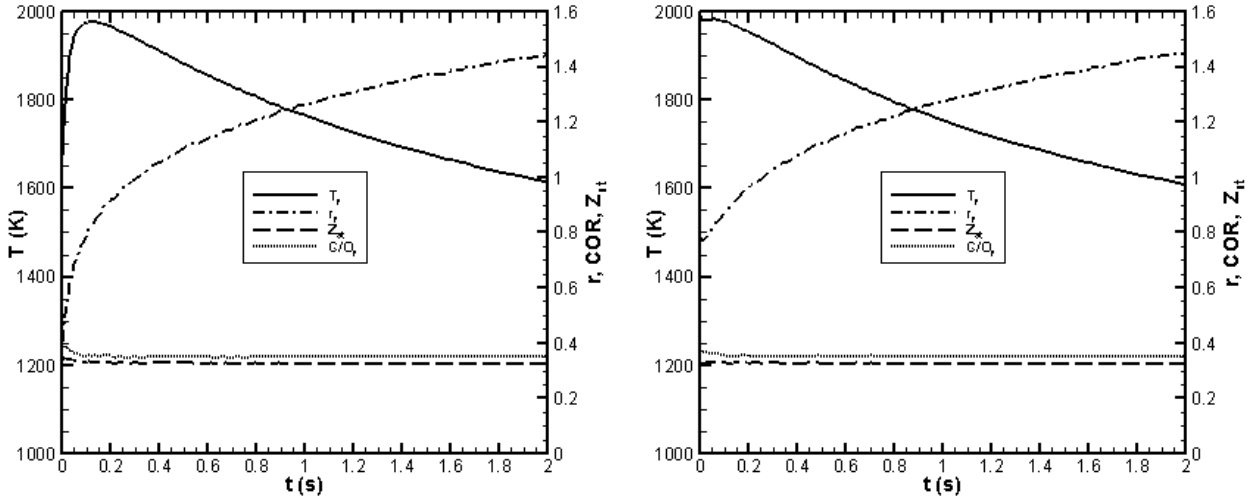

Figure 4.4. Temporal evolution of flame (1) with initial conditions of (a) 0.5 cm, minimum compressed domain, and (b) 1.2 cm compressed domain

The above analysis can be further strengthened by experiments, which showed that Flame (1) turns blue at 2.0 s. The distribution of temperature, C/O atom ratio and stoichiometric mixture fraction at 2 s are then plotted in Fig. 4.5 for the two cases and the results shows that these profiles are identical. Moreover, the molar fractions of some major species at 2 s are plotted in Fig. 4.6 versus the C/O atom ratio, which further confirms that these results are identical.

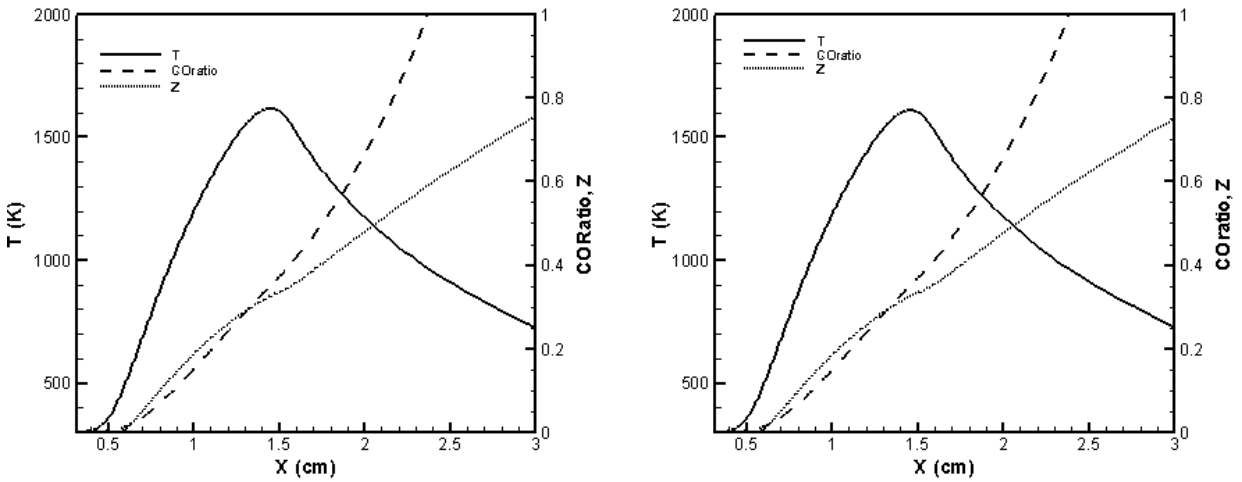

Figure 4.5. Temperature, C/O atom ratio and Z profiles for flame (1) at 2.0 seconds for using (a) 0.5 cm and (b) 1.2 cm as the squeezed domain

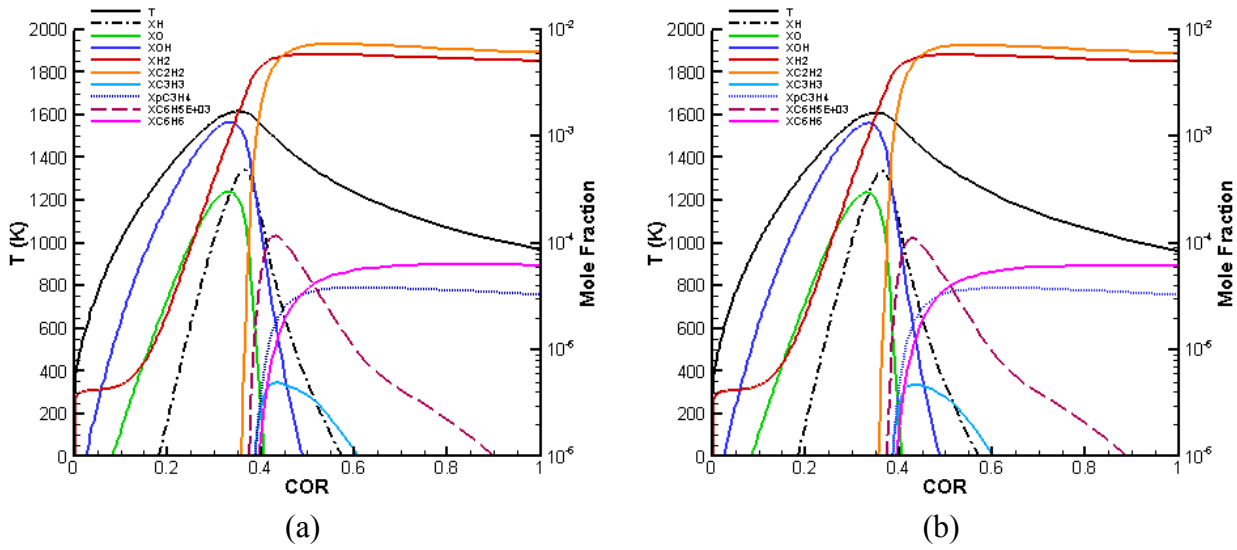

Figure 4.6. Mole fraction of some species for cases (a) and (b) for flame (1) at 2.0 seconds

To ensure that the above observations are independent of the flow direction, similar computations were also performed for Flame (7), which is a normal flame. As for Flame (1), the temporal evolution of temperature, C/O atom ratio, radius and stoichiometric mixture fraction are shown in Fig. 4.7, and distribution of temperature, C/O atom ratio and stoichiometric mixture fraction at 1.5 s are presented in Fig. 4.8, for both compressed domains. Differences between Flames (1) and (7) are that the minimum domain is at 0.55 cm, and the flame reaches its soot free condition at 1.5 s for Flame (7). In consistent with Flame (1), these plots reveal that the results obtained using these initial conditions are identical after 1 s. Because part of the objectives is to compare the results with those of Lecoustre et al. [28], the compressed domain used by Ref. [28] was adopted in this study.

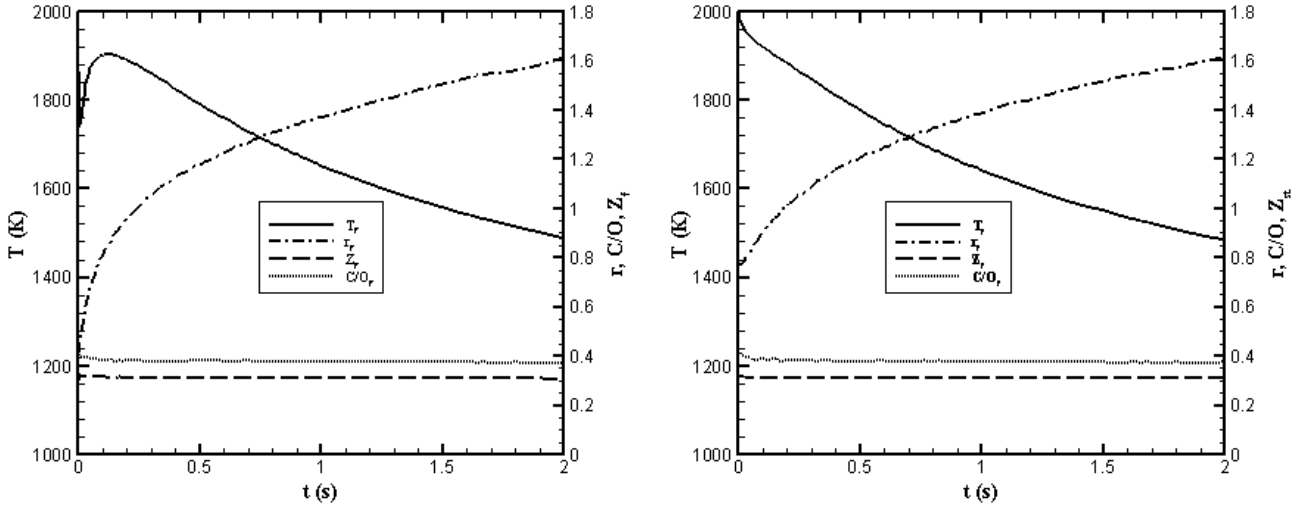

Figure 4.7. Temporal changes in temperature, radius, C/O atom ratio and Z_{st} of flame (7) for a domain size of 20 cm transient solution using initial condition of (a) compressed domain at 0.55 cm and (b) compressed domain at 1.2 cm.

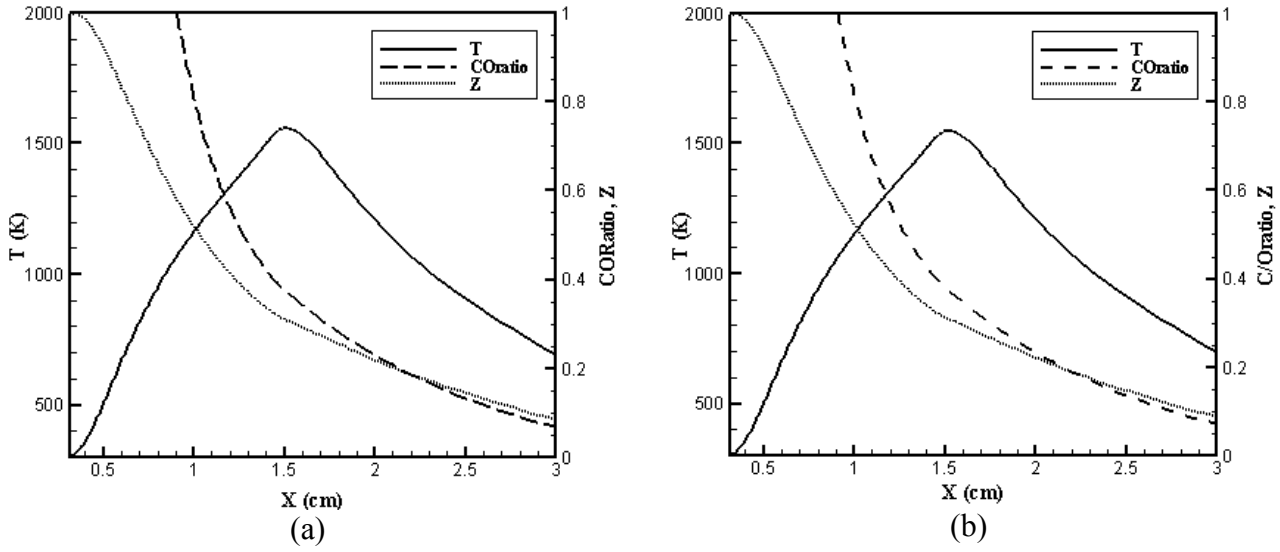

Figure 4.8. Results of transient solution for flame (7) at 1.5s using (a) 0.55 cm compressed domain and (b) 1.2 cm compressed domain

4.3.2 Computational Domain Size

To ensure that the domain size is sufficiently large such that the solution is independent of the selection size, the effect of computation domain size is examined. Lecoustre et al. [28] investigated some sooting limit flames that reach their soot free conditions at 2 s using the same code and claimed that an outer boundary at 20 cm is sufficient while Santa et al. [43] used a domain size of 100 cm. Considerable reduction of the computation times can be achieved if a smaller domain can be adopted. Appropriate domain size can be examined by comparing solutions obtained using these two domain sizes.

The solutions for Flames (1) and (7), similar to those presented in Figs. 4.3, 4.4, 4.6 and 4.7, are plotted in Figs. 4.9 – 4.12 for two domain sizes, 20 cm and 100 cm. In these figures, the initial conditions were generated using a compressed domain of 1.2 cm. These plots reveal that the results are identical, meaning that a domain size of 20 cm is sufficient for this research and the solution is independent of the domain size when it is greater than 20 cm. Observation of the

results reveals that at 2 s after the ignition, the flame region has not reached the outer boundary. As such, 20 cm is sufficient for the domain to be considered infinitely large. The domain of computations for other flames listed in Table 4.1 is then selected to be 20 cm. The structure and time evolution of all the 13 flames are plotted in Appendix B.

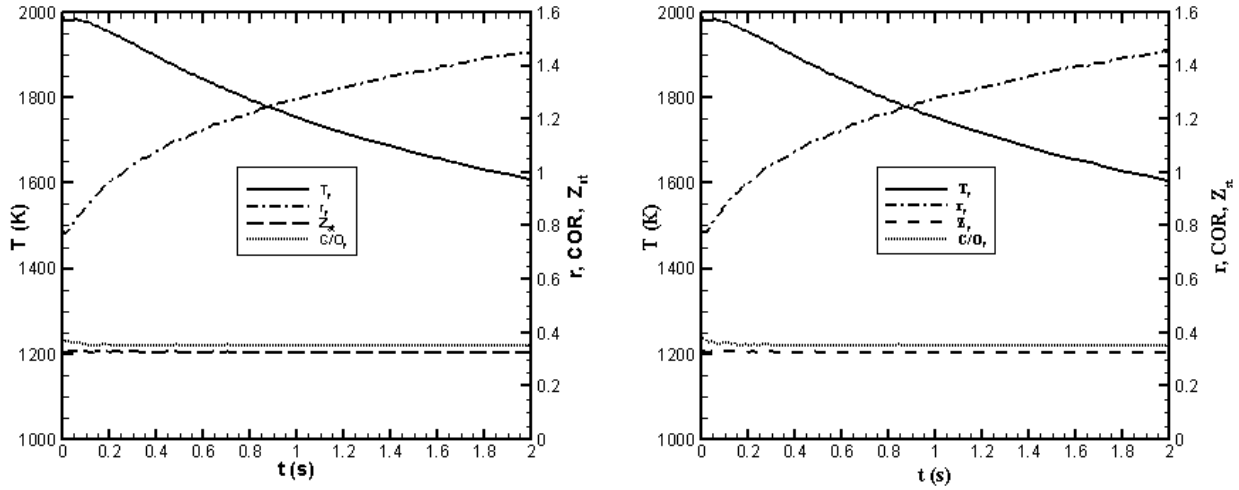

(a) (b)

Figure 4.9. Flame temperature, C/O and Z profiles of flame (1) during the test with the outer boundary at (a) 20cm and (b) 100cm

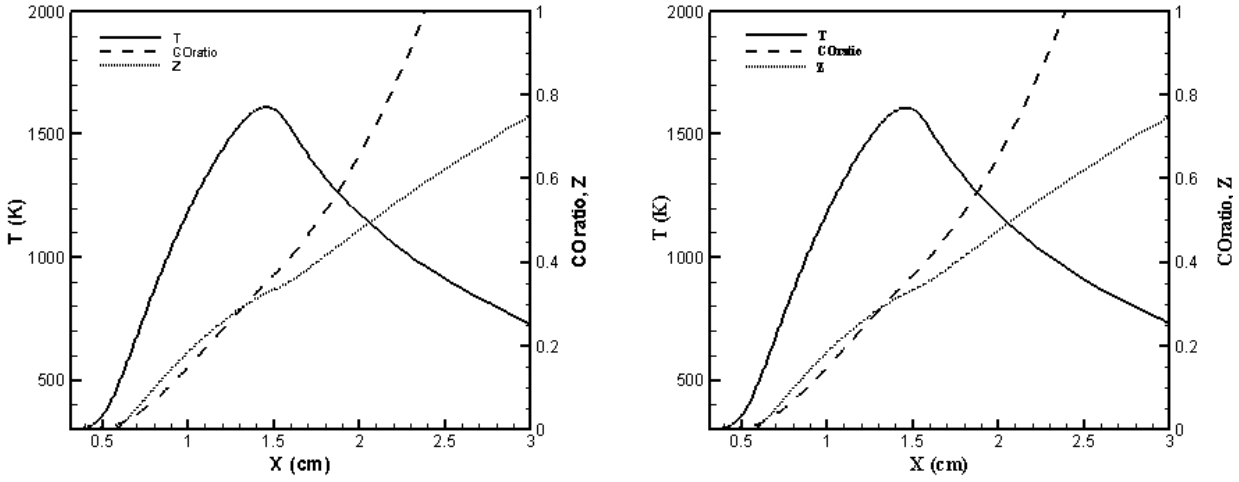

(b)

Figure 4.10. Temperature, C/O and Z profiles of flame (1) at 2.0s with the outer boundary at (a) 20cm and (b) 100cm

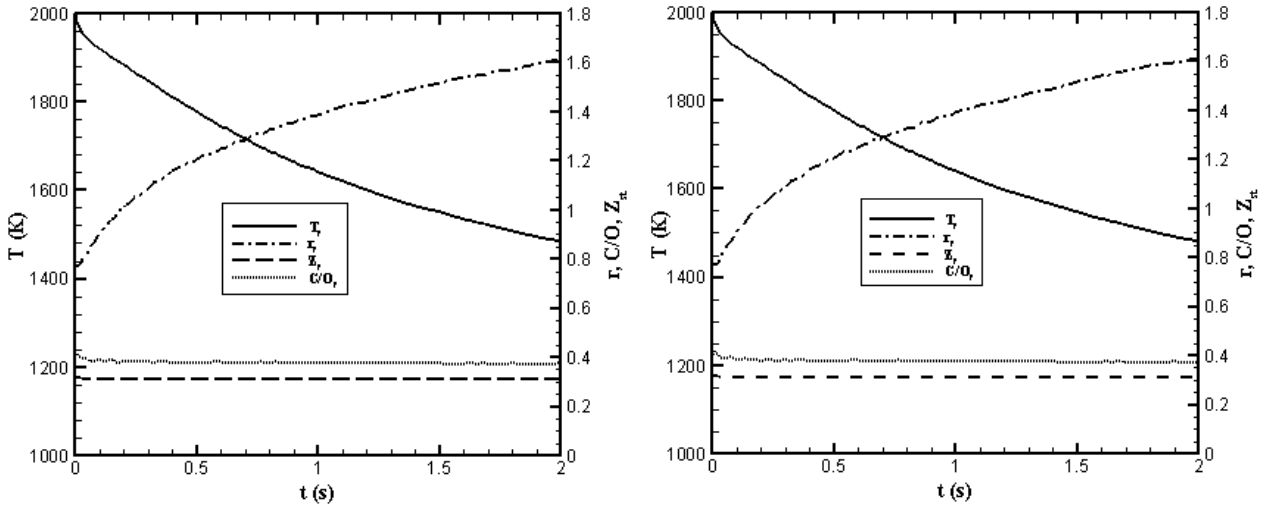

Figure 4.11. Temporal changes in temperature, radius, C/O atom ratio and Z_{st} of flame (7) using a computational domain size of (a) 20cm and (b) 100cm.

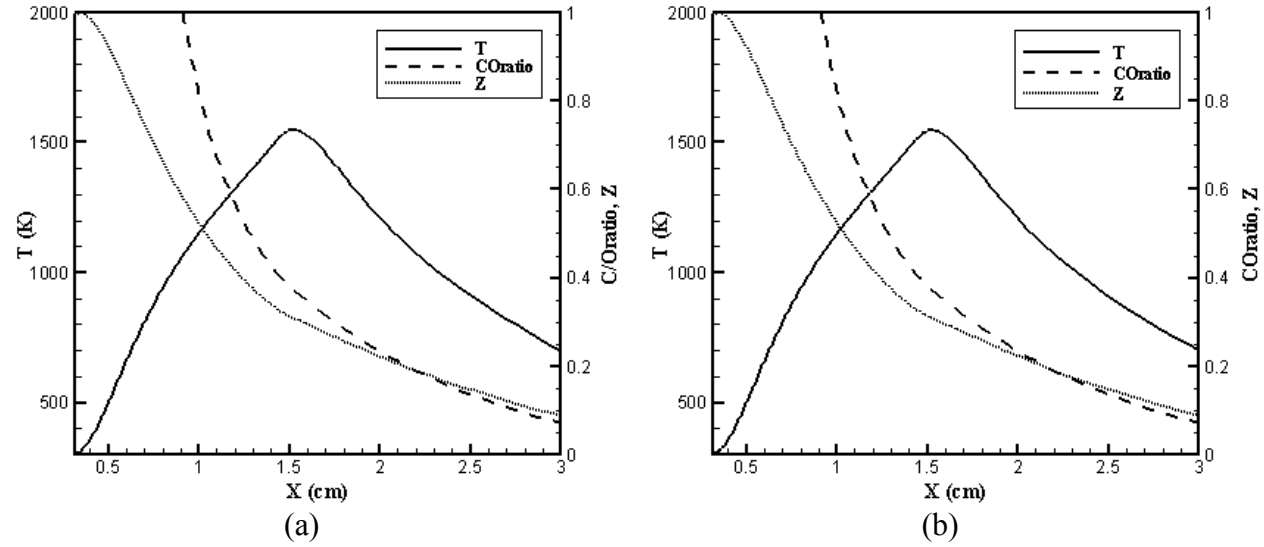

Figure 4.12. Temperature, C/O atom ratio and Z_{st} of flame (7) at its sooting limit using a computational domain size of (a) 20cm and (b) 100cm.

4.4 Identification of the critical C/O atom ratio and temperature

In previous sections, the selection of the boundary conditions and computational domain employed in the study was discussed. Applying those conditions, numerical simulations of the flames listed in Table 4.1 were performed and results were analyzed to determine the critical C/O atom ratio and temperature for these flames at their soot-free conditions. The analysis of numerical results follows that of Lecoustre et al. [28]. It was mentioned in Section 4.1 that previous studies have concluded that soot formation in diffusion flames occurs in a region where both the temperature and C/O atom ratio exceed their respective critical values [28, 43, 44]. According to this concept, formation of soot from diffusion flames may be suppressed by controlling the flame structure such that in regions where the temperature exceeds its critical value, the C/O atom ratio is below its critical value and vise versa. At the moment the flames turn soot free (blue), i.e., reach their soot free limit, these two critical conditions are located at the same radius in space. If the theory is valid, the critical values should be the same for all the flames for a given fuel (e.g., ethylene). The critical values are determined using the following statistical approach.

After the completion of the numerical computations, the temperature and C/O atom ratio distributions at the time the flames reach their respective soot free limits were recorded. For each of the flames, the values of C/O atom ratio corresponding to the temperatures on the fuel side were determined. Next, the average C/O atom ratio, C/O_{mean}, and the standard deviation for all the flames at each specified temperature were computed. The values of C/O_{mean} and the relative standard deviation, C/O*, defined as the standard deviation divided by C/O_{mean}, were plotted

against the temperature as shown in Fig. 4.13. As discussed in the previous paragraph, all the flames should reach the same critical values at their soot free limit if the concept is valid. That is, there should be a temperature at which C/O* = 0. However, because of the uncertainties in microgravity experiments, it is not expected that all the flames reach their soot free limit at exactly the same critical values. The critical values are then identified as the values at where the minimum value of C/O* is attained. Figure 4.13 shows that C/O* has a minimum at T = 1425 K which corresponds to C/O_{mean} = 0.47. This result is consistent with those shown in Figs. 4.10 and 4.12 for Flames (1) and (7). For these flames, in the region where temperature is higher than 1425 K (within a small deviation), the C/O atom ratio falls under the critical value such that the flames are soot free. Similarly, in the region C/O atom ratio exceeds 0.47, the temperature is below 1425 K.

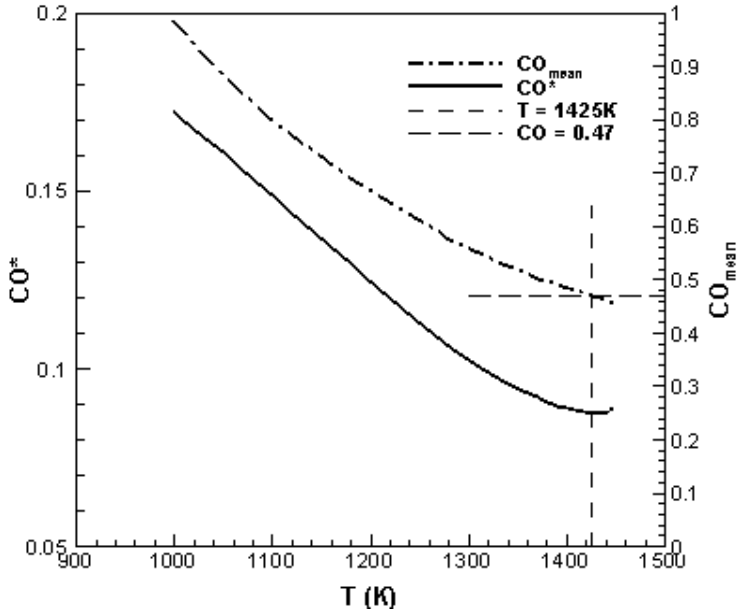

Figure 4.13 Predicted C/O* and C/O_{mean} as a function of temperature for all the flames at their sooting limit

Figure 4.14 shows the temperature profiles of the 13 flames considered in the analysis with respect to their C/O atom ratio at their soot free limit. All these curves converge around C/O = 0.47 and T = 1425 K. This plot provides a better understanding of the determination of critical values. It is worth mentioning that the deviation can be reduced by eliminating some of the cooler flames whose maximum temperatures are close to the critical temperature.

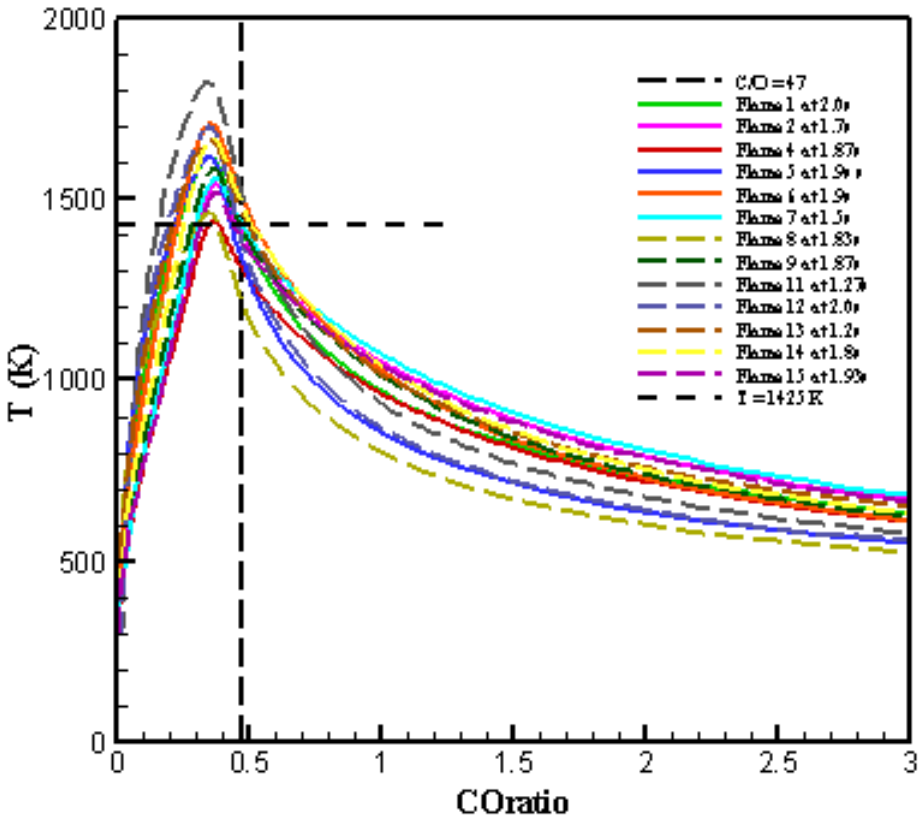

Figure 4.14. Temperature profiles of all the 13 flames at their sooting limit, as a function of their local C/O

The above results agree with the theory that for soot formation to occur, both the temperature and C/O atom ratios should surpass their respective critical values. The values that were obtained

are different from those of Lecoustre et al. [28], 1305 K and 0.53. The difference might be caused by the criteria used to identify the soot free limit. Lecoustre et al. [28] examined their flames at 2 s, right before the termination of the experiments, and defined sooting limits as the conditions when soot formation stops, or when the yellow emission stops increasing. In this research, soot free limits were taken as the conditions when soot is eliminated, or when the flame turns blue. The difference underlines the importance of soot oxidation mechanisms, which are responsible for the elimination of soot, and explains why the critical temperature in this study is higher.

Chapter 5
Conclusions and Recommendations

In this research, spherical microgravity diffusion flames were studied to identify the soot free limit of ethylene flames. Due to their symmetry, one-dimensional models can be adopted which allows for the inclusion of detailed chemistry and transport properties. Experiments were performed using ethylene as the fuel in the drop test facilities provided by NASA Glenn Research Center. Nitrogen was supplied with both the ethylene and oxygen and the flame structure was controlled by the amount of nitrogen content in both of the reactants.

A one-dimensional code with detailed chemistry and transport mechanisms and a realistic radiation model was used to simulate some flames studied in the experiments. The chemistry mechanism included H_2/CO/C1-C4 kinetic models with 111 species and 784 reactions.

Fifteen flames that reach their soot free limits between 1 and 2 seconds were studied. The numerical results were used to analyze the sooting behavior of the flames through the comparison with experimental results. The results are consistent with the theory which indicates that both the temperature and C/O atom ratio must exceed their respective critical values for soot formation to occur. The critical values were found to be T = 1425 K and C/O =0.47 from the 13 flames selected in this work.

This work provided a good insight into the flames at their soot free limit. A chemistry model that includes the formation and oxidation of larger carbon containing molecules is needed to better

understand the formation and destruction of polycyclic aromatic hydrocarbons, which are the precursors leading to soot formation. Because of the 2.2 s limitation in the drop tower tests, the sooting behavior of some flames could not be captured. Extended time allowed for the tests is necessary to advance the knowledge on the soot formation processes. Experiments to be performed in the International Space Station, currently scheduled in 2015, will eliminate the time limitations and allow the study of sooting behavior that cannot be achieved on earth. Use of non-intrusive diagnostic instruments, if possible, will provide additional insight to the soot formation/destruction mechanisms, and approached that can be employed to suppress soot formation from combustion devices.

References

[1] C.J. Cleveland, “Concise Enclopedia of the History of Energy”, Elsevier Inc., First edition 2009.

[2] "Antoine-Laurent Lavoisier." Encyclopedia Britannica. 2011. http://www.britannica.com/EBchecked/topic/332700/Antoine-Laurent-Lavoisier.

[3] E. I. Administration, “Annual energy review 2010,” Energy Information Administration, Tech. Rep., 2011

[4] L.E. Murr, K.M. Garza “Natural and anthropogenic environmental nanoparticulates: Their microstructural characterization and respiratory”, Journal of Atmospheric Environment 43 (2009) 2683-2692.

[5] Department of Environmental Protection, State of New Jersey, 2011 http://www.nj.gov/dep/stopthesoot/dieselhealthconcerns.htm

[6] C.K. Law , “Combustion Physics” Cambridge University Press, 2006.

[7] H. Ross. “Microgravity Combustion: Fire in Free Fall”. NASA Glenn Research Center, Cleveland, OH, USA. Academic Press, 2001

[8] S.D. Tse, D. Zhu, C.J. Sung, Y. Ju, and C.K. Law. “Microgravity Burner-Generated Spherical Diffusion Flames: Experiment and Computation”, Combustion and Flame 125 (2001) 1265–1278

[9] V.R. Lecoustre, “Numerical Investigation of gaseous spherical diffusion flames”, Ph.D dissertation, University of Maryland, 2009.

[10] National Aeronautics and Space Administration, http://facilities.grc.nasa.gov/drop/capabilities.html

[11] P.B. Sunderland, R.L. Axelbaum, D.L. Urban, B.H. Chao, S. Liu, "Effects of structure and hydrodynamics on the sooting behavior of spherical microgravity diffusion flames". Combustion and Flame, 132 (2003) 25-33

[12] K. J. Santa, B. H. Chao, P. B. Sunderland, D. L. Urban, D. P. Stocker, R. L. Axelbaum, "Radiative extinction of gaseous spherical diffusion flames in microgravity" Combustion and Flame, 151 (2007) 665-675

[13] K. Mills and M. Matalon, "Burner-generated spherical diffusion flames," Combustion Science and Technology, 129 (1997) 295‐319

[14] K. Mills and M. Matalon, "Extinction of spherical diffusion flames in the presence of radiant loss," in Symposium (International) on Combustion (1998) 2535‐2542.

[15] B. Chao, C. Law, and J. Tien, "Structure and extinction of diffusion flames with flame radiation," in Symposium (International) on Combustion (1991) 523‐531.

[16] S. Tse, D. Zhu, C. Sung, Y. Ju, and C. Law, "Microgravity burner-generated spherical diffusion flames: experiment and computation," Combustion and Flame, 125 (2001) 1265‐1278

[17] K. Santa, B. Chao, P. Sunderland, D. Urban, D. Stocker, and R. Axelbaum, "Radiative extinction of gaseous spherical diffusion flames in microgravity," Combustion and Flame, 151 (2007) 665‐675

[18] A. Atreya, S. Agrawal, "Effect of radiative heat loss on diffusion flames in quiescent microgravity atmosphere", Combustion and Flame, 115 (1998) 372-382

[19] A. Atreya, S. Agrawal, K. R. Sacksteder, and H. R. Baum, "Observations of methane and ethylene diffusion flames stabilized around a blowing porous sphere under microgravity conditions," in 32nd Aerospace Sciences Meeting and Exhibit, 1994.

[20] S. Berhan, M. Chernovsky, S. Filatyev, A. Atreya, and K. Sacksteder, "The effects of chemical kinetics and radiation on flame radius and temperature prediction of unsteady spherical

diffusion flames in microgravity, comparison with experiments," in 41st Aerospace Sciences Meeting and Exhibit, 2003.

[21] M. Chernovsky, A. Atreya, and K. Sacksteder, "Transient measurements of temperature and radiation intensity in spherical microgravity diffusion flame," in 44nd Aerospace Sciences Meeting and Exhibit, 2006.

[22] M. Chernovsky, A. Atreya, and H. Im, "Effect of CO_2 diluent on fuel versus oxidizer side of spherical diffusion flames in microgravity," Proceedings of the Combustion Institute, 31 (2007) 1005–1013.

[23] Q. Wang, B.H. Chao, "Kinetic and radiative extinctions of spherical burner-stabilized diffusion flames", Combustion and Flame, 158 (2011) 1532–1541

[24] S. Liu, B. Chao, and R. Axelbaum, "A theoretical study on soot inception in spherical burner-stabilized diffusion flames", Combustion and Flame, 140 (2005) 1–23.

[25] P. Sunderland, R. Axelbaum, D. Urban, B. Chao, and S. Liu, "Effects of structure and hydrodynamics on the sooting behavior of spherical microgravity diffusion flames," Combustion and Flame, 132 (2003) 25–33.

[26] J. Du, R.L. Axelbaum, "The effect of flame structure on soot-particle inception in diffusion flames" Combustion and Flame 100 (1995) 367–375

[27] P. Sunderland, D. Urban, D. Stocker, B. Chao, and R. Axelbaum, "Sooting limits of microgravity spherical diffusion flames in oxygen-enriched air and diluted fuel," Combustion Science and Technology, 176 (2004) 2143–2164.

[28] V.R. Lecoustre, P.B. Sunderland, B.H. Chao, R.L. Axelbaum. "Numerical investigation of spherical diffusion flames at their sooting limits", Combustion and Flame, 159 (2012) 194-199.

[29] R. Kee, J. Grcar, M. Smooke, J. Miller, and E. Meeks, "Premix: A FORTRAN Program for Modeling Steady Laminar One-Dimensional Premixed Flames," Sandia National Laboratories Report No. SAND85-8240, Tech. Rep., 1987

[30] R. Kee, F. Rupley, E. Meeks, and J. Miller, "Chemkin-III: a Fortran chemical kinetics package for the analysis of gas-phase chemical and plasma kinetics," Sandia National Laboratories Report No. SAND96-8216, Tech. Rep., 1996

[31] R. Kee, G. Dixon-Lewis, J. Warnatz, M. Coltrin, J. Miller, and H. Moffat, "A Fortran Computer Code Package for the Evaluation of Gas-Phase Multicomponent Transport Properties," Sandia National Laboratories Report No. SAND86-8246, Tech. Rep., 1988

[32] J. Grcar, "The Twopnt program for boundary value problems," Sandia National Laboratories Report No. SAND91-8230, Tech. Rep., 1991

[33] P. Wesseling, "Principles of Computational Fluid Dynamics", Springer Berlin 2001

[34] H. Wang, X. You, A.V. Joshi, Scott G. Davis, Alexander Laskin, Fokion Egolfopoulos & Chung K. Law, USC Mech Version II. High-Temperature Combustion Reaction Model of H2/CO/C1-C4 Compounds. http://ignis.usc.edu/USC_Mech_II.htm, May 2007

[35] Rothman, L.S., Rinsland, C.P., Goldman, A., Massie, S.T., Edwards, D.P., Flaud, J.-M., Perrin, A., Camy-Peyret, C., Dana, V., Mandin, J.-Y., Schroeder, J., Mccann, A., Gamache, R.R., Wattson, R.B., Yoshino, K., Chance, K.V., Jucks, K.W., Brown, L.R., Nemtchinov, V., Varanasi, P., 2003, The HITRAN molecular spectroscopic database: edition of 2000 including updates through 2001. J. Quantitative Spectroscopy and Radiative Transfer, **82**, 5-44.

[36] Carlson, B.G., Lathrop, K.G., 1968, Transport theory - the method of discrete ordinates. In: H. Greenspan, C.N. Kelber, D. Okrent (Eds.) Computing Methods in Reactor Physics. Gordon and Breach, New York.

[37] G. Blanquart, P. Pepiot-Desjardins, H. Pitch. "Chemical mechanism for high temperature combustion of engine relevant fuels with emphasis on soot precursors" Combustion and Flame 156 (2009) 588-607.

[38] K. Narayanaswamy, G. Blanquart, H. Pitch. "A consistent chemical mechanism for oxidation of substituted aromatic species" Combustion and Flame, 157 (2010) 1879-1898.

[39] F. Bisetti, G. Blanquart, M. E. Mueller, H. Pitch. “On the formation and early evolution of soot in turbulent nonpremixed flames” Combustion and Flame, 159 (2012) 317-335.

[40] K. Santa, B. Chao, P. Sunderland, D. Urban, D. Stocker, and R. Axelbaum, “Radiative extinction of gaseous spherical diffusion flames in microgravity,” Combustion and Flame, 151 (2007) 665‐675.

[41] P. Sunderland, R. Axelbaum, D. Urban, B. Chao, and S. Liu, “Effects of structure and hydrodynamics on the sooting behavior of spherical microgravity diffusion flames,” Combustion and Flame,132 (2003) 25–33.

[42] P. Sunderland, D. Urban, D. Stocker, B. Chao, and R. Axelbaum, “Sooting limits of microgravity spherical diffusion flames in oxygen-enriched air and diluted fuel,” Combustion Science and Technology, 176 (2004) 2143‐2164.

[43] S. Tse, D. Zhu, C. Sung, Y. Ju, and C. Law, “Microgravity burner-generated spherical diffusion flames: experiment and computation”, Combustion and Flame, 125 (2001)1265-1278.

[44] B. Kumfer, S. Skeen, and R. Axelbaum, “Soot inception limits in laminar diffusion flames with application to oxy-fuel combustion”, Combustion and Flame, 154 (2008) 546‐556.

[45] B. Kumfer, S. Skeen, R. Chen, and R. Axelbaum, “Measurement and analysis of soot inception limits of oxygen-enriched coflow flames,” Combustion and Flame,147 (2006) 233‐242.

[46] J. Du, R.L. Axelbaum, ” The effect of flame structure on soot-particle inception in diffusion flames”, Combustion and Flame, 100 (1995) 367–375.

[47] J. Warnatz, U. Maas, R.W. Dibble, “Combustion”, 4th edition, Springer, Berlin, 2006

[48] F. Xu, A. M. El-Leathy, C.H. Kim, G. M. Faeth. “Soot surface oxidation in hydrocarbon/air diffusion flames at atmospheric pressure”, Combustion and Flame, 132 (2003) 43-57.

[49] S.B. Dworkin, Q. Zhang, M.J. Thomson, N.A. Slavinskaya, U. Riedel, “Application of an enhanced PAH growth model to soot formation in a laminar coflow ethylene/air diffusion flame”, Combustion and Flame, 158 (2011) 1682-1695.

[50] M.D. Smooke, M.B. Long, B.C. Connelly, M.B. Colket, R.J. Hall, “Soot formation in laminar diffusion flames”, Combustion and Flame, 143 (2005) 613-628.

[51] S.A. Skeen, G. Yablonsky, R.L. Axelbaum, “ Characteristics of non-premixed oxygen-enhanced combustion: II. Flame structure effects on soot precursor kinetics resulting in soot-free flames” Combustion and Flame 157 (2010) 1745-1752

APPENDIX A

USC_Mech 2.0 Chemistry Mechanism

USC_Mech 2.0 is a mechanism optimized for the modeling of natural gas combustion, which includes NO formation and reburn chemistry. It includes the high-temperature chemistry of H2/CO/C1-C4 compounds. Developed in USC Combustion Kinetics Lab, this mechanism contains 784 chemical reactions and 111 species. The reactions are provided below:

The atomic elements considered are O, H, C, N, and AR.

Table A.1 includes the species that are considered in this model:

Table A.1. Species considered in USC_Mech 2.0

AR	N_2	H	O	OH	HO_2	H_2	H_2O
H_2O_2	O_2	C	CH	CH_2	CH_2*	CH_3	CH_4
HCO	CH_2O	CH_3O	CH_2OH	CH_3OH	CO	CO_2	C_2O
C_2H	C_2H_2	H_2CC	C_2H_3	C_2H_4	C_2H_5	C_2H_6	HCCO
HCCOH	CH_2CO	CH_3CO	CH_2CHO	CH_2OCH	CH_3CHO	CH_2OCH_2	C_3H_3
pC_3H_4	aC_3H_4	cC_3H_4	aC_3H_5	CH_3CCH_2	CH_3CHCH	C_3H_6	nC_3H_7
iC_3H_7	C_3H_8	CH_2CHCO	C_2H_3CHO	CH_3CHOCH_2	CH_3CH_2CHO	CH_3COCH_3	C_4H_2
nC_4H_3	iC_4H_3	C_4H_4	nC_4H_5	iC_4H_5	C_4H_5-2	c-C_4H_5	C_4H_6
C4H6-12	C_4H_6-2	C_4H_7	iC_4H_7	C_4H_8-1	$C_4H_8$2	iC_4H_8	pC_4H_9
sC_4H_9	iC_4H_9	tC_4H_9	C_4H_{10}	iC_4H_{10}	H_2C_4O	C_4H_4O	$CH_2CHCHCHO$
$CH_3CHCHCO$	$C_2H_3CHOCH_2$	$C_4H_6O_23$	$CH_3CHCHCHO$	$C_4H_6O_25$	C_5H_4O	$C_5H_5O(1,3)$	$C_5H_5O(2,4)$
C_5H_4OH	C_5H_5OH	C_5H_5	C_5H_6	lC_5H_7	C_6H_2	C_6H_3	l-C_6H_4
o-C_6H_4	C_6H_5	C_6H_6	$C_6H_5CH_2$	$C_6H_5CH_3$	$C_6H_5C_2H$	C_6H_5O	C_6H_5OH
$C_6H_4O_2$	C_6H_5CO	C_6H_5CHO	$C_6H_5CH_2OH$	$OC_6H_4CH_3$	$HOC_6H_4CH_3$	$C_6H_4CH_3$	

And the following reactions:

```
 H+O2 = O+OH                                    2.644E+16  -0.6707 17041.00
 O+H2 = H+OH                                    4.589E+04   2.700   6260.00
 OH+H2 = H+H2O                                  1.734E+08   1.510   3430.00
 OH+OH = O+H2O                                  3.973E+04   2.400  -2110.00
 H+H+M = H2+M                                   1.780E+18  -1.000      0.00
                                              H2/0.0/ H2O/0.0/ CO2/0.0/ AR/0.63/
 H+H+H2 = H2+H2                                 9.000E+16  -0.600      0.00
 H+H+H2O = H2+H2O                               5.624E+19  -1.250      0.00
 H+H+CO2 = H2+CO2                               5.500E+20  -2.000      0.00
 H+OH+M = H2O+M                                 4.400E+22  -2.000      0.00
                                    H2/2.0/ H2O/6.30/ CO/1.75/ CO2/3.6/  AR/0.38/
 O+H+M = OH+M                                   9.428E+18  -1.000      0.00
H2/2.0/ H2O/12.0/ CO/1.75/ CO2/3.6/  AR/0.7/
                                                                    HE/0.7/
 O+O+M = O2+M                                   1.200E+17   -1.000      0.00
                                  H2/2.4/ H2O/15.4/  CO/1.75/ CO2/3.6/  AR/0.83/
```

```
                                                                HE/0.83/
 H+O2(+M) = HO2(+M)                              5.116E+12    0.440      0.00
                                       LOW / 6.328E+19   -1.400      0.00 /
                                       TROE/ 0.5  1E-30  1E+30            /
                              O2/0.85/  H2O/11.89/ CO/1.09/ CO2/2.18/ AR/0.40/
                                                                HE/0.46/
 H2+O2 = HO2+H                                   5.916E+05    2.433  53502.00
 OH+OH(+M) = H2O2(+M)                            1.110E+14   -0.370      0.00
                                     LOW  /  2.010E+17   -0.584  -2293.00
                                     TROE / 0.7346   94.  1756.00  5182.0 /
H2/2.0/ H2O/6.00/ CO/1.75/ CO2/3.6/ AR/0.7/
 HO2+H = O+H2O                                   3.970E+12    0.000    671.00
 HO2+H = OH+OH                                   7.485E+13    0.000    295.00
 HO2+O = OH+O2                                   4.000E+13    0.000      0.00
 HO2+HO2 = O2+H2O2                               1.300E+11    0.000  -1630.00
 HO2+HO2 = O2+H2O2                               3.658E+14    0.000  12000.00
 OH+HO2=H2O+O2                                   1.41E+18    -1.760      60.0
 OH+HO2=H2O+O2                                   1.12E+85   -22.300   26900.0
 OH+HO2=H2O+O2                                   5.37E+70   -16.720   32900.0
 OH+HO2=H2O+O2                                   2.51E+12     2.000   40000.0
 OH+HO2=H2O+O2                                   1.00E+136   -40.000  34800.0
 H2O2+H = HO2+H2                                 6.050E+06    2.000   5200.00
 H2O2+H = OH+H2O                                 2.410E+13    0.000   3970.00
 H2O2+O = OH+HO2                                 9.630E+06    2.000   3970.00
 H2O2+OH = HO2+H2O                               2.000E+12    0.000    427.00
 H2O2+OH = HO2+H2O                               2.670E+41   -7.000  37600.00
 CO+O(+M)=CO2(+M)                                1.362E+10    0.000   2384.00
                                       LOW / 1.173E+24   -2.79    4191.   /
                                  H2/2.0/ H2O/12/ CO/1.75/ CO2/3.6/ AR/0.7/
                                                                HE/0.7/
 CO+OH = CO2+H                                   7.046E+04    2.053  -355.67
 CO+OH = CO2+H                                   5.757E+12   -0.664   331.83
 CO+O2 = CO2+O                                   1.119E+12    0.000  47700.00
 CO+HO2 = CO2+OH                                 1.570E+05    2.180  17942.61
 HCO+H = CO+H2                                    1.200E+14    0.000      0.00
 HCO+O = CO+OH                                   3.000E+13    0.000      0.00
 HCO+O = CO2+H                                   3.000E+13    0.000      0.00
 HCO+OH = CO+H2O                                 3.020E+13    0.000      0.00
 HCO+M = CO+H+M                                  1.870E+17   -1.000  17000.00
                                                 H2/2.0/ H2O/0.0/ CO/1.75/ CO2/3.6/
 HCO+H2O = CO+H+H2O                              2.244E+18   -1.000  17000.00
 HCO+O2 = CO+HO2                                 1.204E+10    0.807   -727.00
 CO+H2(+M) = CH2O(+M)                             4.300E+07    1.500  79600.00
                                     LOW  /  5.070E+27   -3.420  84350.00  /
                                     TROE/  0.9320  197.00  1540.00 10300. /
                 H2/2.0/ H2O/6.0/ CH4/2.0/ CO/1.5/ CO2/2.0/ C2H6/3.0/ AR/0.7/
 C+OH = CO+H                                     5.000E+13    0.000      0.00
 C+O2 = CO+O                                     5.800E+13    0.000    576.00
 CH+H = C+H2                                     1.100E+14    0.000      0.00
 CH+O = CO+H                                     5.700E+13    0.000      0.00
 CH+OH = HCO+H                                   3.000E+13    0.000      0.00
 CH+H2 = CH2+H                                   1.107E+08    1.790   1670.00
 CH+H2O = CH2O+H                                 5.710E+12    0.000   -755.00
 CH+O2 = HCO+O                                   3.300E+13    0.000      0.00
 CH+CO(+M) = HCCO(+M)                            5.000E+13    0.000      0.00
                                     LOW  /  2.690E+28   -3.740   1936.00  /
                                     TROE/  0.5757  237.00  1652.0  5069.0 /
                 H2/2.0/ H2O/6.0/ CH4/2.0/ CO/1.5/ CO2/2.0/ C2H6/3.0/ AR/0.7/
 CH+CO2 = HCO+CO                                 3.400E+12    0.000    690.00
 HCO+H(+M) = CH2O(+M)                            1.090E+12    0.480   -260.00
                                     LOW  /  1.350E+24   -2.570   1425.00  /
                                     TROE/  0.7824  271.0  2755.00  6570.0 /
                H2/2.0/ H2O/6.0/ CH4/2.0/ CO/1.5/ CO2/2.0/ C2H6/3.0/ AR/0.7 /
 CH2+H(+M) = CH3(+M)                             2.500E+16   -0.800      0.00
                                     LOW  /  3.200E+27   -3.140   1230.00  /
                                     TROE/  0.6800   78.00  1995.0  5590.0 /
                 H2/2.0/ H2O/6.0/ CH4/2.0/ CO/1.5/ CO2/2.0/ C2H6/3.0/ AR/0.7/
 CH2+O = HCO+H                                   8.000E+13    0.000      0.00
 CH2+OH = CH2O+H                                 2.000E+13    0.000      0.00
 CH2+OH = CH+H2O                                 1.130E+07    2.000   3000.00
 CH2+H2 = H+CH3                                  5.000E+05    2.000   7230.00
```

```
CH2+O2 = HCO+OH                                 1.060E+13    0.000   1500.00
CH2+O2 = CO2+H+H                                2.640E+12    0.000   1500.00
CH2+HO2 = CH2O+OH                               2.000E+13    0.000      0.00
CH2+C = C2H+H                                   5.000E+13    0.000      0.00
CH2+CO(+M) = CH2CO(+M)                          8.100E+11    0.500   4510.00
                                    LOW  /  2.690E+33   -5.110   7095.00  /
                                    TROE/ 0.5907  275.0  1226.00  5185.00 /
                H2/2.0/ H2O/6.0/ CH4/2.0/ CO/1.5/ CO2/2.0/ C2H6/3.0/ AR/0.7/
CH2+CH = C2H2+H                                 4.000E+13    0.000      0.00
CH2+CH2 = C2H2+H2                               3.200E+13    0.000      0.00
CH2*+N2 = CH2+N2                                1.500E+13    0.000    600.00
CH2*+AR = CH2+AR                                9.000E+12    0.000    600.00
CH2*+H = CH+H2                                  3.000E+13    0.000      0.00
CH2*+O = CO+H2                                  1.500E+13    0.000      0.00
CH2*+O = HCO+H                                  1.500E+13    0.000      0.00
CH2*+OH = CH2O+H                                3.000E+13    0.000      0.00
CH2*+H2 = CH3+H                                 7.000E+13    0.000      0.00
CH2*+O2 = H+OH+CO                               2.800E+13    0.000      0.00
CH2*+O2 = CO+H2O                                1.200E+13    0.000      0.00
CH2*+H2O(+M) = CH3OH(+M)                        2.000E+13    0.000      0.00
                                    LOW  /  2.700E+38   -6.300   3100.00  /
                                    TROE/  0.1507  134.00  2383.0  7265.0 /
                          H2/2.0/ H2O/6.0/ CH4/2.0/ CO/1.5/ CO2/2.0/ C2H6/3.0/
CH2*+H2O = CH2+H2O                              3.000E+13    0.000      0.00
CH2*+CO = CH2+CO                                9.000E+12    0.000      0.00
CH2*+CO2 = CH2+CO2                              7.000E+12    0.000      0.00
CH2*+CO2 = CH2O+CO                              1.400E+13    0.000      0.00
CH2O+H(+M) = CH2OH(+M)                          5.400E+11    0.454   3600.00
                                   LOW  /   1.270E+32   -4.820   6530.00  /
                                   TROE/  0.7187  103.00  1291.00  4160.0 /
                          H2/2.0/ H2O/6.0/ CH4/2.0/ CO/1.5/ CO2/2.0/ C2H6/3.0/
CH2O+H(+M) = CH3O(+M)                           5.400E+11    0.454   2600.00
                                    LOW  /  2.200E+30   -4.800   5560.00  /
                                    TROE/  0.7580   94.00  1555.0 4200.00 /
                          H2/2.0/ H2O/6.0/ CH4/2.0/ CO/1.5/ CO2/2.0/ C2H6/3.0/
CH2O+H = HCO+H2                                 2.300E+10    1.050   3275.00
CH2O+O = HCO+OH                                 3.900E+13    0.000   3540.00
CH2O+OH = HCO+H2O                               3.430E+09    1.180   -447.00
CH2O+O2 = HCO+HO2                               1.000E+14    0.000  40000.00
CH2O+HO2 = HCO+H2O2                             1.000E+12    0.000   8000.00
CH2O+CH = CH2CO+H                               9.460E+13    0.000   -515.00
CH3+H(+M) = CH4(+M)                             1.270E+16   -0.630    383.00
                                   LOW  /   2.477E+33   -4.760   2440.00  /
                                   TROE/  0.7830   74.00  2941.00  6964.0 /
                H2/2.0/ H2O/6.0/ CH4/2.0/ CO/1.5/ CO2/2.0/ C2H6/3.0/ AR/0.7/
CH3+O = CH2O+H                                  8.430E+13    0.000      0.00
CH3+OH(+M) = CH3OH(+M)                          6.300E+13    0.000      0.00
                                    LOW  /  2.700E+38   -6.300   3100.00  /
                                    TROE/  0.2105   83.5 5398.00  8370.0  /
                          H2/2.0/ H2O/6.0/ CH4/2.0/ CO/1.5/ CO2/2.0/ C2H6/3.0/
CH3+OH = CH2+H2O                                5.600E+07    1.600   5420.00
CH3+OH = CH2*+H2O                               2.501E+13    0.000      0.00
CH3+O2 = O+CH3O                                 3.083E+13    0.000  28800.00
CH3+O2 = OH+CH2O                                3.600E+10    0.000   8940.00
CH3+HO2 = CH4+O2                                1.000E+12    0.000      0.00
CH3+HO2 = CH3O+OH                               1.340E+13    0.000      0.00
CH3+H2O2 = CH4+HO2                              2.450E+04    2.470   5180.00
CH3+C = C2H2+H                                  5.000E+13    0.000      0.00
CH3+CH = C2H3+H                                 3.000E+13    0.000      0.00
CH3+HCO = CH4+CO                                8.480E+12    0.000      0.00
CH3+CH2O = CH4+HCO                              3.320E+03    2.810   5860.00
CH3+CH2 = C2H4+H                                4.000E+13    0.000      0.00
CH3+CH2* = C2H4+H                               1.200E+13    0.000   -570.00
CH3+CH3(+M) = C2H6(+M)                          2.120E+16   -0.970    620.00
                                    LOW  /  1.770E+50   -9.670   6220.00  /
                                    TROE/  0.5325  151.0  1038.00  4970.0 /
                H2/2.0/ H2O/6.0/ CH4/2.0/ CO/1.5/ CO2/2.0/ C2H6/3.0/ AR/0.7/
CH3+CH3 = H+C2H5                                4.990E+12    0.100  10600.00
CH3+HCCO = C2H4+CO                              5.00E+13     0.0        0.0
CH3+C2H = C3H3+H                                2.41E+13     0.0        0.0
CH3O+H(+M) = CH3OH(+M)                          5.000E+13    0.000      0.00
```

```
                                    LOW  /  8.600E+28   -4.000   3025.00  /
                                    TROE/  0.8902  144.0  2838.00 45569.0 /
                          H2/2.0/ H2O/6.0/ CH4/2.0/ CO/1.5/ CO2/2.0/ C2H6/3.0/
CH3O+H = CH2OH+H                          3.400E+06    1.600      0.00
CH3O+H = CH2O+H2                          2.000E+13    0.000      0.00
CH3O+H = CH3+OH                           3.200E+13    0.000      0.00
CH3O+H = CH2*+H2O                         1.600E+13    0.000      0.00
CH3O+O = CH2O+OH                          1.000E+13    0.000      0.00
CH3O+OH = CH2O+H2O                        5.000E+12    0.000      0.00
CH3O+O2 = CH2O+HO2                        4.280E-13    7.600  -3530.00
CH2OH+H(+M) = CH3OH(+M)                   1.800E+13    0.000     0.00
                                    LOW  /  3.000E+31   -4.800  3300.00   /
                                    TROE/  0.7679  338.00  1812.0 5081.0  /
   H2/2.0/ H2O/6.0/ CH4/2.0/ CO/1.5/ CO2/2.0/ C2H6/3.0/
CH2OH+H = CH2O+H2                         2.000E+13    0.000     0.00
CH2OH+H = CH3+OH                          1.200E+13    0.000     0.00
CH2OH+H = CH2*+H2O                        6.000E+12    0.000     0.00
CH2OH+O = CH2O+OH                         1.000E+13    0.000     0.00
CH2OH+OH = CH2O+H2O                       5.000E+12    0.000     0.00
CH2OH+O2 = CH2O+HO2                       1.800E+13    0.000   900.00
CH4+H = CH3+H2                            6.600E+08    1.620 10840.00
CH4+O = CH3+OH                            1.020E+09    1.500  8600.00
CH4+OH = CH3+H2O                          1.000E+08    1.600  3120.00
CH4+CH = C2H4+H                           6.000E+13    0.000     0.00
CH4+CH2 = CH3+CH3                         2.460E+06    2.000  8270.00
CH4+CH2* = CH3+CH3                        1.600E+13    0.000  -570.00
CH4+C2H = C2H2+CH3                        1.810E+12    0.0     500.0
CH3OH+H = CH2OH+H2                        1.700E+07    2.100  4870.00
CH3OH+H = CH3O+H2                         4.200E+06    2.100  4870.00
CH3OH+O = CH2OH+OH                        3.880E+05    2.500  3100.00
CH3OH+O = CH3O+OH                         1.300E+05    2.500  5000.00
CH3OH+OH = CH2OH+H2O                      1.440E+06    2.000  -840.00
CH3OH+OH = CH3O+H2O                       6.300E+06    2.000  1500.00
CH3OH+CH3 = CH2OH+CH4                     3.000E+07    1.500  9940.00
CH3OH+CH3 = CH3O+CH4                      1.000E+07    1.500  9940.00
C2H+H(+M) = C2H2(+M)                      1.000E+17   -1.000     0.00
                                     LOW  /  3.750E+33   -4.800  1900.00   /
                                    TROE/  0.6464  132.00  1315.00 5566.0 /
               H2/2.0/ H2O/6.0/ CH4/2.0/ CO/1.5/ CO2/2.0/ C2H6/3.0/ AR/0.7/
C2H+O = CH+CO                             5.000E+13    0.000     0.00
C2H+OH = H+HCCO                           2.000E+13    0.000     0.00
C2H+O2 = HCO+CO                           5.000E+13    0.000  1500.00
C2H+H2 = H+C2H2                           4.900E+05    2.500   560.00
C2O+H = CH+CO                             5.000E+13    0.000     0.00
C2O+O = CO+CO                             5.000E+13    0.000     0.00
C2O+OH = CO+CO+H                          2.000E+13    0.000     0.00
C2O+O2 = CO+CO+O                          2.000E+13    0.000     0.00
HCCO+H = CH2*+CO                          1.000E+14    0.000     0.00
HCCO+O = H+CO+CO                          1.000E+14    0.000     0.00
HCCO+O2 = OH+2CO                          1.600E+12    0.000   854.00
HCCO+CH = C2H2+CO                         5.000E+13    0.000     0.00
HCCO+CH2 = C2H3+CO                        3.000E+13    0.000     0.00
HCCO+HCCO = C2H2+CO+CO                    1.000E+13    0.000     0.00
HCCO+OH = C2O+H2O                         3.000E+13    0.000     0.00
C2H2 (+M) = H2CC (+M)                     8.000E+14   -0.520  50750.00
                                    LOW /   2.450E+15   -0.640  49700.00  /
     H2/2.0/ H2O/6.0/ CH4/2.0/ CO/1.5/ CO2/2.0/ C2H6/3.0/C2H2/2.5/ C2H4/2.5/
C2H3 (+M) = C2H2+H (+M)                   3.860E+08    1.620  37048.2
                                    LOW  /  2.565E+27   -3.400  35798.72  /
                                    TROE/  1.9816  5383.7  4.2932 -0.0795 /
     H2/2.0/ H2O/6.0/ CH4/2.0/ CO/1.5/ CO2/2.0/ C2H6/3.0/ AR/0.7/ C2H2/3.00/
                                                                 C2H4/3.00/
C2H2+O = C2H+OH                           4.600E+19   -1.410  28950.00
C2H2+O = CH2+CO                           4.080E+06    2.000   1900.00
C2H2+O = HCCO + H                         1.632E+07    2.000   1900.00
C2H2+OH = CH2CO+H                         2.180E-04    4.500  -1000.00
C2H2+OH = HCCOH+H                         5.040E+05    2.300  13500.00
C2H2+OH = C2H+H2O                         3.370E+07    2.000  14000.00
C2H2+OH = CH3+CO                          4.830E-04    4.000  -2000.00
C2H2+HCO = C2H3+CO                        1.000E+07    2.000   6000.00
C2H2+CH2 = C3H3+H                         1.200E+13    0.000   6620.00
```

```
C2H2+CH2* = C3H3+H                          2.000E+13    0.000      0.00
C2H2+C2H = C4H2+H                           9.600E+13    0.000      0.00
C2H2+C2H (+M) = nC4H3 (+M)                  8.300E+10    0.899   -363.00
                                    LOW   /1.240E+31   -4.718   1871.00  /
                                    TROE  /1.0 100. 5613. 13387.         /
                        H2/2.0/ H2O/6.0/ CH4/2.0/ CO/1.5/ CO2/2.0/ C2H6/3.0/
                                                          C2H2/2.5/ C2H4/2.5/
C2H2+C2H (+M) = iC4H3 (+M)                  8.300E+10    0.899    -363.00
                                    LOW   /1.240E+31   -4.718    1871.00 /
                                    TROE   /1.0 100. 5613. 13387.        /
                        H2/2.0/ H2O/6.0/ CH4/2.0/ CO/1.5/ CO2/2.0/ C2H6/3.0/
                                                        C2H2/2.5/ C2H4/2.5/
C2H2+HCCO = C3H3+CO                         1.00E+11     0.000    3000.00
C2H2+CH3 = pC3H4+H                          2.56E+09     1.10    13644.0
C2H2+CH3 = aC3H4+H                          5.14E+09     0.86    22153.0
C2H2+CH3 = CH3CCH2                          4.99E+22    -4.39    18850.0
C2H2+CH3 = CH3CHCH                          3.20E+35    -7.76    13300.0
C2H2+CH3 = aC3H5                            2.68E+53    -12.82   35730.0
H2CC+H = C2H2+H                             1.000E+14    0.000       0.00
H2CC+OH = CH2CO+H                           2.000E+13    0.000       0.00
H2CC+O2 = HCO+HCO                           1.000E+13    0.000       0.00
H2CC+C2H2 (+M) = C4H4 (+M)                  3.500E+05    2.055   -2400.00
                                      LOW /1.400E+60  -12.599    7417.00 /
                                      TROE /0.980 56.0 580.0 4164.0      /
                        H2/2.0/ H2O/6.0/ CH4/2.0/ CO/1.5/ CO2/2.0/ C2H6/3.0/
                                                        C2H2/3.00/ C2H4/3.00/
H2CC+C2H4 = C4H6                            1.00E+12     0.0         0.0
CH2CO+H (+M) = CH2CHO (+M)                  3.300E+14   -0.060    8500.00
                                    LOW     /3.800E+41   -7.640   11900.00 /
                                    TROE    /0.337 1707. 3200. 4131.       /
    H2/2/ H2O/6/ CH4/2/ CO/1.5/ CO2/2/ C2H6/3/ AR/0.7/ C2H2/3.00/ C2H4/3.00/
CH2CO+H = HCCO+H2                           5.000E+13    0.000    8000.00
CH2CO+H = CH3+CO                            1.500E+09    1.430    2690.00
CH2CO+O = HCCO+OH                           1.000E+13    0.000    8000.00
CH2CO+O = CH2+CO2                           1.750E+12    0.000    1350.00
CH2CO+OH = HCCO+H2O                         7.500E+12    0.000    2000.00
HCCOH+H = CH2CO+H                           1.000E+13    0.000       0.00
C2H3+H(+M) = C2H4(+M)                       6.080E+12    0.270     280.00
                                     LOW  /  1.400E+30   -3.860    3320.00 /
                                    TROE/  0.7820  207.50  2663.00  6095.00/
               H2/2.0/ H2O/6.0/ CH4/2.0/ CO/1.5/ CO2/2.0/ C2H6/3.0/ AR/0.7/
                                                        C2H2/3.00/ C2H4/3.00/
C2H3+H = C2H2+H2                            9.000E+13    0.000       0.00
C2H3+H = H2CC+H2                            6.000E+13    0.000       0.00
C2H3+O = CH2CO+H                            4.800E+13    0.000       0.00
C2H3+O = CH3+CO                             4.800E+13    0.000       0.00
C2H3+OH = C2H2+H2O                          3.011E+13    0.000       0.00
C2H3+O2 = C2H2+HO2                          1.340E+06    1.610    -383.40
C2H3+O2 = CH2CHO+O                          3.000E+11    0.290      11.00
C2H3+O2 = HCO+CH2O                          4.600E+16   -1.390    1010.00
C2H3+HO2 = CH2CHO+OH                        1.000E+13    0.000       0.00
C2H3+H2O2 = C2H4+HO2                        1.210E+10    0.000    -596.00
C2H3+HCO = C2H4+CO                          9.033E+13    0.000       0.00
C2H3+HCO = C2H3CHO                          1.800E+13    0.00        0.0
C2H3+CH3 = C2H2+CH4                         3.920E+11    0.000       0.00
C2H3+CH3 (+M) = C3H6(+M)                    2.500E+13    0.000       0.00
                                    LOW  / 4.270E+58  -11.940    9769.80 /
                                    TROE / 0.175  1340.6 60000.0 10139.8 /
     H2/2/ H2O/6/ CH4/2/ CO/1.5/ CO2/2/ C2H6/3/ AR/0.7/C2H2/3.00/ C2H4/3.00/
C2H3+CH3 = aC3H5+H                          1.500E+24   -2.830    18618.0
C2H3 + C2H2 = C4H4 + H                      2.00E+18     -1.68   10600.
C2H3 + C2H2 = nC4H5                         9.30E+38     -8.76   12000.
C2H3 + C2H2 = iC4H5                         1.60E+46    -10.98   18600
C2H3 + C2H3 = C4H6                          1.50E+42     -8.84   12483.
C2H3 + C2H3 = iC4H5 + H                     1.20E+22     -2.44   13654.
C2H3 + C2H3 = nC4H5 + H                     2.40E+20     -2.04   15361.
C2H3+C2H3 = C2H2+C2H4                       9.600E+11    0.00        0.
CH2CHO = CH3+CO                             7.800E+41   -9.147   46900.00
CH2CHO+H (+M) = CH3CHO (+M)                 1.000E+14    0.000       0.00
                                    LOW     /5.200E+39   -7.297    4700.00 /
                                    TROE    /0.55 8900. 4350. 7244.        /
```

```
            H2/2/ H2O/6/ CH4/2/ CO/1.5/ CO2/2/ C2H6/3/ C2H2/3.00/ C2H4/3.00/
CH2CHO+H = CH3CO+H                              5.000E+12    0.000       0.00
CH2CHO+H = CH3+HCO                              9.000E+13    0.000       0.00
CH2CHO+H = CH2CO+H2                             2.000E+13    0.000    4000.00
CH2CHO+O = CH2CO+OH                             2.000E+13    0.000    4000.00
CH2CHO+OH = CH2CO+H2O                           1.000E+13    0.000    2000.00
CH2CHO+O2 = CH2CO+HO2                           1.400E+11    0.000       0.00
CH2CHO+O2 = CH2O+CO+OH                          1.800E+10    0.000       0.00 B
CH3+CO (+M) = CH3CO (+M)                        4.850E+07    1.650    6150.00
                                    LOW     /7.800E+30   -5.395    8600.00 /
                                    TROE    /0.258 598. 21002. 1773.       /
    H2/2/ H2O/6/ CH4/2/ CO/1.5/ CO2/2/ C2H6/3/ AR/0.7/ C2H2/3.00/ C2H4/3.00/
CH3CO+H (+M) = CH3CHO (+M)                      9.600E+13    0.000      0.00
                                    LOW     /3.850E+44   -8.569    5500.00 /
                                    TROE    /1.0000 2900. 2900. 5132.      /
            H2/2/ H2O/6/ CH4/2/ CO/1.5/ CO2/2/ C2H6/3/ C2H2/3.00/ C2H4/3.00/
CH3CO+H = CH3+HCO                               9.600E+13    0.000      0.00
CH3CO+O = CH2CO+OH                              3.900E+13    0.000      0.00
CH3CO+O = CH3+CO2                               1.500E+14    0.000      0.00
CH3CO+OH = CH2CO+H2O                            1.200E+13    0.000      0.00
CH3CO+OH = CH3+CO+OH                            3.000E+13    0.000      0.00
CH3CO+HO2 = CH3+CO2+OH                          3.000E+13    0.000      0.00
CH3CO+H2O2 = CH3CHO+HO2                         1.800E+11    0.000   8226.00
CH3 + HCO (+M) = CH3CHO (+M)                    1.800E+13    0.000       0.00
                                    LOW  /  2.200E+48   -9.588    5100.00 /
                                    TROE /  0.6173 13.076 2078. 5093.     /
                        H2/2.0/ H2O/6.0/ CH4/2.0/ CO/1.5/ CO2/2.0/ C2H6/3.0/
                                                          C2H2/3.00/ C2H4/3.00/
CH3CHO+H = CH3CO+H2                             4.100E+09    1.160    2400.00
CH3CHO+H = CH4+HCO                              5.000E+10    0.0        00.00
CH3CHO+O = CH3CO+OH                             5.800E+12    0.000    1800.00
CH3CHO+OH = CH3CO+H2O                           2.350E+10    0.730   -1110.00
CH3CHO+CH3 = CH3CO+CH4                          2.000E-06    5.600    2460.00
CH3CHO+HCO = CO+HCO+CH4                         8.000E+12    0.000   10400.00
CH3CHO+O2 = CH3CO+HO2                           3.000E+13    0.000   39100.00
CH2OCH2 = CH3+HCO                               3.630E+13    0.000   57200.00
CH2OCH2 = CH3CHO                                7.260E+13    0.000   57200.00
CH2OCH2 = CH4+CO                                1.210E+13    0.000   57200.00
CH2OCH2+H = CH2OCH+H2                           2.000E+13    0.000    8300.00
CH2OCH2+H = C2H3+H2O                            5.000E+09    0.000    5000.00
CH2OCH2+H = C2H4+OH                             9.510E+10    0.000    5000.00
CH2OCH2+O = CH2OCH+OH                           1.910E+12    0.000    5250.00
CH2OCH2+OH = CH2OCH+H2O                         1.780E+13    0.000    3610.00
CH2OCH2+CH3 = CH2OCH+CH4                        1.070E+12    0.000   11830.00
CH2OCH+M = CH3+CO+M                             3.160E+14    0.000   12000.00
CH2OCH+M = CH2CHO+M                             5.000E+09    0.000       0.00
CH2OCH+M = CH2CO+H+M                            3.000E+13    0.000    8000.00
C2H4(+M) = H2+H2CC(+M)                          8.000E+12    0.440 88770.00
                                    LOW  /  7.000E+50   -9.310 99860.00   /
                                    TROE / 0.7345  180.0  1035.00  5417.0 /
                H2/2.0/ H2O/6.0/ CH4/2.0/ CO/1.5/ CO2/2.0/ C2H6/3.0/ AR/0.7/
C2H4+H(+M) = C2H5(+M)                           1.367E+09    1.463   1355.00
                                    LOW  /  2.027E+39   -6.642   5769.00  /
                                    TROE / -0.569  299.0  9147.0  -152.40 /
                H2/2.0/ H2O/6.0/ CH4/2.0/ CO/1.5/ CO2/2.0/ C2H6/3.0/ AR/0.7/
C2H4+H = C2H3+H2                                5.070E+07    1.900  12950.00
C2H4+O = C2H3+OH                                1.510E+07    1.900   3740.00
C2H4+O = CH3+HCO                                1.920E+07    1.830    220.00
C2H4+O = CH2+CH2O                               3.840E+05    1.830    220.00
C2H4+OH = C2H3+H2O                              3.600E+06    2.000   2500.00
C2H4+HCO = C2H5+CO                              1.000E+07    2.000   8000.00
C2H4+CH = aC3H4+H                               3.000E+13    0.000      0.00
C2H4+CH = pC3H4+H                               3.000E+13    0.000      0.00
C2H4+CH2 = aC3H5+H                              2.000E+13    0.000   6000.00
C2H4+CH2* = H2CC+CH4                            5.000E+13    0.000      0.00
C2H4+CH2* = aC3H5+H                             5.000E+13    0.000      0.00
C2H4+CH3 = C2H3+CH4                             2.270E+05    2.000   9200.00
C2H4+CH3 = nC3H7                                3.300E+11    0.00    7700.0
C2H4+C2H = C4H4+H                               1.200E+13    0.000      0.00
C2H4+O2 = C2H3+HO2                              4.220E+13    0.000  60800.00
C2H4+C2H3 = C4H7                                7.93E+38    -8.47   14220.0
```

```
C2H4+HO2 = CH2OCH2+OH                       2.820E+12    0.000  17100.00
C2H5+H(+M) = C2H6(+M)                       5.210E+17   -0.990  1580.00
                                  LOW  / 1.990E+41   -7.080  6685.00   /
                                  TROE / 0.8422  125.0  2219.00 6882.0 /
              H2/2.0/ H2O/6.0/ CH4/2.0/ CO/1.5/ CO2/2.0/ C2H6/3.0/ AR/0.7/
C2H5+H = C2H4+H2                            2.000E+12    0.000     0.00
C2H5+O = CH3+CH2O                           1.604E+13    0.000     0.00
C2H5+O = CH3CHO+H                           8.020E+13    0.000     0.00
C2H5+O2 = C2H4+HO2                          2.000E+10    0.000     0.00
C2H5+HO2 = C2H6+O2                          3.000E+11    0.000     0.00
C2H5+HO2 = C2H4+H2O2                        3.000E+11    0.000     0.00
C2H5+HO2 = CH3+CH2O+OH                      2.400E+13    0.000     0.00
C2H5+H2O2 = C2H6+HO2                        8.700E+09    0.000   974.00
C2H5+CH3(+M) = C3H8(+M)                     4.90E+14  -0.50        0.0
                                  LOW  / 6.80E+61 -13.42     6000.0    /
                                  TROE / 1.000  1000.0  1433.9  5328.8 /
                           H2/2/ H2O/6/ CH4/2/ CO/1.5/ CO2/2/ C2H6/3/ AR/0.7/
C2H5+C2H3(+M) = C4H81(+M)                   1.50E+13   0.00        0.0
                                  LOW  / 1.55E+56 -11.79     8984.5    /
                                  TROE / 0.198 2277.9 60000.0 5723.2   /
                           H2/2/ H2O/6/ CH4/2/ CO/1.5/ CO2/2/ C2H6/3/ AR/0.7/
C2H5+C2H3 = aC3H5+CH3                       3.90E+32  -5.22    19747.0
C2H6+H = C2H5+H2                            1.15E+08    1.900   7530.00
C2H6+O = C2H5+OH                            8.98E+07    1.920   5690.00
C2H6+OH = C2H5+H2O                          3.54E+06    2.120    870.00
C2H6+CH2* = C2H5+CH3                        4.00E+13    0.000   -550.00
C2H6+CH3 = C2H5+CH4                         6.14E+06    1.740  10450.00
C3H3+H = pC3H4                              1.50E+13    0.0        0.0
C3H3+H = aC3H4                              2.50E+12    0.0        0.0
C3H3+O = CH2O+C2H                           2.00E+13    0.0        0.0
C3H3+O2 = CH2CO+HCO                         3.00E+10    0.0     2868.0
C3H3+HO2 = OH+CO+C2H3                       8.00E+11    0.0        0.0
C3H3+HO2 = aC3H4+O2                         3.00E+11    0.0        0.0
C3H3+HO2 = pC3H4+O2                         2.50E+12    0.0        0.0
C3H3+HCO = aC3H4+CO                         2.50E+13    0.0        0.0
C3H3+HCO = pC3H4+CO                         2.50E+13    0.0        0.0
C3H3+HCCO = C4H4+CO                         2.50E+13    0.0        0.0
C3H3+CH = iC4H3+H                           5.00E+13    0.0        0.0
C3H3+CH2 = C4H4+H                           5.00E+13    0.0        0.0
C3H3+CH3 (+M) = C4H612 (+M)                 1.50E+12    0.0        0.0
                                   LOW /2.60E+57 -11.94     9770.0    /
                                   TROE /0.175 1340.6 60000.0 9769.8  /
              H2/2.0/ H2O/6.0/ CH4/2.0/ CO/1.5/ CO2/2.0/ C2H6/3.0/ AR/0.7/
C3H3+C2H2 = C5H5                            6.870E+55 -12.5    42025.0
C3H3+C3H3 => C6H5+H                         5.000E+12   0.0        0.0
C3H3+C3H3 => C6H6                           2.000E+12   0.0        0.0
C3H3+C4H4 = C6H5CH2                         6.53E+5    1.28    -4611.0
C3H3+C4H6 = C6H5CH3+H                       6.53E+5    1.28    -4611.0
aC3H4+H = C3H3+H2                           1.30E+06    2.0     5500.0
aC3H4+H = CH3CHCH                           5.40E+29   -6.09   16300.0
aC3H4+H = CH3CCH2                           9.46E+42   -9.43   11190.0
aC3H4+H = aC3H5                             1.52E+59  -13.54   26949.0
aC3H4+O = C2H4+CO                           2.00E+07    1.8     1000.0
aC3H4+OH = C3H3+H2O                         5.30E+06    2.0     2000.0
aC3H4+CH3 = C3H3+CH4                        1.30E+12   0.00     7700.0
aC3H4+CH3 = iC4H7                           2.00E+11   0.00     7500.0
aC3H4+C2H = C2H2+C3H3                       1.00E+13    0.0        0.0
pC3H4 = cC3H4                               1.20E+44  -9.92    69250.0
pC3H4 = aC3H4                               5.15E+60 -13.93    91117.0
pC3H4+H = aC3H4+H                           6.27E+17  -0.91    10079.0
pC3H4+H = CH3CCH2                           1.66E+47 -10.58    13690.0
pC3H4+H = CH3CHCH                           5.50E+28 -5.74      4300.0
pC3H4+H = aC3H5                             4.91E+60 -14.37    31644.0
pC3H4+H = C3H3+H2                           1.30E+06   2.0      5500.0
pC3H4+C3H3 = aC3H4+C3H3                     6.14E+06   1.74    10450.
pC3H4+O = HCCO+CH3                          0.73E+13   0.0      2250.0
pC3H4+O = C2H4+CO                           1.00E+13   0.0      2250.0
pC3H4+OH = C3H3+H2O                         1.00E+06   2.0       100.0
pC3H4+C2H = C2H2+C3H3                       1.00E+13   0.0        0.0
pC3H4+CH3 = C3H3+CH4                        1.80E+12   0.0      7700.0
cC3H4 = aC3H4                               4.89E+41  -9.17    49594.0
```

```
aC3H5+H(+M) = C3H6(+M)                          2.00E+14   0.00        0.0
                                    LOW  / 1.33E+60 -12.00   5967.8      /
                                    TROE / 0.020  1096.6  1096.6  6859.5 /
                          H2/2/ H2O/6/ CH4/2/ CO/1.5/ CO2/2/ C2H6/3/ AR/0.7/
aC3H5+H = aC3H4+H2                              1.80E+13   0.00        0.0
aC3H5+O = C2H3CHO+H                             6.00E+13   0.00        0.0
aC3H5+OH = C2H3CHO+H+H                          4.20E+32  -5.16    30126.0
aC3H5+OH = aC3H4+H2O                            6.00E+12   0.00        0.0
aC3H5+O2 = aC3H4+HO2                            4.99E+15  -1.40    22428.0
aC3H5+O2 = CH3CO+CH2O                           1.19E+15  -1.01    20128.0
aC3H5+O2 = C2H3CHO+OH                           1.82E+13  -0.41    22859.0
aC3H5+HO2 = C3H6+O2                             2.66E+12   0.00        0.0
aC3H5+HO2 = OH+C2H3+CH2O                        6.60E+12   0.00        0.0
aC3H5+HCO = C3H6+CO                             6.00E+13   0.00        0.0
aC3H5+CH3(+M) = C4H81(+M)                       1.00E+14  -0.32     -262.3
                                    LOW  / 3.91E+60 -12.81     6250.0    /
                                    TROE / 0.104  1606.0 60000.0  6118.4 /
                          H2/2/ H2O/6/ CH4/2/ CO/1.5/ CO2/2/ C2H6/3/ AR/0.7/
aC3H5+CH3 = aC3H4+CH4                           3.00E+12  -0.32     -131.0
aC3H5 = CH3CCH2                                 7.06E+56 -14.08    75868.0
aC3H5 = CH3CHCH                                 5.00E+51 -13.02    73300.0
aC3H5+C2H2 = lC5H7                              8.38E+30 -6.242    12824.0
CH3CCH2 = CH3CHCH                               1.50E+48 -12.71    53900.0
CH3CCH2+H = pC3H4+H2                            3.34E+12   0.00        0.0
CH3CCH2+O = CH3+CH2CO                           6.00E+13   0.00        0.0
CH3CCH2+OH = CH3+CH2CO+H                        5.00E+12   0.00        0.0
CH3CCH2+O2 = CH3CO+CH2O                         1.00E+11   0.00        0.0
CH3CCH2+HO2 = CH3+CH2CO+OH                      2.00E+13   0.00        0.0
CH3CCH2+HCO = C3H6+CO                           9.00E+13   0.00        0.0
CH3CCH2+CH3 = pC3H4+CH4                         1.00E+11   0.00        0.0
CH3CCH2+CH3 = iC4H8                             2.00E+13   0.00        0.0
CH3CHCH+H = pC3H4+H2                            3.34E+12   0.00        0.0
CH3CHCH+O = C2H4+HCO                            6.00E+13   0.00        0.0
CH3CHCH+OH = C2H4+HCO+H                         5.00E+12   0.00        0.0
CH3CHCH+O2 = CH3CHO+HCO                         1.00E+11   0.00        0.0
CH3CHCH+HO2 = C2H4+HCO+OH                       2.00E+13   0.00        0.0
CH3CHCH+HCO = C3H6+CO                           9.00E+13   0.00        0.0
CH3CHCH+CH3 = pC3H4+CH4                         1.00E+11   0.00        0.0
C3H6+H(+M) = nC3H7(+M)                          1.33E+13   0.00     3260.7
                                    LOW  / 6.26E+38  -6.66     7000.0    /
                                    TROE / 1.000  1000.0  1310.0 48097.0 /
                          H2/2/ H2O/6/ CH4/2/ CO/1.5/ CO2/2/ C2H6/3/ AR/0.7/
C3H6+H(+M) = iC3H7(+M)                          1.33E+13   0.00     1559.8
                                    LOW  / 8.70E+42  -7.50     4721.8    /
                                    TROE / 1.000  1000.0   645.4  6844.3 /
                          H2/2/ H2O/6/ CH4/2/ CO/1.5/ CO2/2/ C2H6/3/ AR/0.7/
C3H6+H = C2H4+CH3                               8.00E+21  -2.39    11180.0
C3H6+H = aC3H5+H2                               1.73E+05   2.50     2490.0
C3H6+H = CH3CCH2+H2                             4.00E+05   2.50     9790.0
C3H6+H = CH3CHCH+H2                             8.04E+05   2.50    12283.0
C3H6+O = CH2CO+CH3+H                            0.80E+08   1.65      327.0
C3H6+O = C2H3CHO+H+H                            0.40E+08   1.65      327.0
C3H6+O = C2H5+HCO                               3.50E+07   1.65     -972.0
C3H6+O = aC3H5+OH                               1.80E+11   0.70     5880.0
C3H6+O = CH3CCH2+OH                             6.00E+10   0.70     7630.0
C3H6+O = CH3CHCH+OH                             1.21E+11   0.70     8960.0
C3H6+OH = aC3H5+H2O                             3.10E+06   2.00     -298.0
C3H6+OH = CH3CCH2+H2O                           1.10E+06   2.00     1450.0
C3H6+OH = CH3CHCH+H2O                           2.14E+06   2.00     2778.0
C3H6+HO2 = aC3H5+H2O2                           9.60E+03   2.60    13910.0
C3H6+CH3 = aC3H5+CH4                            2.20E+00   3.50     5675.0
C3H6+CH3 = CH3CCH2+CH4                          8.40E-01   3.50    11660.0
C3H6+CH3 = CH3CHCH+CH4                          1.35E+00   3.50    12848.0
C3H6+C2H3 = C4H6+CH3                            7.23E+11   0.0      5000.0
C3H6+HO2 = CH3CHOCH2+OH                         1.09E+12   0.00    14200.00
C2H3CHO+H = C2H4+HCO                            1.08E+11   0.454    5820.00
C2H3CHO+O = C2H3+OH+CO                          3.00E+13   0.00     3540.00
C2H3CHO+O = CH2O+CH2CO                          1.90E+07   1.80      220.00
C2H3CHO+OH = C2H3+H2O+CO                        3.43E+09   1.18     -447.00
C2H3CHO+CH3 = CH2CHCO+CH4                       2.00E+13   0.000   11000.00
C2H3CHO+C2H3 = C4H6+HCO                         2.80E+21  -2.440   14720.00
```

```
CH2CHCO = C2H3+CO                           1.00E+14   0.000   27000.00
CH2CHCO+H = C2H3CHO                         1.00E+14   0.000      00.00
CH3CHOCH2 = CH3CH2CHO                       1.840E+14  0.000   58500.00
CH3CHOCH2 = C2H5+HCO                        2.450E+13  0.000   58500.00
CH3CHOCH2 = CH3+CH2CHO                      2.450E+13  0.000   58800.00
CH3CHOCH2 = CH3COCH3                        1.010E+14  0.000   59900.00
CH3CHOCH2 = CH3+CH3CO                       4.540E+13  0.000   59900.00
iC3H7+H(+M) = C3H8(+M)                      2.40E+13   0.00        0.0
                                  LOW  / 1.70E+58 -12.08    11263.7    /
                                  TROE / 0.649  1213.1  1213.1 13369.7 /
                        H2/2/ H2O/6/ CH4/2/ CO/1.5/ CO2/2/ C2H6/3/ AR/0.7/
iC3H7+H = CH3+C2H5                          1.40E+28  -3.94    15916.0
iC3H7+H = C3H6+H2                           3.20E+12   0.00        0.0
iC3H7+O = CH3CHO+CH3                        9.60E+13   0.00        0.0
iC3H7+OH = C3H6+H2O                         2.40E+13   0.00        0.0
iC3H7+O2 = C3H6+HO2                         1.30E+11   0.00        0.0
iC3H7+HO2 = CH3CHO+CH3+OH                   2.40E+13   0.00        0.0
iC3H7+HCO = C3H8+CO                         1.20E+14   0.00        0.0
iC3H7+CH3 = CH4 + C3H6                      2.20E+14  -0.68        0.0
nC3H7+H(+M) = C3H8(+M)                      3.60E+13   0.00        0.0
                                  LOW  / 3.01E+48  -9.32     5833.6    /
                                  TROE / 0.498  1314.0  1314.0 50000.0 /
                        H2/2/ H2O/6/ CH4/2/ CO/1.5/ CO2/2/ C2H6/3/ AR/0.7/
nC3H7+H = C2H5+CH3                          3.70E+24  -2.92    12505.0
nC3H7+H = C3H6+H2                           1.80E+12   0.00        0.0
nC3H7+O = C2H5+CH2O                         9.60E+13   0.00        0.0
nC3H7+OH = C3H6+H2O                         2.40E+13   0.00        0.0
nC3H7+O2 = C3H6+HO2                         9.00E+10   0.00        0.0
nC3H7+HO2 = C2H5+OH+CH2O                    2.40E+13   0.00        0.0
nC3H7+HCO = C3H8+CO                         6.00E+13   0.00        0.0
nC3H7+CH3 = CH4+C3H6                        1.10E+13   0.00        0.0
C3H8+H = H2+nC3H7                           1.30E+06   2.54     6756.0
C3H8+H = H2+iC3H7                           1.30E+06   2.40     4471.0
C3H8+O = nC3H7+OH                           1.90E+05   2.68     3716.0
C3H8+O = iC3H7+OH                           4.76E+04   2.71     2106.0
C3H8+OH = nC3H7+H2O                         1.40E+03   2.66      527.0
C3H8+OH = iC3H7+H2O                         2.70E+04   2.39      393.0
C3H8+O2 = nC3H7+HO2                         4.00E+13   0.00    50930.0
C3H8+O2 = iC3H7+HO2                         4.00E+13   0.00    47590.0
C3H8+HO2 = nC3H7+H2O2                       4.76E+04   2.55    16490.0
C3H8+HO2 = iC3H7+H2O2                       9.64E+03   2.60    13910.0
C3H8+CH3 = CH4+nC3H7                        9.03E-01   3.65     7153.0
C3H8+CH3 = CH4+iC3H7                        1.51E+00   3.46     5480.0
C4H2 + H = nC4H3                            1.10E+42  -8.72    15300.0
C4H2 + H = iC4H3                            1.10E+30  -4.92    10800.0
C4H2+OH = H2C4O+H                           6.60E+12    0.0     -410.
C4H2+C2H = C6H2+H                           9.60E+13    0.0        0.
C4H2 + C2H = C6H3                           4.50E+37   -7.68    7100.0
H2C4O+H = C2H2+HCCO                         5.00E+13    0.0     3000.
H2C4O+OH = CH2CO+HCCO                       1.00E+07    2.0     2000.
nC4H3 = iC4H3                               4.10E+43   -9.49   53000.0
nC4H3 + H = iC4H3 + H                       2.50E+20   -1.67   10800.0
nC4H3 + H = C2H2 + H2CC                     6.30E+25   -3.34   10014.0
nC4H3 + H = C4H4                            2.00E+47  -10.26   13070.0
nC4H3+H = C4H2+H2                           3.00E+13    0.00        0.
nC4H3+OH = C4H2+H2O                         2.00E+12    0.00        0.
nC4H3 + C2H2 = l-C6H4 + H                   2.50E+14   -0.56    10600.
nC4H3 + C2H2 = C6H5                         9.60E+70  -17.77    31300.
nC4H3 + C2H2 = o-C6H4 + H                   6.90E+46  -10.01    30100.
iC4H3 + H = C2H2 + H2CC                     2.80E+23   -2.55    10780.0
iC4H3 + H = C4H4                            3.40E+43   -9.01    12120.0
iC4H3+H = C4H2+H2                           6.00E+13    0.00        0.
iC4H3+OH = C4H2+H2O                         4.00E+12    0.00        0.
iC4H3+O2 = HCCO+CH2CO                       7.86E+16   -1.80        0.
C4H4 + H = nC4H5                            1.30E+51  -11.92     16500.
C4H4 + H = iC4H5                            4.90E+51  -11.92     17700.
C4H4+H = nC4H3+H2                           6.65E+05    2.53     12240.
C4H4+H = iC4H3+H2                           3.33E+05    2.53      9240.
C4H4+OH = nC4H3+H2O                         3.10E+07    2.0      3430.
C4H4+OH = iC4H3+H2O                         1.55E+07    2.0       430.
C4H4+O = C3H3+HCO                           6.00E+08    1.45     -860.
```

C4H4+C2H = l-C6H4+H	1.20E+13	0.0	0.
nC4H5 = iC4H5	1.50E+67	-16.89	59100.
nC4H5 + H = iC4H5 + H	3.10E+26	-3.35	17423.
nC4H5+H = C4H4+H2	1.50E+13	0.00	0.
nC4H5+OH = C4H4+H2O	2.00E+12	0.00	0.
nC4H5+HCO = C4H6+CO	5.00E+12	0.0	0.
nC4H5+HO2 = C2H3+CH2CO+OH	6.60E+12	0.0	0.
nC4H5+H2O2 = C4H6+HO2	1.21E+10	0.0	-596.
nC4H5+HO2 = C4H6+O2	6.00E+11	0.0	0.
nC4H5+O2 = CH2CHCHCHO+O	3.00E+11	0.29	11.
nC4H5+O2 = HCO+C2H3CHO	9.20E+16	-1.39	1010.
nC4H5 + C2H2 = C6H6 + H	1.60E+16	-1.33	5400.
nC4H5+C2H3 = C6H6+H2	1.84E-13	7.07	-3611.
iC4H5+H = C4H4+H2	3.0E+13	0.00	0.
iC4H5+H = C3H3+CH3	2.00E+13	0.0	2000.
iC4H5+OH = C4H4+H2O	4.0E+12	0.00	0.
iC4H5+HCO = C4H6+CO	5.00E+12	0.0	0.
iC4H5+HO2 = C4H6+O2	6.000E+11	0.00	0.
iC4H5+HO2 = C2H3+CH2CO+OH	6.60E+12	0.0	0.
iC4H5+H2O2 = C4H6+HO2	1.21E+10	0.000	-596.
iC4H5+O2 = CH2CO+CH2CHO	2.16E+10	0.00	2500.
C4H5-2 = iC4H5	1.5E+67	-16.89	59100.
iC4H5+H = C4H5-2+H	3.1E+26	-3.35	17423.
C4H5-2+HO2 = OH+C2H2+CH3CO	8.00E+11	0.0	0.
C4H5-2+O2 = CH3CO+CH2CO	2.16E+10	0.00	2500.
C4H5-2+C2H2 = C6H6+H	5.00E+14	0.00	25000.
C4H5-2+C2H4 = C5H6+CH3	5.00E+14	0.000	25000.
C4H6 = iC4H5 + H	5.70E+36	-6.27	112353.
C4H6 = nC4H5 + H	5.30E+44	-8.62	123608.
C4H6 = C4H4+H2	2.50E+15	0.0	94700.
C4H6+H = nC4H5+H2	1.33E+06	2.53	12240.
C4H6+H = iC4H5+H2	6.65E+05	2.53	9240.
C4H6+H = C2H4+C2H3	1.46E+30	-4.34	21647.
C4H6+H = pC3H4+CH3	2.00E+12	0.0	7000.
C4H6+H = aC3H4+CH3	2.00E+12	0.0	7000.
C4H6+O = nC4H5+OH	0.75E+07	1.90	3740.
C4H6+O = iC4H5+OH	0.75E+07	1.90	3740.
C4H6+O = CH3CHCHCO+H	1.5E+08	1.45	-860.
C4H6+O = CH2CHCHCHO+H	4.5E+08	1.45	-860.
C4H6+OH = nC4H5+H2O	6.20E+06	2.0	3430.
C4H6+OH = iC4H5+H2O	3.10E+06	2.0	430.
C4H6+HO2 = C4H6O25+OH	1.20E+12	0.0	14000.
C4H6+HO2 = C2H3CHOCH2+OH	4.80E+12	0.0	14000.
C4H6+CH3 = nC4H5+CH4	2.00E+14	0.0	22800.
C4H6+CH3 = iC4H5+CH4	1.00E+14	0.0	19800.
C4H6+C2H3 = nC4H5+C2H4	5.00E+13	0.0	22800.
C4H6+C2H3 = iC4H5+C2H4	2.50E+13	0.0	19800.
C4H6+C3H3 = nC4H5+aC3H4	1.00E+13	0.0	22500.
C4H6+C3H3 = iC4H5+aC3H4	0.50E+13	0.0	19500.
C4H6+aC3H5 = nC4H5+C3H6	1.00E+13	0.0	22500.
C4H6+aC3H5 = iC4H5+C3H6	0.50E+13	0.0	19500.
C4H6+C2H3 = C6H6+H2+H	5.62E+11	0.0	3240.
C4H612 = iC4H5+H	4.20E+15	0.0	92600.
C4H612+H = C4H6+H	2.00E+13	0.0	4000.
C4H612+H = iC4H5+H2	1.70E+05	2.5	2490.
C4H612+H = aC3H4+CH3	2.00E+13	0.0	2000.
C4H612+H = pC3H4+CH3	2.00E+13	0.0	2000.
C4H612+CH3 = iC4H5+CH4	7.00E+13	0.0	18500.
C4H612+O = CH2CO+C2H4	1.20E+08	1.65	327.
C4H612+O = iC4H5+OH	1.80E+11	0.70	5880.
C4H612+OH = iC4H5+H2O	3.10E+06	2.00	-298.
C4H612 = C4H6	3.00E+13	0.0	65000.
C4H6-2 = C4H6	3.00E+13	0.000	65000.
C4H6-2 = C4H612	3.00E+13	0.000	67000.
C4H6-2+H = C4H612+H	2.00E+13	0.0	4000.
C4H6-2+H = C4H5-2+H2	3.40E+05	2.5	2490.
C4H6-2+H = CH3+pC3H4	2.60E+5	2.500	1000.
C4H6-2 = H+C4H5-2	5.00E+15	0.000	87300.
C4H6-2+CH3 = C4H5-2+CH4	1.40E+14	0.0	18500.
C2H3CHOCH2 = C4H6O23	2.00E+14	0.0	50600.
C4H6O23 = CH3CHCHCHO	1.95E+13	0.0	49400.

```
C4H6O23 = C2H4+CH2CO                          5.75E+15   0.0      69300.
C4H6O23 = C2H2+CH2OCH2                        1.00E+16   0.0      75800.
C4H6O25 = C4H4O+H2                            5.30E+12   0.0      48500.
C4H4O = CO+pC3H4                              1.78E+15   0.0      77500.
C4H4O = C2H2+CH2CO                            5.01E+14   0.0      77500.
CH3CHCHCHO = C3H6+CO                          3.90E+14    0.0      69000.
CH3CHCHCHO+H = CH2CHCHCHO+H2                  1.70E+5     2.5       2490.
CH3CHCHCHO+H = CH3CHCHCO+H2                   1.00E+5     2.5       2490.
CH3CHCHCHO+H = CH3+C2H3CHO                    4.00E+21   -2.390    11180.
CH3CHCHCHO+H = C3H6+HCO                       4.00E+21   -2.390    11180.
CH3CHCHCHO+CH3 = CH2CHCHCHO+CH4               2.10E+00    3.50      5675.
CH3CHCHCHO+CH3 = CH3CHCHCO+CH4                1.10E+00    3.50      5675.
CH3CHCHCHO+C2H3 = CH2CHCHCHO+C2H4             2.21E+00    3.50      4682.
CH3CHCHCHO+C2H3 = CH3CHCHCO+C2H4              1.11E+00    3.50      4682.
CH3CHCHCO = CH3CHCH+CO                        1.00E+14    0.0      30000.
CH3CHCHCO+H = CH3CHCHCHO                      1.00E+14    0.0         00.
CH2CHCHCHO = aC3H5+CO                         1.00E+14    0.0      25000.
CH2CHCHCHO+H = CH3CHCHCHO                     1.00E+14    0.0         00.
C4H7 = C4H6+H                                 2.48E+53 -12.30     52000.0
C4H7+H(+M) = C4H81(+M)                        3.60E+13   0.00         0.0
                                        LOW  / 3.01E+48  -9.32      5833.6   /
                                        TROE / 0.498  1314.0  1314.0 50000.0 /
                          H2/2/ H2O/6/ CH4/2/ CO/1.5/ CO2/2/ C2H6/3/ AR/0.7/
C4H7+H = CH3+aC3H5                            2.00E+21  -2.00     11000.0
C4H7+H = C4H6+H2                              1.80E+12   0.00         0.0
C4H7+O2 = C4H6+HO2                            1.00E+11   0.00         0.0
C4H7+HO2 = CH2O+OH+aC3H5                      2.40E+13   0.00         0.0
C4H7+HCO = C4H81+CO                           6.00E+13   0.00         0.0
C4H7+CH3 = C4H6+CH4                           1.10E+13   0.00         0.0
iC4H7+H(+M) = iC4H8(+M)                       2.00E+14   0.00         0.0
                                        LOW  / 1.33E+60 -12.00      5967.8   /
                                        TROE / 0.020  1096.6  1096.6  6859.5 /
                          H2/2/ H2O/6/ CH4/2/ CO/1.5/ CO2/2/ C2H6/3/ AR/0.7/
iC4H7+H = CH3CCH2+CH3                         2.60E+45  -8.19     37890.0
iC4H7+O = CH2O+CH3CCH2                        9.00E+13   0.00         0.0
iC4H7+HO2 = CH3CCH2+CH2O+OH                   4.00E+12   0.00         0.0
C4H81+H(+M) = pC4H9(+M)                       1.33E+13   0.00      3260.7
                                        LOW  / 6.26E+38  -6.66      7000.0   /
                                        TROE / 1.000  1000.0  1310.0 48097.0 /
                          H2/2/ H2O/6/ CH4/2/ CO/1.5/ CO2/2/ C2H6/3/ AR/0.7/
C4H81+H(+M) = sC4H9(+M)                       1.33E+13   0.00      1559.8
                                        LOW  / 8.70E+42  -7.50      4721.8   /
                                        TROE / 1.000  1000.0   645.4  6844.3 /
                          H2/2/ H2O/6/ CH4/2/ CO/1.5/ CO2/2/ C2H6/3/ AR/0.7/
C4H81+H = C2H4+C2H5                           1.60E+22  -2.39     11180.0
C4H81+H = C3H6+CH3                            3.20E+22  -2.39     11180.0
C4H81+H = C4H7+H2                             6.50E+05   2.54      6756.0
C4H81+O = nC3H7+HCO                           3.30E+08   1.45      -402.0
C4H81+O = C4H7+OH                             1.50E+13   0.00      5760.0

C4H81+O = C4H7+OH                             2.60E+13   0.00      4470.0

C4H81+OH = C4H7+H2O                           7.00E+02   2.66       527.0
C4H81+O2 = C4H7+HO2                           2.00E+13   0.00     50930.0
C4H81+HO2 = C4H7+H2O2                         1.00E+12   0.00     14340.0
C4H81+CH3 = C4H7+CH4                          4.50E-01   3.65      7153.0
C4H82+H(+M) = sC4H9(+M)                       1.33E+13   0.00      1559.8
                                        LOW  / 8.70E+42  -7.50      4721.8   /
                                        TROE / 1.000  1000.0   645.4  6844.3 /
                          H2/2/ H2O/6/ CH4/2/ CO/1.5/ CO2/2/ C2H6/3/ AR/0.7/
C4H82+H = C4H7+H2                             3.40E+05   2.50      2490.0
C4H82+O = C2H4+CH3CHO                         2.40E+08   1.65       327.0
C4H82+OH = C4H7+H2O                           6.20E+06   2.00      -298.0
C4H82+O2 = C4H7+HO2                           5.00E+13   0.00     53300.0
C4H82+HO2 = C4H7+H2O2                         1.90E+04   2.60     13910.0
C4H82+CH3 = C4H7+CH4                          4.40E+00   3.50      5675.0
iC4H8+H(+M) = iC4H9(+M)                       1.33E+13   0.00      3260.7
                                        LOW  / 6.26E+38  -6.66      7000.0  /
                                        TROE / 1.000  1000.0  1310.0 48097.0 /
                          H2/2/ H2O/6/ CH4/2/ CO/1.5/ CO2/2/ C2H6/3/ AR/0.7/
iC4H8+H = iC4H7+H2                            1.20E+06   2.54      6760.0
```

```
 iC4H8+H = C3H6+CH3                          8.00E+21  -2.39     11180.0
 iC4H8+O = CH3+CH3+CH2CO                     1.20E+08   1.65       327.0
 iC4H8+O = iC3H7+HCO                         3.50E+07   1.65      -972.0
 iC4H8+O = iC4H7+OH                          2.90E+05   2.50      3640.0
 iC4H8+OH = iC4H7+H2O                        1.50E+08   1.53       775.0
 iC4H8+HO2 = iC4H7+H2O2                      2.00E+04   2.55     15500.0
 iC4H8+O2 = iC4H7+HO2                        2.70E+13   0.00     50900.0
 iC4H8+CH3 = iC4H7+CH4                       9.10E-01   3.65      7150.0
 C2H4+C2H5 = pC4H9                           1.50E+11   0.00      7300.0
 pC4H9+H(+M) = C4H10(+M)                     3.60E+13   0.00         0.0
                                    LOW  / 3.01E+48  -9.32      5833.6   /
                                    TROE / 0.498  1314.0  1314.0 50000.0 /
                           H2/2/ H2O/6/ CH4/2/ CO/1.5/ CO2/2/ C2H6/3/ AR/0.7/
 pC4H9+H = C2H5+C2H5                         3.70E+24  -2.92     12505.0
 pC4H9+H = C4H81+H2                          1.80E+12   0.00         0.0
 pC4H9+O = nC3H7+CH2O                        9.60E+13   0.00         0.0
 pC4H9+OH = C4H81+H2O                        2.40E+13   0.00         0.0
 pC4H9+O2 = C4H81+HO2                        2.70E+11   0.00         0.0
 pC4H9+HO2 = nC3H7+OH+CH2O                   2.40E+13   0.00         0.0
 pC4H9+HCO = C4H10+CO                        9.00E+13   0.00         0.0
 pC4H9+CH3 = C4H81+CH4                       1.10E+13   0.00         0.0
 C3H6+CH3(+M) = sC4H9(+M)                    1.70E+11   0.00      7403.6
                                    LOW  / 2.31E+28  -4.27      1831.0   /
                                    TROE / 0.565 60000.0   534.2  3007.2 /
                           H2/2/ H2O/6/ CH4/2/ CO/1.5/ CO2/2/ C2H6/3/ AR/0.7/
 sC4H9+H(+M) = C4H10(+M)                     2.40E+13   0.00         0.0
                                    LOW  / 1.70E+58 -12.08     11263.7   /
                                    TROE / 0.649  1213.1  1213.1 13369.7 /
                           H2/2/ H2O/6/ CH4/2/ CO/1.5/ CO2/2/ C2H6/3/ AR/0.7/
 sC4H9+H = C2H5+C2H5                         1.40E+28  -3.94     15916.0
 sC4H9+H = C4H81+H2                          3.20E+12   0.00         0.0
 sC4H9+H = C4H82+H2                          2.10E+12   0.00         0.0
 sC4H9+O = CH3CHO+C2H5                       9.60E+13   0.00         0.0
 sC4H9+OH = C4H81+H2O                        2.40E+13   0.00         0.0
 sC4H9+OH = C4H82+H2O                        1.60E+13   0.00         0.0
 sC4H9+O2 = C4H81+HO2                        5.10E+10   0.00         0.0
 sC4H9+O2 = C4H82+HO2                        1.20E+11   0.00         0.0
 sC4H9+HO2 = CH3CHO+C2H5+OH                  2.40E+13   0.00         0.0
 sC4H9+HCO = C4H10+CO                        1.20E+14   0.00         0.0
 sC4H9+CH3 = CH4+C4H81                       2.20E+14  -0.68         0.0
 sC4H9+CH3 = CH4+C4H82                       1.50E+14  -0.68         0.0
 C3H6+CH3(+M) = iC4H9(+M)                    9.60E+10   0.00      8003.6
                                    LOW  / 1.30E+28  -4.27      2431.1   /
                                    TROE / 0.565 60000.0   534.2  3007.2 /
                           H2/2/ H2O/6/ CH4/2/ CO/1.5/ CO2/2/ C2H6/3/ AR/0.7/
 iC4H9+H(+M) = iC4H10(+M)                    3.60E+13   0.00         0.0
                                    LOW  / 3.27E+56 -11.74      6430.8   /
                                    TROE / 0.506  1266.6  1266.6 50000.0 /
                           H2/2/ H2O/6/ CH4/2/ CO/1.5/ CO2/2/ C2H6/3/ AR/0.7/
 iC4H9+H = iC3H7+CH3                         1.90E+35  -5.83     22470.0
 iC4H9+H = iC4H8+H2                          9.00E+11   0.00         0.0
 iC4H9+O = iC3H7+CH2O                        9.60E+13   0.00         0.0
 iC4H9+OH = iC4H8+H2O                        1.20E+13   0.00         0.0
 iC4H9+O2 = iC4H8+HO2                        2.40E+10   0.00         0.0
 iC4H9+HO2 = iC3H7+CH2O+OH                   2.41E+13   0.00         0.0
 iC4H9+HCO = iC4H10+CO                       3.60E+13   0.00         0.0
 iC4H9+CH3 = iC4H8+CH4                       6.00E+12  -0.32         0.0
 tC4H9(+M) = iC4H8+H(+M)                     8.30E+13   0.00     38150.4
LOW  / 1.90E+41  -7.36     36631.7   /
                                    TROE / 0.293   649.0 60000.0  3425.9 /
                           H2/2/ H2O/6/ CH4/2/ CO/1.5/ CO2/2/ C2H6/3/ AR/0.7/
 tC4H9+H(+M) = iC4H10(+M)                    2.40E+13   0.00         0.0
                                    LOW  / 1.47E+61 -12.94      8000.0   /
                                    TROE / 0.000  1456.4  1000.0 10000.5 /
                           H2/2/ H2O/6/ CH4/2/ CO/1.5/ CO2/2/ C2H6/3/ AR/0.7/
 tC4H9+H = iC3H7+CH3                         2.60E+36  -6.12     25640.0
 tC4H9+H = iC4H8+H2                          5.42E+12   0.00         0.0
 tC4H9+O = iC4H8+OH                          1.80E+14   0.00         0.0
 tC4H9+O = CH3COCH3+CH3                      1.80E+14   0.00         0.0
 tC4H9+OH = iC4H8+H2O                        1.80E+13   0.00         0.0
 tC4H9+O2 = iC4H8+HO2                        4.80E+11   0.00         0.0
```

```
tC4H9+HO2 = CH3+CH3COCH3+OH                 1.80E+13   0.00         0.0
tC4H9+HCO = iC4H10+CO                       6.00E+13   0.00         0.0
tC4H9+CH3 = iC4H8+CH4                       3.80E+15  -1.00         0.0
CH3COCH3+H = H2+CH2CO+CH3                   1.30E+06   2.54      6756.0
CH3COCH3+O = OH+CH2CO+CH3                   1.90E+05   2.68      3716.0
CH3COCH3+OH = H2O+CH2CO+CH3                 3.20E+07   1.80       934.0
CH3+CH3CO = CH3COCH3                        4.00E+15  -0.80         0.0
nC3H7+CH3(+M) = C4H10(+M)                   1.93E+14  -0.32         0.0
                                    LOW  / 2.68E+61 -13.24      6000.0   /
                                    TROE / 1.000  1000.0  1433.9  5328.8 /
                          H2/2/ H2O/6/ CH4/2/ CO/1.5/ CO2/2/ C2H6/3/ AR/0.7/
C2H5+C2H5(+M) = C4H10(+M)                   1.88E+14  -0.50         0.0   !
                                    LOW  / 2.61E+61 -13.42      6000.0   /
                                    TROE / 1.000  1000.0  1433.9  5328.8 /
                          H2/2/ H2O/6/ CH4/2/ CO/1.5/ CO2/2/ C2H6/3/ AR/0.7/
C4H10+H = pC4H9+H2                          9.20E+05   2.54      6756.0
C4H10+H = sC4H9+H2                          2.40E+06   2.40      4471.0
C4H10+O = pC4H9+OH                          4.90E+06   2.40      5500.0
C4H10+O = sC4H9+OH                          4.30E+05   2.60      2580.0
C4H10+OH = pC4H9+H2O                        3.30E+07   1.80       954.0
C4H10+OH = sC4H9+H2O                        5.40E+06   2.00      -596.0
C4H10+O2 = pC4H9+HO2                        4.00E+13   0.00     50930.0
C4H10+O2 = sC4H9+HO2                        8.00E+13   0.00     47590.0
C4H10+HO2 = pC4H9+H2O2                      4.76E+04   2.55     16490.0
C4H10+HO2 = sC4H9+H2O2                      1.90E+04   2.60     13910.0
C4H10+CH3 = pC4H9+CH4                       9.03E-01   3.65      7153.0
C4H10+CH3 = sC4H9+CH4                       3.00E+00   3.46      5480.0
iC3H7+CH3(+M) = iC4H10(+M)                  1.40E+15  -0.68         0.0
                                    LOW  / 4.16E+61 -13.33      3903.4   /
                                    TROE / 0.931 60000.0  1265.3  5469.8 /
                          H2/2/ H2O/6/ CH4/2/ CO/1.5/ CO2/2/ C2H6/3/ AR/0.7/
iC4H10+H = iC4H9+H2                         1.80E+06   2.54      6760.0
iC4H10+H = tC4H9+H2                         6.00E+05   2.40      2580.0
iC4H10+O = iC4H9+OH                         4.30E+05   2.50      3640.0
iC4H10+O = tC4H9+OH                         1.57E+05   2.50      1110.0
iC4H10+OH = iC4H9+H2O                       2.30E+08   1.53       775.0
iC4H10+OH = tC4H9+H2O                       5.73E+10   0.51        64.0
iC4H10+HO2 = iC4H9+H2O2                     3.00E+04   2.55     15500.0
iC4H10+HO2 = tC4H9+H2O2                     3.60E+03   2.55     10500.0
iC4H10+O2 = iC4H9+HO2                       4.00E+13   0.00     50900.0
iC4H10+O2 = tC4H9+HO2                       4.00E+13   0.00     44000.0
iC4H10+CH3 = iC4H9+CH4                      1.36E+00   3.65      7150.0
iC4H10+CH3 = tC4H9+CH4                      9.00E-01   3.46      4600.0
C6H2 + H = C6H3                             1.10E+30  -4.92    10800.0
C6H3 + H = C4H2 + C2H2                      2.80E+23  -2.55    10780.0
C6H3 + H = l-C6H4                           3.40E+43  -9.01    12120.0
C6H3+H = C6H2+H2                            3.00E+13   0.00        0.0
C6H3+OH = C6H2+H2O                          4.00E+12   0.00        0.0
l-C6H4 + H = C6H5                           1.70E+78 -19.72    31400.
l-C6H4 + H = o-C6H4+ H                      1.40E+54 -11.70    34500.
l-C6H4 + H = C6H3 + H2                      1.330E+06   2.530    9240.00
l-C6H4 + OH = C6H3 + H2O                    3.100E+06   2.000     430.00
C4H2 + C2H2 = o-C6H4                        5.00E+78  -19.31    67920.
o-C6H4 + OH = CO + C5H5                     1.00E+13    0.00        0.
C6H5 + CH3 = C6H5CH3                                1.380E+13   0.000      46.0
C6H5CH3 + O2 = C6H5CH2 + HO2                3.000E+14   0.000   42992.00
C6H5CH3 + OH = C6H5CH2 + H2O                1.620E+13   0.000    2770.00
C6H5CH3 + OH = C6H4CH3 + H2O                1.333E+08   1.420    1450.00
C6H5CH3 + H = C6H5CH2 + H2                  1.259E+14   0.000    8359.00
C6H5CH3 + H = C6H6 + CH3                    1.930E+06   2.170    4163.00
C6H5CH3 + O = OC6H4CH3 + H                  2.600E+13   0.000    3795.00
C6H5CH3 + CH3 = C6H5CH2 + CH4               3.160E+11   0.000    9500.00
C6H5CH3 + C6H5 = C6H5CH2 + C6H6             2.103E+12   0.000    4400.00
C6H5CH3 + HO2 = C6H5CH2 + H2O2              3.975E+11   0.000   14069.00
C6H5CH3 + HO2 = C6H4CH3 + H2O2              5.420E+12   0.000   28810.00
C6H5CH2 + H (+M) = C6H5CH3 (+M)             1.000E+14   0.000       0.00
                                    LOW   /1.100E+103 -24.63   14590.00  /
                                   TROE   /0.431    383.   152.   4730.  /
                                 H2/2/ H2O/6/ CH4/2/ CO/1.5/ CO2/2/ C2H6/3/
C6H5CH2 + H = C6H5 + CH3                    1.500E+66 -13.940   64580.00
C6H5CH2 + O = C6H5CHO + H                   4.000E+14   0.000       0.00
```

```
C6H5CH2 + OH  = C6H5CH2OH                    2.000E+13   0.000       0.00
C6H5CH2 + HO2 = C6H5CHO + H + OH             5.000E+12   0.000       0.00
C6H5CH2 + C6H5OH = C6H5CH3 + C6H5O           1.050E+11   0.000    9500.00
C6H5CH2 + HOC6H4CH3 = C6H5CH3 + OC6H4CH3     1.050E+11   0.000    9500.00
C6H5CH2OH + OH = C6H5CHO + H2O + H           5.000E+12   0.000       0.00
C6H5CH2OH + H = C6H5CHO + H2 + H             8.000E+13   0.000    8235.00
C6H5CH2OH + H = C6H6 + CH2OH                 1.200E+13   0.000    5148.00
C6H5CH2OH + C6H5 = C6H5CHO + C6H6 + H        1.400E+12   0.000    4400.00
C6H5 + HCO = C6H5CHO                         1.000E+13   0.000       0.00
C6H5CHO = C6H5CO + H                         3.980E+15   0.000   86900.00
C6H5CHO + O2 = C6H5CO + HO2                  1.020E+13   0.000   38950.00
C6H5CHO + OH = C6H5CO + H2O                  2.350E+10    0.730  -1110.00
C6H5CHO + H = C6H5CO + H2                    4.100E+09    1.160   2400.00
C6H5CHO + H = C6H6 + HCO                     1.930E+06   2.170    4163.00
C6H5CHO + O = C6H5CO + OH                    5.800E+12    0.000   1800.00
C6H5CHO + C6H5CH2 = C6H5CO + C6H5CH3         2.000E-06    5.600   2460.00
C6H5CHO + CH3 = C6H5CO + CH4                 2.000E-06    5.600   2460.00
C6H5CHO + C6H5 = C6H5CO + C6H6               2.103E+12   0.000    4400.00
C6H5CO + H2O2 = C6H5CHO + HO2                1.800E+11    0.000   8226.00
OC6H4CH3 + H (+M) = HOC6H4CH3 (+M)           1.000E+14   0.000       0.00
                                    LOW  / 4.000E+93 -21.840   13880.0   /
                                    TROE / 0.043 304.2 60000. 5896.4     /
                                 H2/2.0/ H2O/6.0/ CH4/2.0/ CO/1.5/ CO2/2.0/
OC6H4CH3 + H = C6H5O + CH3                   1.930E+06   2.170    4163.00
OC6H4CH3 + O = C6H4O2 + CH3                  8.000E+13   0.000       0.00
HOC6H4CH3 + OH = OC6H4CH3 + H2O              6.000E+12   0.000       0.00
HOC6H4CH3 + H = OC6H4CH3 + H2                1.150E+14   0.000   12400.00
HOC6H4CH3 + H = C6H5CH3 + OH                 2.210E+13   0.000    7910.00
HOC6H4CH3 + H = C6H5OH + CH3                 1.200E+13   0.000    5148.00
C6H5CO = C6H5 + CO                           5.270E+14   0.000   29013.00
C6H5 + H (+M) = C6H6 (+M)                    1.000E+14   0.000       0.00
                                    LOW  / 6.600E+75 -16.300    7000.00
                                    TROE / 1.0 0.1 584.9 6113.           /
                                 H2/2.0/ H2O/6.0/ CH4/2.0/ CO/1.5/ CO2/2.0/
C6H6 + OH = C6H5 + H2O                       3.985E+05   2.286    1058.00
C6H6 + OH = C6H5OH + H                       1.300E+13   0.000   10600.00
C6H6 + O = C6H5O + H                         1.390E+13   0.000    4910.00
C6H6 + O = C5H5 + HCO                        1.390E+13   0.000    4530.00
C6H5 + H2 = C6H6 + H                         5.707E+04   2.430    6273.00
C6H5 (+M) = o-C6H4 + H (+M)                  4.300E+12   0.616    77313.
                                     LOW/ 1.000E+84 -18.866    90064    /
                                     TROE/ 0.902, 696., 358., 3856.     /
                                 H2/2.0/ H2O/6.0/ CH4/2.0/ CO/1.5/ CO2/2.0/
C6H5 + H = o-C6H4 + H2                       2.000E+11   1.100   24500.00
C6H5 + O2 = C6H5O + O                        2.600E+13   0.000    6120.00
C6H5 + O2 = C6H4O2 + H                       3.000E+13   0.000    8980.00
C6H5 + O = C5H5 + CO                         1.000E+14   0.000       0.00
C6H5 + OH = C6H5O + H                        3.000E+13   0.000       0.00
C6H5 + HO2 = C6H5O + OH                      3.000E+13   0.000       0.00
C6H5 + HO2 = C6H6 + O2                       1.000E+12   0.000       0.00
C6H5 + CH4 = C6H6 + CH3                      3.890E-03   4.570    5256.00
C6H5 + C2H6 = C6H6 + C2H5                    2.100E+11   0.000    4443.00
C6H5 + CH2O = C6H6 + HCO                     8.550E+04    2.190     38.00
C6H4O2 = C5H4O + CO                          7.400E+11   0.000   59000.00
C6H4O2 + H =  CO + C5H5O(1,3)                4.300E+09   1.450    3900.00
C6H4O2 + O = 2CO + C2H2 + CH2CO              3.000E+13   0.000    5000.00
C6H5O + H = C5H5 + HCO                  1.000E+13   0.000   12000.00
C6H5O + H = C5H6 + CO                    5.000E+13   0.000       0.00
C6H5O = CO + C5H5                            3.760E+54 -12.060   72800.00
C6H5O + O = C6H4O2 + H                       2.600E+10   0.470     795.00
C6H5OH = C5H6 + CO                           1.000E12    0.000   60808.00
C6H5OH + OH = C6H5O + H2O                    2.950E+06   2.000   -1312.00
C6H5OH + H = C6H5O + H2                      1.150E+14   0.000   12398.00
C6H5OH + O = C6H5O + OH                      2.810E+13   0.000    7352.00
C6H5OH + C2H3 = C6H5O + C2H4                 6.000E+12   0.000       0.00
C6H5OH + nC4H5 = C6H5O + C4H6                6.000E+12   0.000       0.00
C6H5OH + C6H5 = C6H5O + C6H6                 4.910E+12   0.000    4400.00
C5H6 + H = C2H2 + aC3H5                      7.740E+36  -6.180   32890.00
C5H6 + H = lC5H7                             8.270E+126 -32.30   82348.00
C5H6 + H = C5H5 + H2                         3.030E+08   1.710    5590.00
C5H6 + O = C5H5 + OH                         4.770E+04   2.710    1106.00
```

```
 C5H6 + O = C5H5O(1,3) + H                  8.910E+12  -0.150     590.00
 C5H6 + O = C5H5O(1,3) + H                  5.600E+12  -0.060     200.00
 C5H6 + O = nC4H5 + CO + H                  8.700E+51 -11.090   33240.00
 C5H6 + OH = C5H5 + H2O                     3.080E+06   2.000       0.00
 C5H6 + HO2 = C5H5 + H2O2                   1.100E+04   2.600   12900.00
 C5H6 + O2 = C5H5 + HO2                     4.000E+13   0.000   37150.00
 C5H6 + HCO = C5H5 + CH2O                   1.080E+08   1.900   16000.00
 C5H6 + CH3 = C5H5 + CH4                    0.180E+00   4.000       0.00
 C5H5 + H (+M)= C5H6 (+M)                   1.000E+14   0.000       0.00
                                  LOW  / 4.400E+80 -18.280    12994.0  /
                                  TROE / 0.068 400.7 4135.8 5501.9     /
                                H2/2.0/ H2O/6.0/ CH4/2.0/ CO/1.5/ CO2/2.0/
 C5H5 + O2 = C5H5O(2,4) + O                 7.780E+15  -0.730   48740.00
 C5H5 + O = C5H5O(2,4)                                1.120E-12   5.870  -17310.00
 C5H5 + O = C5H4O + H                       5.810E+13  -0.020      20.00
 C5H5 + O = nC4H5 + CO                      3.200E+13  -0.17      440.00
 C5H5 + OH = C5H4OH + H                     3.510E+57 -12.180   48350.00
 C5H5 + OH = C5H5O(2,4) + H                 1.360E+51 -10.460   57100.00
 C5H5 + HO2 = C5H5O(2,4) + OH               6.270E+29  -4.690   11650.00
 C5H5 + OH = C5H5OH                         6.490E+14  -0.850   -2730.00
 C5H5 + OH = C5H5OH                         1.150E+43  -8.760   18730.00
 C5H5 + OH = C5H5OH                         1.060E+59 -13.080   33450.00
 C5H5 + O2 = C5H4O + OH                     1.800E+12   0.080   18000.00
 C5H5OH + H = C5H5O(2,4) + H2               1.150E+14   0.000   15400.00
 C5H5OH + H = C5H4OH + H2                   1.200E+05   2.500    1492.00
 C5H5OH + OH = C5H5O(2,4) + H2O             6.000E+12   0.000       0.00
 C5H5OH + OH = C5H4OH + H2O                 3.080E+06   2.000       0.00
 C5H5O(2,4) + H = C5H5OH                    1.000E+14   0.000       0.00
 C5H5O(2,4) = C5H4O + H                     2.000E+13   0.000   30000.00
 C5H5O(2,4) + O2 = C5H4O + HO2              1.000E+11   0.000       0.00
 C5H4O + H = C5H5O(1,3)                     2.000E+13   0.000    2000.00
 C5H5O(1,3) =  c-C4H5 + CO                  1.000E+12   0.000   36000.00
 C5H5O(1,3) + O2 = C5H4O + HO2              1.000E+11   0.000       0.00
 C5H4OH = C5H4O + H                         2.100E+13   0.000   48000.00
 C5H4O = 2C2H2+ CO                          6.200E+41  -7.870   98700.00
 C5H4O + H = CO + c-C4H5                    4.300E+09   1.450    3900.00
 C5H4O + O = CO + HCO + C3H3                6.200E+08   1.450    -858.00
 c-C4H5 + H = C4H6                          1.000E+13   0.000       0.00
 c-C4H5 + H = C2H4 + C2H2                   1.000E+13   0.000       0.00
 c-C4H5 + O = CH2CHO + C2H2                 1.000E+14   0.000       0.00
 c-C4H5 + O2 = CH2CHO + CH2CO               4.800E+11   0.000   19000.00
 c-C4H5 = C4H4 + H                          3.000E+12   0.000   52000.00
 c-C4H5 = C2H3 + C2H2                       2.000E+12   0.000   58000.00
 aC3H5 + C2H3 = lC5H7 + H                   1.000E+13   0.000       0.00
 lC5H7 + O = C2H3CHO + C2H3                 5.000E+13   0.000       0.00
 lC5H7 + OH = C2H3CHO + C2H4                2.000E+13   0.000       0.00
END
```

Appendix B

Soot-free flame structures and time evolution

Figures B.1 through B. 13 show the structure of the 13 sooting limit flames considered in this study at their sooting limit. For all of these flames, it can be observed that scalar dissipation rate profiles have more drastic changes in the regions with the temperatures high enough to produce soot (1250-1650K). This shows that taking residence time into account as well as T and C/O in the study of sooting behavior of flames might provide a better insight for a global soot-free condition.

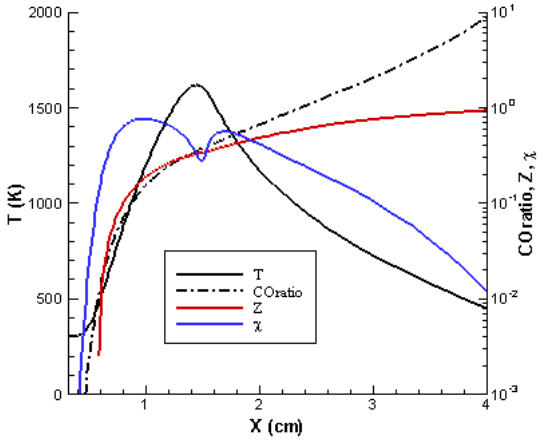

Figure B.1. Predicted T, C/O, Z and χ of flame 1at its sooting limit 2.0 s.

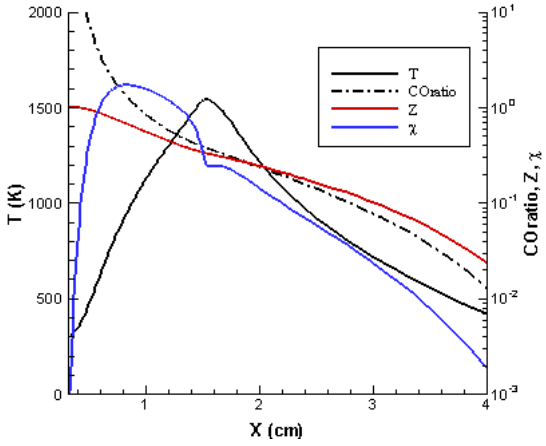

Figure B.2. Predicted T, C/O, Z and χ of flame 2at its sooting limit 1.7 s.

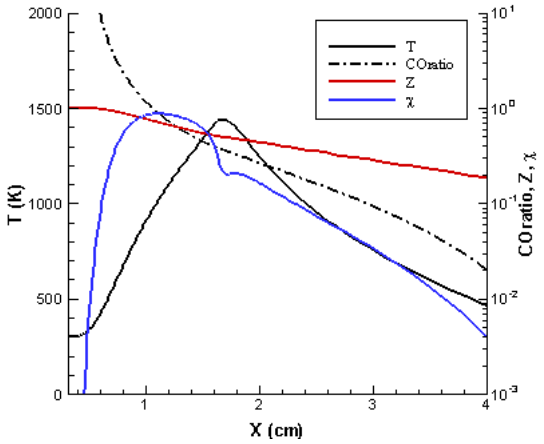

Figure B.3. Predicted T, C/O, Z and χ of flame 4 at its sooting limit 1.87 s.

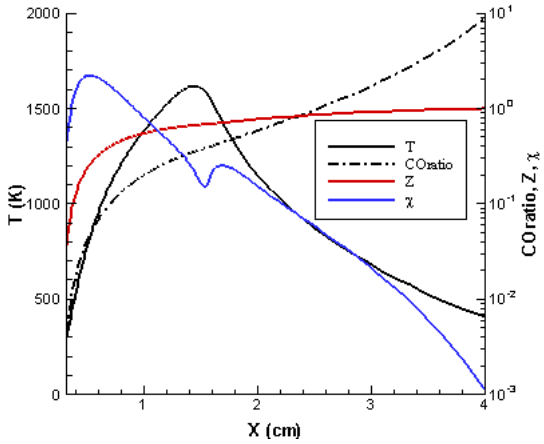

Figure B.4. Predicted T, C/O, Z and χ of flame 5 at its sooting limit 1.9 s.

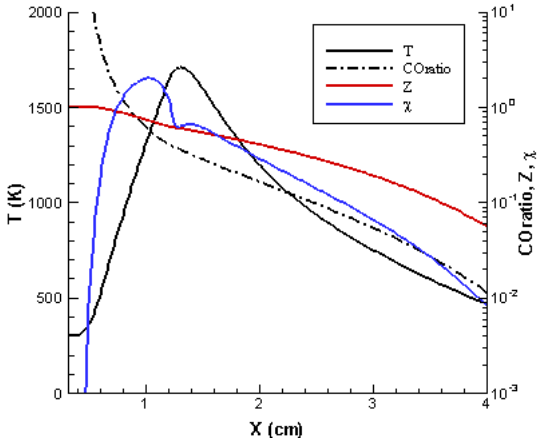

Figure B.5. Predicted T, C/O, Z and χ of flame 6 at its sooting limit 1.9 s.

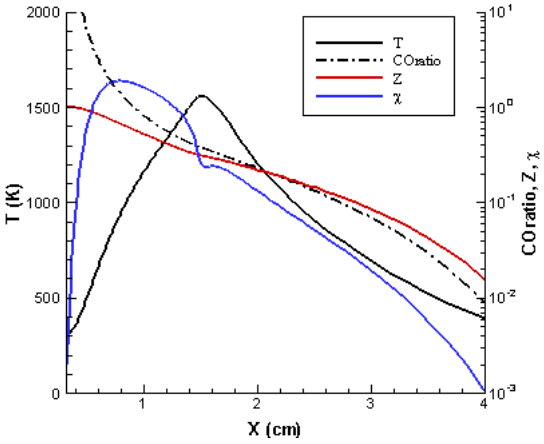

Figure B.6. Predicted T, C/O, Z and χ of flame 7 at its sooting limit 1.5 s.

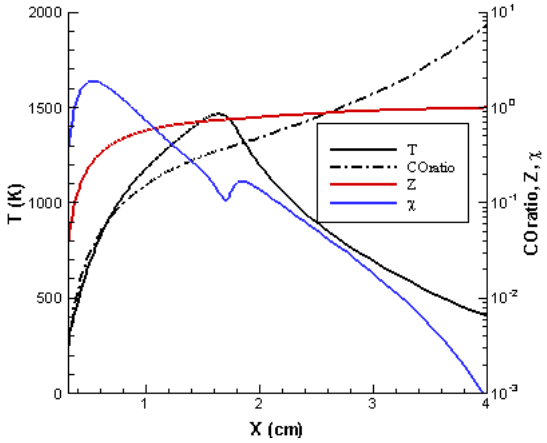

Figure B.7. Predicted T, C/O, Z and χ of flame 8 at its sooting limit 1.83 s.

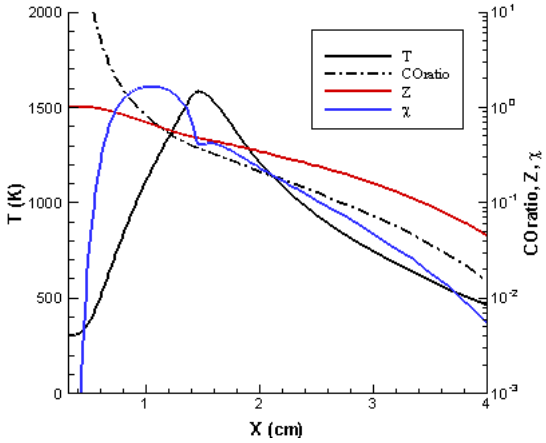

Figure B.8. Predicted T, C/O, Z and χ of flame 9 at its sooting limit 1.87 s.

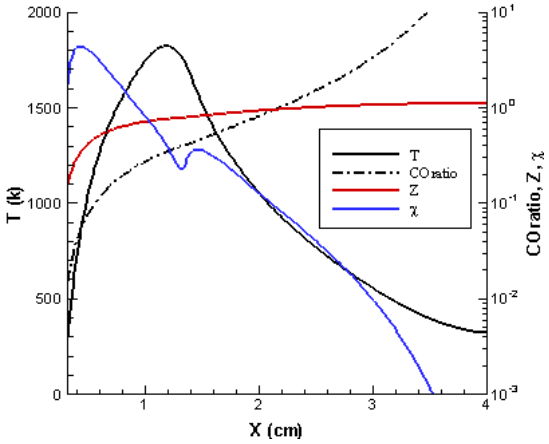

Figure B.9. Predicted T, C/O, Z and χ of flame 11 at its sooting limit 1.27 s.

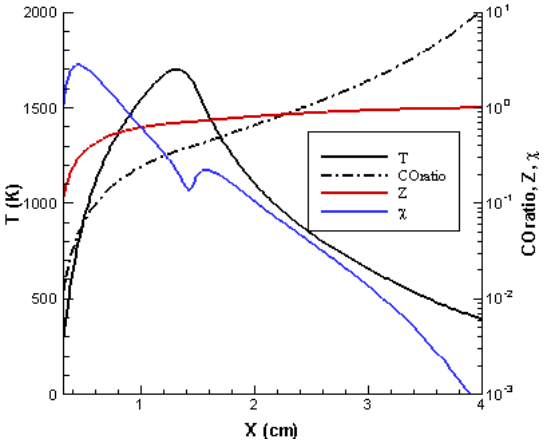

Figure B.10. Predicted T, C/O, Z and χ of flame 12 at its sooting limit 2.0 s.

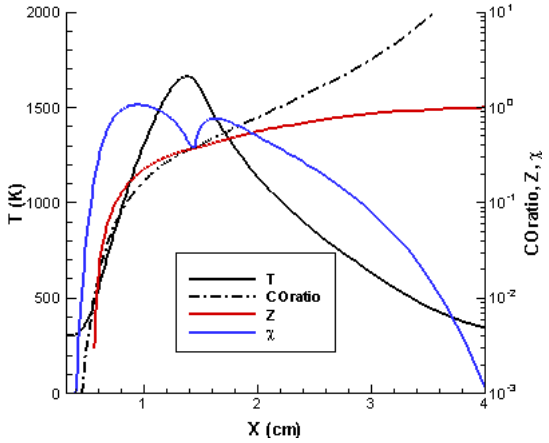

Figure B.11. Predicted T, C/O, Z and χ of flame 13 at its sooting limit 1.2 s.

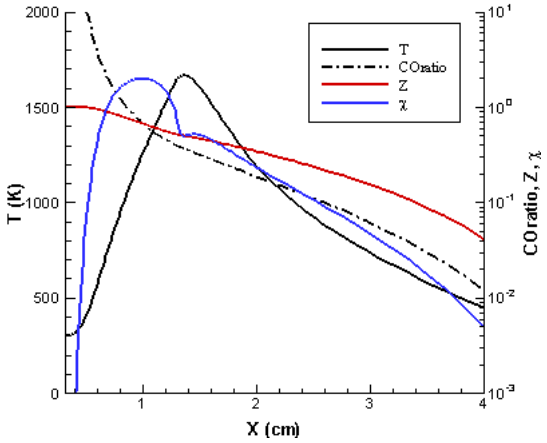

Figure B.12. Predicted T, C/O, Z and χ of flame 14 at its sooting limit 1.8 s.

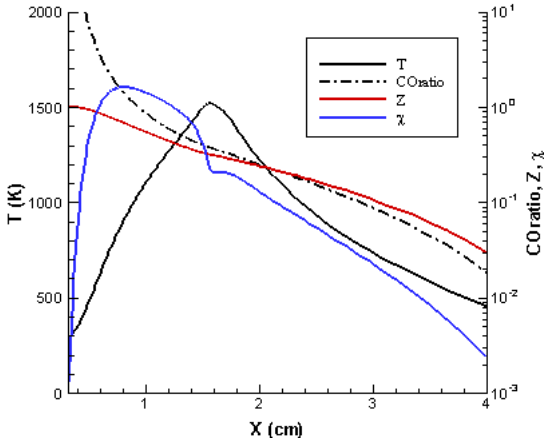

Figure B.13. Predicted T, C/O, Z and χ of flame 15 at its sooting limit 1.93 s.

And the following plots represent the temporal evolution of these flames over the duration of the experiment. It can be noticed that none of these flames have reached the steady-state condition at their soot-free limit, indicating the need for longer time of experiments in order to study sooting behaviors under steady-state conditions.

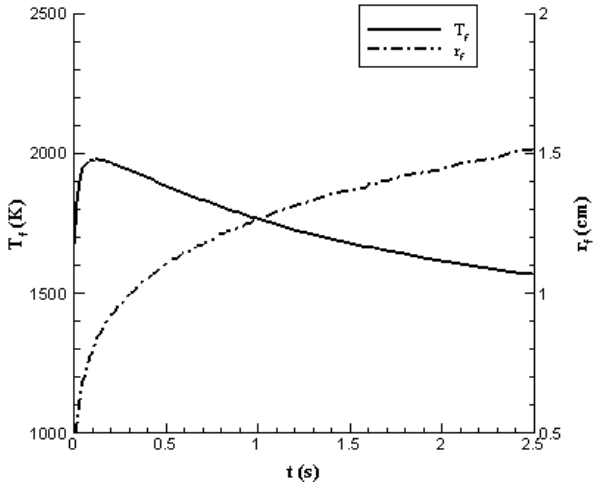

Figure B. 14. Predicted temporal evolution of flame temperature and radius for flame 1, from 0 to 2.5 s.

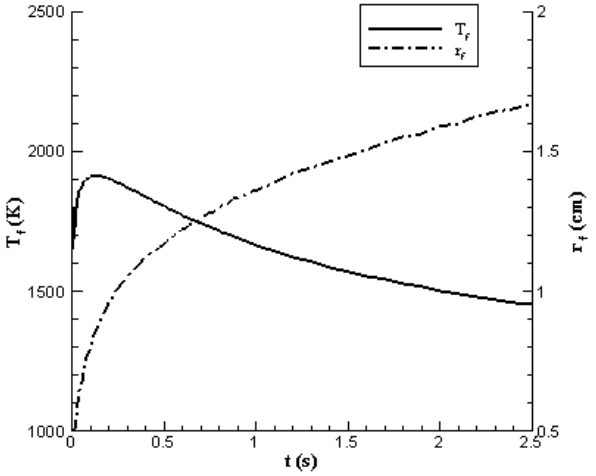

Figure B. 15. Predicted temporal evolution of flame temperature and radius for flame 2, from 0 to 2.5 s.

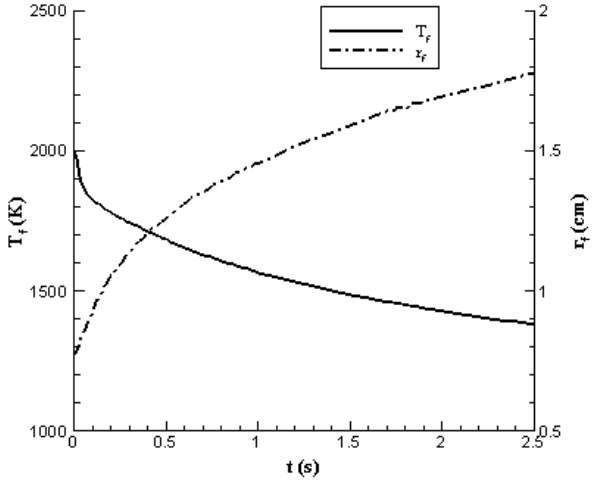

Figure B. 16. Predicted temporal evolution of flame temperature and radius for flame 4, from 0 to 2.5 s.

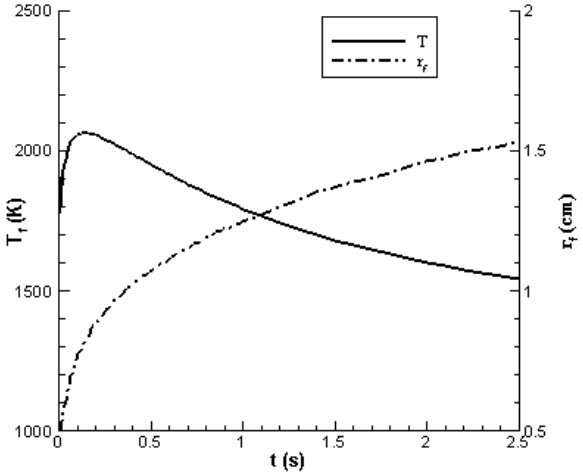

Figure B. 17. Predicted temporal evolution of flame temperature and radius for flame 5, from 0 to 2.5 s.

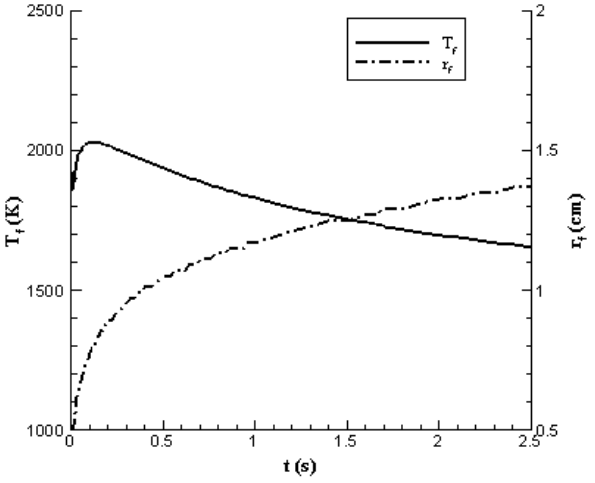

Figure B. 18. Predicted temporal evolution of flame temperature and radius for flame 6, from 0 to 2.5 s.

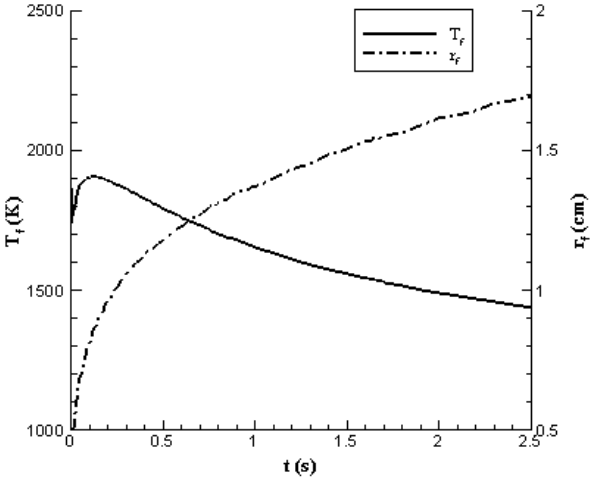

Figure B. 19. Predicted temporal evolution of flame temperature and radius for flame 7, from 0 to 2.5 s.

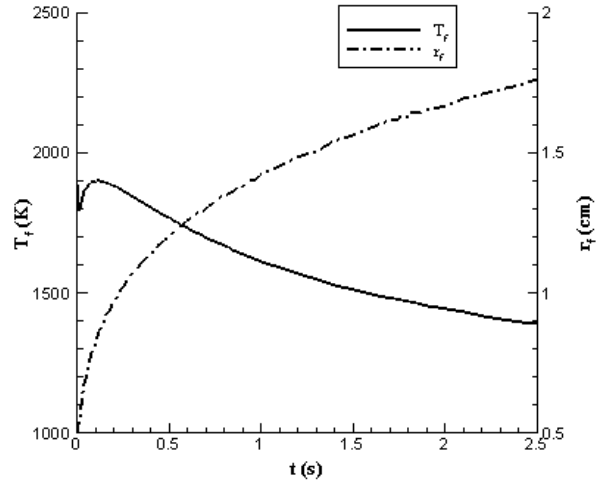

Figure B. 20. Predicted temporal evolution of flame temperature and radius for flame 8, from 0 to 2.5 s.

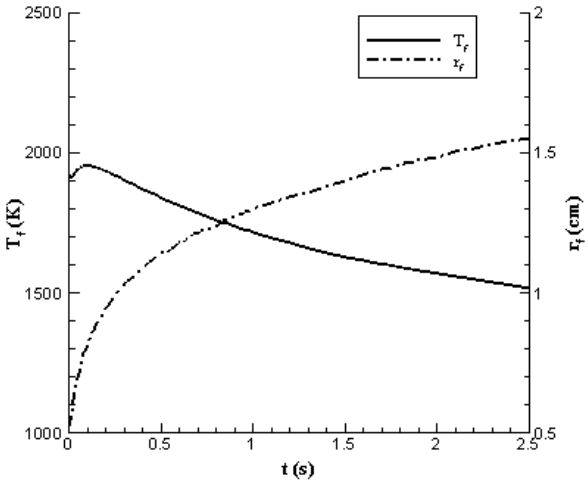

Figure B. 21. Predicted temporal evolution of flame temperature and radius for flame 9, from 0 to 2.5 s.

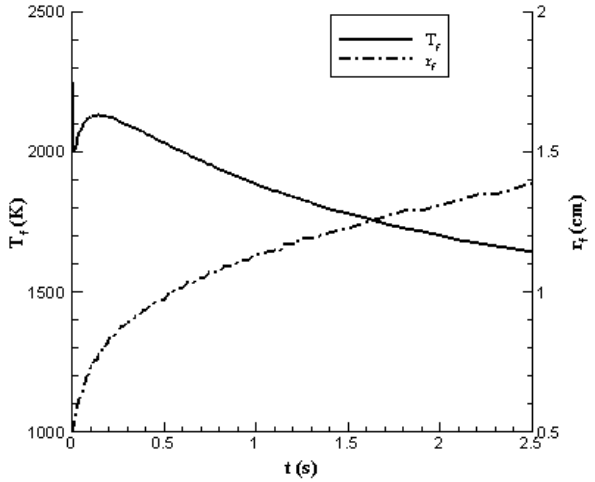

Figure B. 22. Predicted temporal evolution of flame temperature and radius for flame 11, from 0 to 2.5 s.

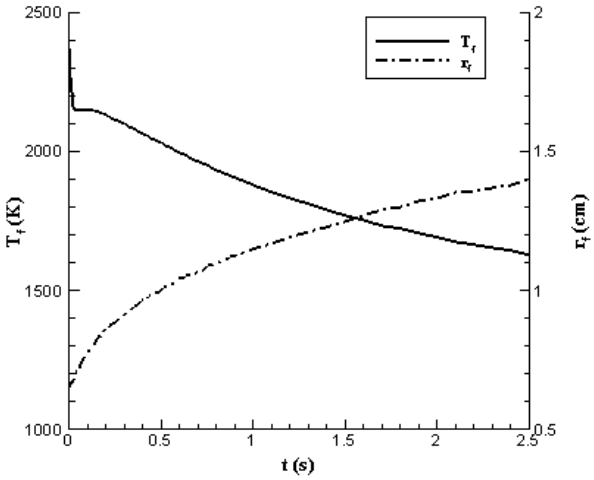

Figure B. 23. Predicted temporal evolution of flame temperature and radius for flame 12, from 0 to 2.5 s.

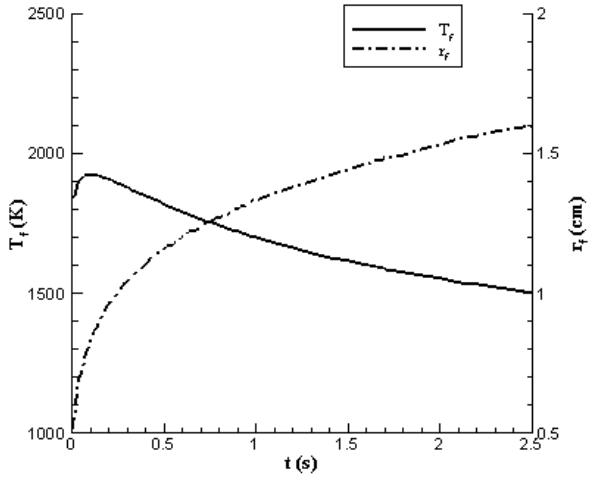

Figure B. 24. Predicted temporal evolution of flame temperature and radius for flame 13, from 0 to 2.5 s.

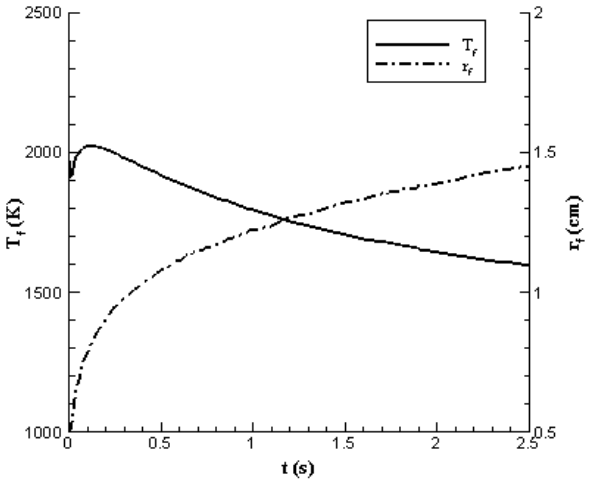

Figure B. 25. Predicted temporal evolution of flame temperature and radius for flame 14, from 0 to 2.5 s.

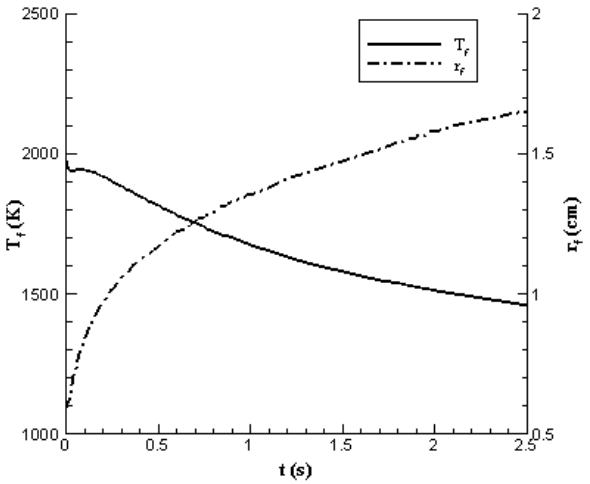

Figure B. 26. Predicted temporal evolution of flame temperature and radius for flame 15, from 0 to 2.5 s.